



8-2013

X-ray crystal structures of: $[\text{Rh}_2(\text{N}-\{2,4,6\text{-CH}_3\}\text{C}_6\text{H}_2)\text{COCH}_3)_4] \cdot 2\text{NCC}_6\text{H}_4$
AND
 $\text{Ba}_{1.5}[\text{Fe}(\text{C}_{10}\text{H}_{13}\text{N}_2\text{O}_7)][\text{Co}(\text{CN})_6] \cdot 9\text{H}_2\text{O}$;
two crystallographic challenges

Kenneth K. Kpogo

East Tennessee State University

Follow this and additional works at: <https://dc.etsu.edu/etd>

 Part of the [Inorganic Chemistry Commons](#)

Recommended Citation

Kpogo, Kenneth K., "X-ray crystal structures of: $[\text{Rh}_2(\text{N}-\{2,4,6\text{-CH}_3\}\text{C}_6\text{H}_2)\text{COCH}_3)_4] \cdot 2\text{NCC}_6\text{H}_4$ AND $\text{Ba}_{1.5}[\text{Fe}(\text{C}_{10}\text{H}_{13}\text{N}_2\text{O}_7)][\text{Co}(\text{CN})_6] \cdot 9\text{H}_2\text{O}$; two crystallographic challenges" (2013). *Electronic Theses and Dissertations*. Paper 1175. <https://dc.etsu.edu/etd/1175>

This Thesis - Open Access is brought to you for free and open access by the Student Works at Digital Commons @ East Tennessee State University. It has been accepted for inclusion in Electronic Theses and Dissertations by an authorized administrator of Digital Commons @ East Tennessee State University. For more information, please contact digilib@etsu.edu.

X-ray Crystal Structures Of: $[\text{Rh}_2(\text{N}-\{2,4,6-\text{CH}_3\}\text{C}_6\text{H}_2)\text{COCH}_3)_4] \cdot 2\text{NCC}_6\text{H}_4$ AND
 $\text{Ba}_{1.5}[\text{Fe}(\text{C}_{10}\text{H}_{13}\text{N}_2\text{O}_7)][\text{Co}(\text{CN})_6] \cdot 9\text{H}_2\text{O}$; Two Crystallographic Challenges

A thesis
presented to
the faculty of the Department of Chemistry
East Tennessee State University
in partial fulfilment
of the requirements for the degree
Master of Science in Chemistry

by
Kenneth Kwame Kpogo
August 2013

Dr. Cassandra T. Eagle, Chair
Dr. Scott Kirkby
Dr. Peng Sun

Keywords: X-ray Crystal Structure, Dirhodium, Barium, Iron, Cobalt, EDTA, HEDTA,
Phenylacetamide, dimeric rhodium, iron-nitrile-cobalt, cobalt-nitrile-iron, Rh_2L_4 .

ABSTRACT

X-ray Crystal Structures Of: $[\text{Rh}_2(\text{N}-\{2,4,6-\text{CH}_3\}\text{C}_6\text{H}_2)\text{COCH}_3)_4] \cdot 2\text{NCC}_6\text{H}_5$ and $\text{Ba}_{1.5}[\text{Fe}(\text{C}_{10}\text{H}_{13}\text{N}_2\text{O}_7)][\text{Co}(\text{CN})_6] \cdot 9\text{H}_2\text{O}$; Two Crystallographic Challenges

by

Kenneth K. Kpogo

The novel compound $[\text{Rh}_2(\text{N}-\{2,4,6-\text{CH}_3\}\text{C}_6\text{H}_2)\text{COCH}_3)_4]$ was synthesized. Crystal structures of $[\text{Rh}_2(\text{N}-\{2,4,6-\text{CH}_3\}\text{C}_6\text{H}_2)\text{COCH}_3)_4] \cdot 2\text{NCC}_6\text{H}_5$ and $\text{Ba}_{1.5}[\text{Fe}(\text{C}_{10}\text{H}_{13}\text{N}_2\text{O}_7)][\text{Co}(\text{CN})_6] \cdot 9\text{H}_2\text{O}$ were determined employing a Rigaku Mercury375R/M CCD (XtaLAB mini) diffractometer with graphite monochromated Mo-K α radiation. For $[\text{Rh}_2(\text{N}-\{2,4,6-\text{CH}_3\}\text{C}_6\text{H}_2)\text{COCH}_3)_4] \cdot 2\text{NCC}_6\text{H}_5$, the space group was P-421c(#114) with unit cell dimensions: $a = 11.0169(14)\text{\AA}$, $c = 21.499(3)\text{\AA}$, $V = 2609.4(6)\text{\AA}^3$. Each rhodium had approximately octahedral coordination and was bound to another rhodium atom, two nitrogens (*trans* to each other), two oxygens (*trans* to each other), and one benzonitrile nitrogen (*trans* to rhodium). For $\text{Ba}_{1.5}[\text{Fe}(\text{C}_{10}\text{H}_{13}\text{N}_2\text{O}_7)][\text{Co}(\text{CN})_6] \cdot 9\text{H}_2\text{O}$ the space group was: P-1(#2) with unit cell dimensions: $a = 13.634\text{\AA}$, $b = 13.768\text{\AA}$, $c = 17.254\text{\AA}$ and $\alpha = 84.795^\circ$, $\beta = 87.863^\circ$, $\gamma = 78.908^\circ$, $V = 3164.5\text{\AA}^3$. The iron atom (nearly octahedral) was coordinated to one chelating ligand (derived from ethylenediaminetetraacetic acid) and the nitrogen of a cyanide ligand. The carbon of the cyanide ligand was bound to cobalt (octahedral). Thus, the cyanide ligand serves as a bridge between the two metals.

DEDICATION

This thesis is dedicated to my wife Josephine, my mother Bridget, and my son Kenneth Jr.

ACKNOWLEDGEMENTS

I am grateful to God for His guidance and protection throughout my life and especially my graduate studies at ETSU. I thank my supervisor, Dr. Cassandra T Eagle, for her professional guidance and constructive critique of this research. My sincere gratitude also goes to Dr. Scott Kirkby and Dr. Peng Sun for serving on my committee and for their advice and suggestions on this work. Dr Chu-Ngi Ho, I thank you so much for guiding me. I thank the faculty and staff of the Department of Chemistry ETSU, especially Dr. Reza Mohseni, Ms. Barbara Rasnick, Ms. Jillian Quirante, Mr. Tom Webster, and Mr. Walt Witt. I am grateful to Dr. Lee Daniels of Rigaku for training me in X-ray crystallography and all the help he gave me in solving crystal structures.

My gratitude goes to my sweet mother who instilled in me the value of education and has cared and guided me throughout my life. Mum, thank you for believing in my abilities. My love goes to my dearest wife and son, Josephine and Kenneth Jr., for their assured love and prayers during my studies. I thank all the graduate students in the chemistry department and all members of Shades of Africa for a wonderful social experience on campus. Finally, I thank Nkongho Atem-Tambe, Landon Zink, Albert Smith, and Jennie Tan for shared ideas.

TABLE OF CONTENTS

	Page
ABSTRACT.....	2
DEDICATION.....	3
ACKNOWLEDGEMENTS.....	4
LIST OF TABLES.....	7
LIST OF FIGURES.....	9
Chapter	
1. INTRODUCTION.....	11
Single-Crystal X-ray Crystallography.....	11
Deriving Bragg's Law.....	12
Dirhodium Compounds.....	17
Bonding in Tetrakis (carboxylamidate) Dirhodium (II).....	20
Preparation and Classification of Tetrakis (carboxylamidate) Dirhodium (II).....	22
2. EXPERIMENTAL.....	25
Reagents.....	25
Synthesis of Starting Materials.....	25
Sodium Acetate Trihydrate.....	26
Tetrakis (carboxylate) Dirhodium(II).....	26
N-(2, 4, 6-trimethylphenyl) Acetamide.....	27
Tetrakis [μ -(N-{2, 4,6-trimethylphenyl} Acetamidato- κ N: κ O)] Dirhodium (II), $[\text{Rh}_2(\text{N}-\{2,4,6-\text{CH}_3\}\text{C}_6\text{H}_2)\text{COCH}_3)_4]$	32
Flash Column Chromatography.....	33
Characterization of Tetrakis (trimethylphenylacetamidate) Dirhodium (II).....	35
Nuclear Magnetic Resonance (NMR) Analysis.....	35
Synthesis of $[\text{Rh}_2(\text{N}-\{2,4,6-\text{CH}_3\}\text{C}_6\text{H}_2)\text{COCH}_3)_4] \cdot 2\text{NCC}_6\text{H}_4$ by Vapor Diffusion Method.....	43
X-ray Crystallographic Studies.....	43
$[\text{Rh}_2(\text{N}-\{2,4,6-\text{CH}_3\}\text{C}_6\text{H}_2)\text{COCH}_3)_4] \cdot 2\text{NCC}_6\text{H}_5$	44
Data Collection.....	44

Data Reduction	45
Structure Solution and Refinement.....	45
Ba _{1.5} [Fe(C ₁₀ H ₁₃ N ₂ O ₇)] [Co(CN) ₆] · 9H ₂ O	46
Data Collection	46
Data Reduction	47
Structure Solution and Refinement.....	47
3. RESULTS AND DISCUSSION	49
Preamble.....	49
N-(2,4,6-trimethylphenyl) Acetamide	49
[Rh ₂ (N-{2,4,6-CH ₃ }C ₆ H ₂)COCH ₃) ₄] · 2NCC ₆ H ₄	49
Ba _{1.5} [Fe(C ₁₀ H ₁₃ N ₂ O ₇)] [Co(CN) ₆] · 9H ₂ O	54
4. CONCLUSION.....	59
REFERENCES	61
APPENDICES	65
Appendix A: Crystallographic Report for [Rh ₂ (N-{2,4,6-CH ₃ }C ₆ H ₂)COCH ₃) ₄] · 2NCC ₆ H ₄	65
Appendix B: Crystallographic Report for Ba _{1.5} [Fe(C ₁₀ H ₁₃ N ₂ O ₇)] [Co(CN) ₆] · 9H ₂ O	81
Appendix C: Authored Publication	112
VITA.....	113

LIST OF TABLES

Table	Page
Table 1: Elemental analysis of $\text{Ba}_{1.5}[\text{Fe}(\text{C}_{10}\text{H}_{13}\text{N}_2\text{O}_7)][\text{Co}(\text{CN})_6]\cdot 9\text{H}_2\text{O}$	54
Table 2: (Appendix A $[\text{Rh}_2(\text{N}-\{2,4,6-\text{CH}_3\}\text{C}_6\text{H}_2)\text{COCH}_3)_4]\cdot 2\text{NCC}_6\text{H}_4$): Atomic coordinates and $B_{\text{iso}}/B_{\text{eq}}$ and occupancy.	68
Table 3: (Appendix A $[\text{Rh}_2(\text{N}-\{2,4,6-\text{CH}_3\}\text{C}_6\text{H}_2)\text{COCH}_3)_4]\cdot 2\text{NCC}_6\text{H}_4$): Atomic coordinates and B_{iso} and occupancy involving hydrogen atoms.	68
Table 4: (Appendix A $[\text{Rh}_2(\text{N}-\{2,4,6-\text{CH}_3\}\text{C}_6\text{H}_2)\text{COCH}_3)_4]\cdot 2\text{NCC}_6\text{H}_4$): Anisotropic displacement parameters.	69
Table 5: (Appendix A $[\text{Rh}_2(\text{N}-\{2,4,6-\text{CH}_3\}\text{C}_6\text{H}_2)\text{COCH}_3)_4]\cdot 2\text{NCC}_6\text{H}_4$): Bond lengths (Å). 69	69
Table 6: (Appendix A $[\text{Rh}_2(\text{N}-\{2,4,6-\text{CH}_3\}\text{C}_6\text{H}_2)\text{COCH}_3)_4]\cdot 2\text{NCC}_6\text{H}_4$): Bond lengths involving hydrogens (Å).	70
Table 7: (Appendix A $[\text{Rh}_2(\text{N}-\{2,4,6-\text{CH}_3\}\text{C}_6\text{H}_2)\text{COCH}_3)_4]\cdot 2\text{NCC}_6\text{H}_4$): Bond angles ($^\circ$). 71	71
Table 8: (Appendix A $[\text{Rh}_2(\text{N}-\{2,4,6-\text{CH}_3\}\text{C}_6\text{H}_2)\text{COCH}_3)_4]\cdot 2\text{NCC}_6\text{H}_4$): Bond angles involving hydrogens ($^\circ$).....	71
Table 9: (Appendix A $[\text{Rh}_2(\text{N}-\{2,4,6-\text{CH}_3\}\text{C}_6\text{H}_2)\text{COCH}_3)_4]\cdot 2\text{NCC}_6\text{H}_4$): Torsion Angles ($^\circ$). (Those having bond angles > 160 degrees are excluded.)	72
Table 10: (Appendix A $[\text{Rh}_2(\text{N}-\{2,4,6-\text{CH}_3\}\text{C}_6\text{H}_2)\text{COCH}_3)_4]\cdot 2\text{NCC}_6\text{H}_4$): Intramolecular contacts less than 3.60 Å.....	73
Table 11: (Appendix A $[\text{Rh}_2(\text{N}-\{2,4,6-\text{CH}_3\}\text{C}_6\text{H}_2)\text{COCH}_3)_4]\cdot 2\text{NCC}_6\text{H}_4$): Intramolecular contacts less than 3.60 Å involving hydrogens.....	74
Table 12: (Appendix A $[\text{Rh}_2(\text{N}-\{2,4,6-\text{CH}_3\}\text{C}_6\text{H}_2)\text{COCH}_3)_4]\cdot 2\text{NCC}_6\text{H}_4$): Intermolecular contacts less than 3.60 Å involving hydrogens.....	76
Table 13: (Appendix B $\text{Ba}_{1.5}[\text{Fe}(\text{C}_{10}\text{H}_{13}\text{N}_2\text{O}_7)][\text{Co}(\text{CN})_6]\cdot 9\text{H}_2\text{O}$): Atomic coordinates and $B_{\text{iso}}/B_{\text{eq}}$ and occupancy.....	84
Table 14: (Appendix B $\text{Ba}_{1.5}[\text{Fe}(\text{C}_{10}\text{H}_{13}\text{N}_2\text{O}_7)][\text{Co}(\text{CN})_6]\cdot 9\text{H}_2\text{O}$): Atomic coordinates and B_{iso} and occupancy involving hydrogen atoms.	88
Table 15: (Appendix B $\text{Ba}_{1.5}[\text{Fe}(\text{C}_{10}\text{H}_{13}\text{N}_2\text{O}_7)][\text{Co}(\text{CN})_6]\cdot 9\text{H}_2\text{O}$): Anisotropic displacement parameters	89
Table 16: (Appendix B $\text{Ba}_{1.5}[\text{Fe}(\text{C}_{10}\text{H}_{13}\text{N}_2\text{O}_7)][\text{Co}(\text{CN})_6]\cdot 9\text{H}_2\text{O}$): Bond lengths (Å).	93
Table 17: (Appendix B $\text{Ba}_{1.5}[\text{Fe}(\text{C}_{10}\text{H}_{13}\text{N}_2\text{O}_7)][\text{Co}(\text{CN})_6]\cdot 9\text{H}_2\text{O}$): Bond lengths involving hydrogens (Å).	96
Table 18: (Appendix B $\text{Ba}_{1.5}[\text{Fe}(\text{C}_{10}\text{H}_{13}\text{N}_2\text{O}_7)][\text{Co}(\text{CN})_6]\cdot 9\text{H}_2\text{O}$): Bond angles ($^\circ$).	97

Table 19: (Appendix B Ba_{1.5}[Fe(C₁₀H₁₃N₂O₇)] [Co(CN)₆]·9H₂O): Bond angles involving hydrogens (°)..... 103

Table 20: (Appendix B Ba_{1.5}[Fe(C₁₀H₁₃N₂O₇)] [Co(CN)₆]·9H₂O): Torsion Angles (°). (Those having bond angles > 160 degrees are excluded.) 105

LIST OF FIGURES

Figures	Page
Figure 1: A scheme of Bragg's Law showing incident rays far from 45 degrees	12
Figure 2: A schematic representation of lattice points in a plane	14
Figure 3: A diagram of a unit cell showing miller indices	15
Figure 4: A schematic representation of the Crystallographic method	16
Figure 5: Schematic representation of the 'octahedral' geometry of the pseudo fourfold symmetry structure of $\text{Rh}_2(\text{O}_2\text{CR})_4$, (R = alkane).....	18
Figure 6: Sketal structure of a typical Tetrakis(carboxylamidate) dirhodium(II)	19
Figure 7: A diagram of various isomeric structures of tetrakis(carboxylamidate) dirhodium(II).....	19
Figure 8: A scheme of a 2,2- <i>cis</i> isomer of $[\text{Rh}_2(\text{NPhCOCH}_3)_4]$	19
Figure 9: Schematic representation of coordination of Tetrakis(carboxylamidate) dirhodium(II).....	20
Figure 10: A combination of Atomic Orbitals showing Metal-Metal bonding-antibonding interactions.....	21
Figure 11: Metal-Ligand interactions in MO of tetrakis(carboxylamidate) dirhodium(II). ...	22
Figure 12: IR of N-(2,4,6-trimethylphenyl)-acetamide	29
Figure 13a: ^1H NMR spectrum of 2,4,6-trimethylphenyl acetamide	30
Figure 13b: ^{13}C NMR spectrum of 2,4,6-trimethylphenyl acetamide	31
Figure 14a: ^1H NMR of the 2,2- <i>trans</i> isomer of $[\text{Rh}_2(\text{N}-\{2,4,6-\text{CH}_3\}\text{C}_6\text{H}_2)\text{COCH}_3)_4]$	37
Figure 14b: ^{13}C NMR of the 2,2- <i>trans</i> isomer of $[\text{Rh}_2(\text{N}-\{2,4,6-\text{CH}_3\}\text{C}_6\text{H}_2)\text{COCH}_3)_4]$	38
Figure 15a: ^1H NMR of the 2,2- <i>cis</i> isomer of $[\text{Rh}_2(\text{N}-\{2,4,6-\text{CH}_3\}\text{C}_6\text{H}_2)\text{COCH}_3)_4]$	39
Figure 15b: ^{13}C NMR of the 2,2- <i>cis</i> isomer of $[\text{Rh}_2(\text{N}-\{2,4,6-\text{CH}_3\}\text{C}_6\text{H}_2)\text{COCH}_3)_4]$	40
Figure 16a: ^1H NMR of the 3,1 isomer of $[\text{Rh}_2(\text{N}-\{2,4,6-\text{CH}_3\}\text{C}_6\text{H}_2)\text{COCH}_3)_4]$	41
Figure 16b: ^{13}C NMR of the 3,1 isomer of $[\text{Rh}_2(\text{N}-\{2,4,6-\text{CH}_3\}\text{C}_6\text{H}_2)\text{COCH}_3)_4]$	42

Figure 17: ORTEP of Bis(benzonitrile)-2,2-trans-tetrakis[μ -(N-{2,4,6-trimethylphenyl})Acetamidato- κ N: κ O)] dirhodium(II) with thermal ellipsoids at 30% probability and hydrogen atoms arbitrarily small.....	52
Figure 18: Packing diagram of the Bis(benzonitrile)-2,2-trans-tetrakis[μ -(N-{2,4,6-Trimethylphenyl})Acetamidato- κ N: κ O)] dirhodium(II) viewed along the <i>a</i> -axis. H-atoms omitted for clarity	53
Figure 19: Packing diagram of the Bis(benzonitrile)-2,2-trans-tetrakis[μ -(N-{2,4,6-Trimethylphenyl})Acetamidato- κ N: κ O)] dirhodium(II) viewed along the <i>c</i> -axis to emphasize the pseudo fourfold symmetry orientation. H-atoms omitted for clarity	53
Figure 20: ORTEP of Ba _{1.5} [Fe(HEDTA)][Co(CN) ₆].9H ₂ O showing thermal ellipsoids at 30% probability and hydrogen atoms arbitrarily small.....	57
Figure 21: A symmetry extension diagram of Ba _{1.5} [Fe(HEDTA)][Co(CN) ₆].9H ₂ O.	58
Figure 22: Packing diagram of Ba _{1.5} [Fe(HEDTA)][Co(CN) ₆].9H ₂ O viewed along the <i>a</i> -axis. H-atoms omitted for clarity.....	58

CHAPTER 1

INTRODUCTION

Single-Crystal X-ray Crystallography

A crystal is made of atoms arranged in a pattern that is repetitive, periodically in three dimensional space.¹ This pattern can consist of a single atom, group of atoms, a particular molecule, or a group of molecules.²

X-rays are produced with X-ray tubes or synchrotron radiation. In an X-ray tube, X-rays are created when a focused electron source accelerated over a high electrical energy field hits a fixed or revolving solid target. As these electrons have a collision with atoms in the target and slow down, a constant spectrum of X-rays is emitted. This is called Bremsstrahlung radiation. The energetic electrons also emit inner shell electrons in atoms through the ionization process.³

X-rays interact with electrons in the atom. When X-rays hit electrons, some of these X-rays are deflected from the direction in which they were originally travelling. If the wavelength of these deflected X-rays does not change (meaning that X-rays do not lose any energy), the process is called elastic scattering (Thompson Scattering). Only momentum has been transferred in the scattering process. These types of X-rays are the ones measured in diffraction experiments.⁴ However, in the inelastic scattering process (Compton Scattering), X-rays transmit some of their energy to the electrons and the deflected X-rays lose energy and hence have different wavelength than the incident X-rays.

As the X-rays interact with the electrons in the atoms of matter that is crystalline with the atoms ordered in planes, and the distances between the atoms are of the same magnitude as the wavelength of the X-rays, then constructive and destructive interference will occur.

The result is diffraction in which X-rays are ‘reflected’ at angles based on the spaces between the atoms ordered in the crystalline matter.³

Deriving Bragg's Law

Bragg's Law is obtained by taking into account the conditions needed to make the phases of the rays correspond when the incident angle and the reflecting angle are equal. The incident rays are always in phase and parallel up to the point at which the top beam hits the uppermost plane at atom z as in Figure 1. The second incident ray continues to the second plane where it is reflected by the second atom B. The second incident ray must go the extra distance AB + BC if the two rays are to keep travelling adjacent and parallel. This extra distance must be an integral (n) multiple of the wavelength (λ) for the phases of the two rays to be the same:

$$n\lambda = AB + BC \tag{1.1}$$

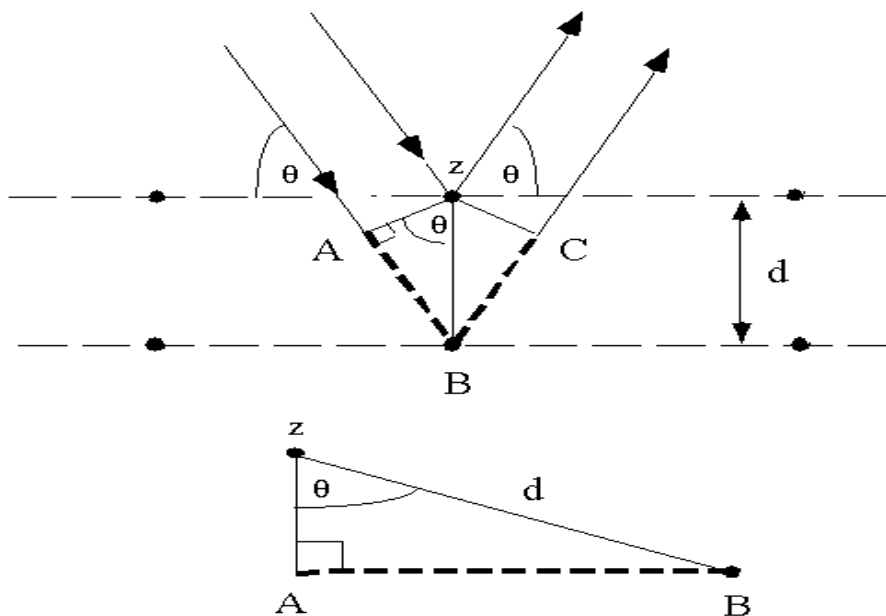


Figure 1: A scheme of Bragg's Law showing incident rays far from 45 degrees

$$n\lambda=AB+BC \quad (1.2)$$

Identifying d as the hypotenuse of the right triangle ABz , we can use trigonometry to relate d and θ to the distance $(AB + BC)$. The distance AB is opposite θ so,

$$AB=d\sin\theta \quad (1.3).$$

Because $AB = BC$ eq. (1.2) becomes,

$$n\lambda=2AB \quad (1.4)$$

Substituting eq. (1.3) in eq. (1.4) we have,

$$n\lambda=2d\cdot\sin\theta \quad (1.5)$$

Crystals have a lot of planes passing through their atoms. These planes have specific inter-planar distances that will give a typical angle of diffracted X-rays. The relationship between wavelength, the atomic spacing 'd', and the angle 'θ' was explained as Bragg's Law. If the incident wavelength is known and the 'reflected' angle can be measured with an X-ray diffractometer then the inter-atomic distance can be calculated from the Bragg equation. A set of 'd-spaces' obtained from a single compound represents the set of planes that can pass through the atoms and can be compared with sets of d-spaces obtained from reference compounds.

The orientation of a surface or a crystal plane may be defined by considering how that plane intersects the main crystallographic axes of the solid.⁵ The application of specific rules leads to the assignment of the Miller Indices (hkl). Miller indices are a group of three numbers that indicate the orientation in space of a plane or set of parallel planes of atoms in a crystal.

If each atom in the crystal is represented by a point and these points are joined by lines as shown in figure 2 below, the resultant lattice is divided into a number of identical blocks called unit cells; the intersecting edges of one of the unit cells defines a set of crystallographic axes, and the Miller indices are obtained by the intersection of the plane with these axes. The reciprocals of these intercepts are calculated, and fractions are eliminated to give the three Miller indices (hkl).⁶

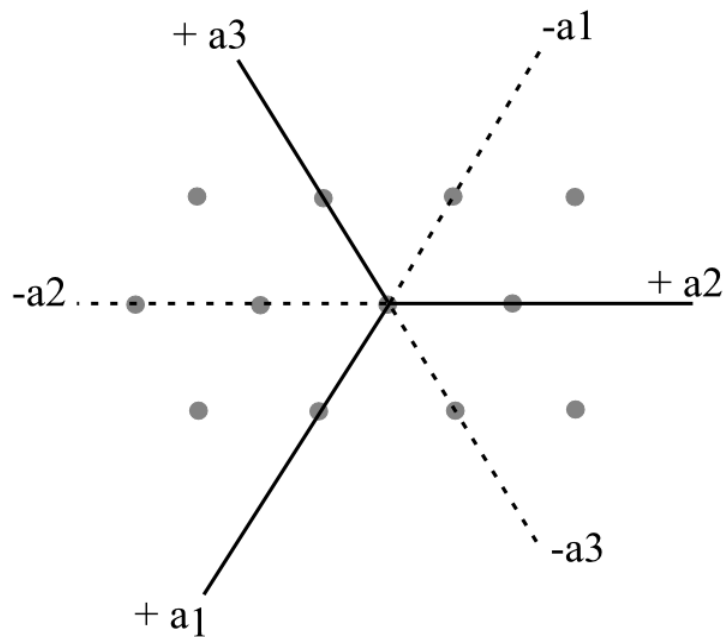


Figure 2: A schematic representation of lattice points in a plane

A plane parallel to two axes but cutting the third axis at a length equal to one edge of a unit cell has Miller indices of (100) , (010) , or (001) as shown in figure 3 depending upon

the axis cut; and a plane cutting all three axes at lengths equal to the edges of a unit cell has Miller indices of (111).⁵ This scheme was devised by a British mineralogist and crystallographer William Hallowes Miller in 1839. The Miller indices scheme has the advantage of eliminating all fractions from the notation for a plane.⁶

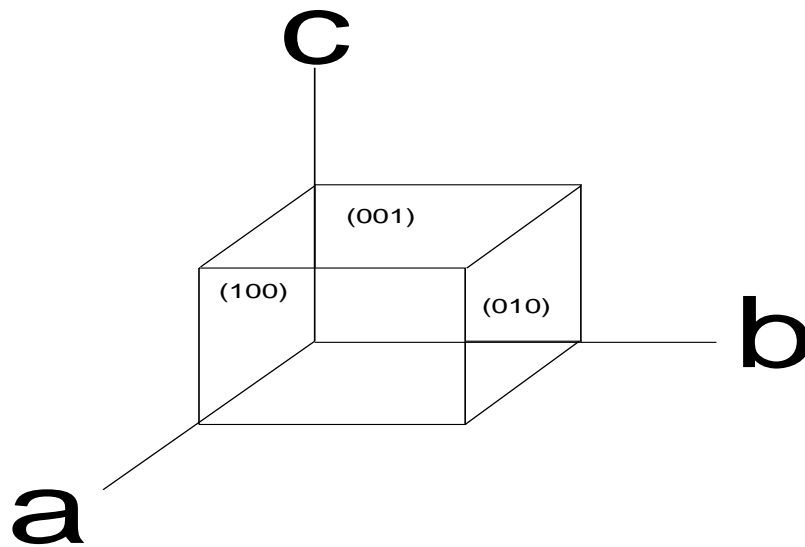


Figure 3: A diagram of a unit cell showing miller indices

During single crystal X-ray diffraction experiment as illustrated in figure 4 below, a crystal is mounted onto a mitogen loop on a magnetic cap that is placed onto a goniometer and is immersed in X-rays of a specific wavelength (0.71075 \AA). The crystal is rotated continuously about one of the unit cell axes, and the incident X-ray beam is normal to this axis. As the crystal is rotated, the atoms in a crystal structure absorb X-ray radiation and emit the radiation outward, creating both constructive and destructive interference, which is called diffraction.

These rays of diffracted radiation are sent out in the corresponding directions, and the constructive interference from diffracted beams creates a diffraction pattern on the photographic plate. From the angles of the X-ray beams and intensities determined by diffraction patterns, the 3D structure of the atoms of the crystal can be constructed. The intensity of the diffraction patterns depends on the size of the crystal, the condition of the crystal, and the thermal vibrations in the crystal structure. The angles of the diffraction beams also give insight on the specific details of the structure of the atoms, such as the distances of the bonds of the atoms.⁷

Overview of the X-ray Crystallographic Method

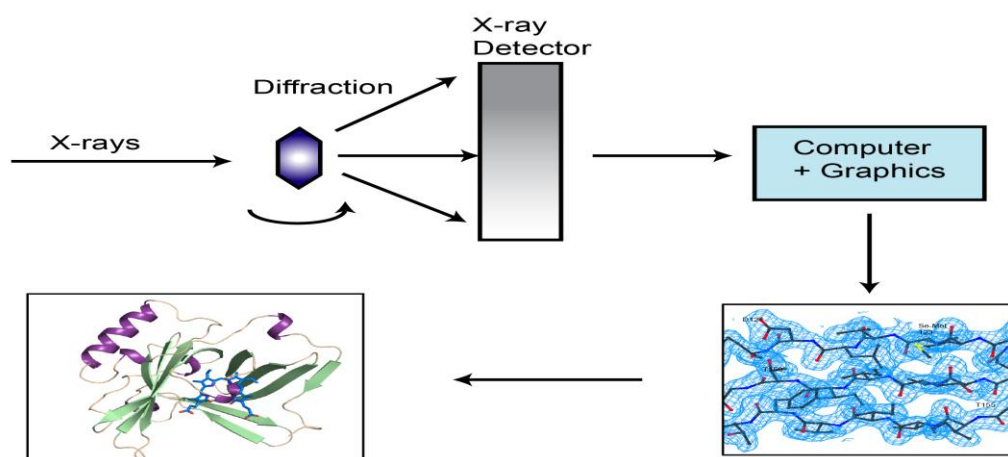


Figure 4: A schematic representation of the Crystallographic Method

In order to determine the positions of the atoms within a unit cell, the atomic structural parameters (temperature, thermal motion, partial occupancy of atomic sites, etc.) can be refined. Because an atom does not vibrate equally in all directions (anisotropically), it is difficult to pinpoint the exact location of an atom. By adjusting these parameters, the values of the structure factors will change, but the best set of parameters are those which will produce the most accurate values of inter atomic distances and bond angles. The measure of

correctness of a structure is given by the residual or R-value calculated by the following formula:

$$R = \frac{\sum |F_{\text{observed}} - F_{\text{calculated}}|}{\sum |F_{\text{observed}}|} \quad (1.6)$$

F is the structure factor. The structure factor F_{hkl} is a mathematical function that defines the amplitude and phase of a wave diffracted from crystal lattice planes characterised by Miller indices (h,k,l .)

The term R factor in crystallography is a degree of agreement between the amplitudes of the structure factors calculated from a model and those from the original diffraction data. The R factor is calculated during each cycle of least-squares structure refinement to determine the quality and progress of this agreement. The final R factor is reported in percentages. An R of 0.20 (20%) may indicate a correct structure, with the best possible values of the experimental atomic parameters; however, R should be considerably less than 0.10 (10%), and an R value of 0.005 (5%) or less implies that the results are probably very reliable.

Dirhodium Compounds

Dirhodium compounds with bridging ligands are very important in the field of metal-metal bonding chemistry. They have unique properties such as structural rigidity, ease of ligand exchange, availability of open diaxial sites for coordination with Lewis bases, and low oxidation potentials. They have become highly efficient catalysts for a variety of applications.^{8,9,10,11,12}

Tetrakis (acetate) dirhodium(II) was first used as a catalyst for the decomposition of diazo compounds by Teyssie and co-workers in 1973.¹³ The air-stable compound has become the single most used catalyst for metal carbene transformations since then.¹³ There are four

bridging acetate ligands and one vacant coordination site per metal atom¹⁴ that show an ‘octahedral’ geometry whose ligand arrangement at each rhodium face resembles that of a circular wall as shown in figure 5 below whose periphery is electron rich and its center is electron deficient.¹⁵

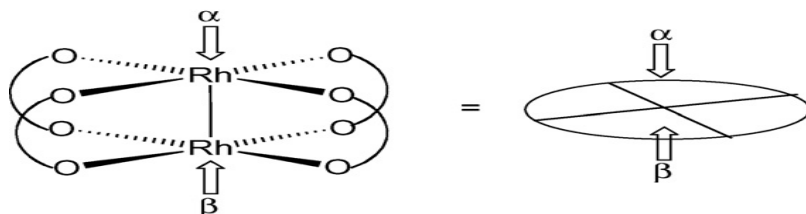


Figure 5: Schematic representation of the ‘octahedral’ geometry of the pseudo fourfold symmetry structure of $\text{Rh}_2(\text{O}_2\text{CR})_4$, (R = alkane)

Replacing the acetate ligands with other carboxylates changes the physical and chemical properties of the tetrakis(carboxylate) dirhodium(II) according to the characteristics of its ligands.¹⁶ Tetrakis(prolinates) dirhodium(II), for instance, have high solubility in nonpolar solvents¹⁷ and tetrakis(phenylacetate) dirhodium(II) was introduced as a highly efficient catalyst for carbon-hydrogen insertion reactions of α -diazo- β -keto esters.¹⁸

The first synthesis of a tetrakis (carboxylamidate) dirhodium(II), see Figure 6, occurred in 1983 when tetrakis(carboxylamidate) dirhodium(II) was isolated from a melt of acetamide containing tetrakis(acetate) dirhodium(II).¹⁹ Multiple isomers are possible as can be seen in figure 7, but the one in figure 8 in which two nitrogen atoms and two oxygen atoms are bound to each rhodium with the two nitrogen atoms *cis* to each other (the *cis*-2,2 isomer) is dominant.¹⁹ In catalytic reactions with diazocarbonyl compounds, the carboxamidates exhibited lower reactivity for diazo decomposition than the corresponding carboxylates, but higher selectivities.

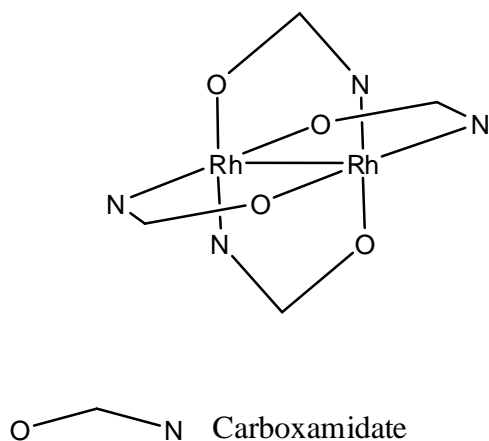


Figure 6: Sketal structure of a typical Tetrakis (carboxylamidate) Dirhodium(II)

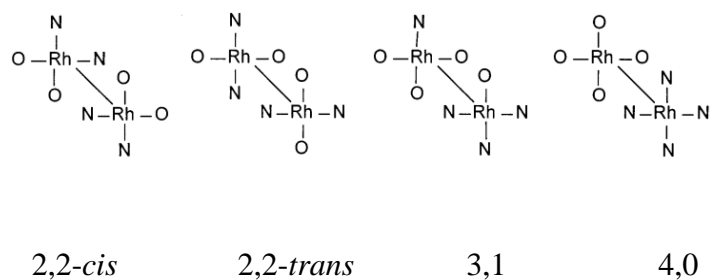


Figure 7: A diagram of various isomeric structures of tetrakis (carboxylamidate) dirhodium(II)

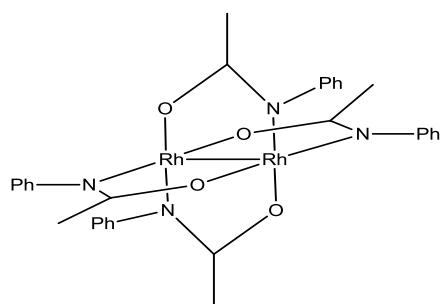


Figure 8: A scheme of a 2, 2-*cis* isomer of $[\text{Rh}_2(\text{NPhCOCH}_3)_4]$

When the dirhodium core interacts with four bridging ligands, bonding takes place. This can be expressed as a metal centered dsp^2 hybrid atomic orbital (AO). Based on the

coordinate system, the dsp^2 hybrid orbital is made up of the s , p_x , y , and dx^2-y^2 atomic orbitals (AO). The basic structure in figure 9 results as a combination of two empty dsp^2 AO and 4 sp^2 orbitals of a μ -bridging X=C-Y donor ligand. This combination leaves four d -orbitals and one p -orbital on each of the metal atoms that can combine in the bonding/anti-bonding interactions.²⁰

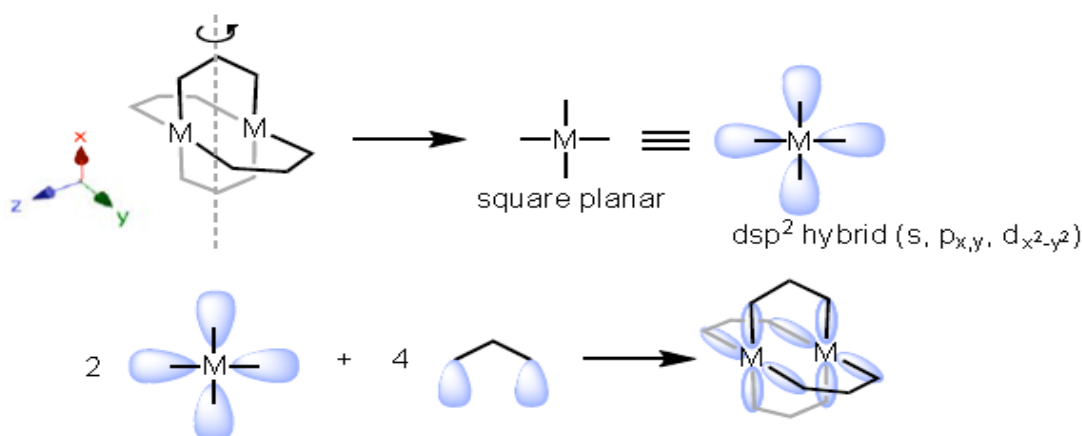


Figure 9: Schematic representation of coordination of Tetrakis(carboxylamidate) dirhodium(II)²⁰

Bonding in Tetrakis (carboxylamidate) Dirhodium(II)

The bonding in Rh_2L_4 (where L = carboxylate or carboxylamide) complexes is usually discussed within the context of the description in figure 10. Rh_2L_4 is made of two rhodium atoms that are surrounded by four bridging carboxylate groups. These bridging carboxylate ligands have a -1 charge each. Because the tetrakis(carboxylate) dirhodium(II) is a neutral complex, the rhodium atoms share a plus 4 charge, hence each rhodium atom has a +2 oxidation state.²¹ The fundamental Rh_2^{4+} complex is a d^7-d^7 dimer with 14 d -electrons.

When the electrons are placed into the MO diagram an electronic configuration of $\sigma^2\pi^4\delta^2\delta^*\pi^*4$ for Rh_2^{4+} and an overall Rh-Rh single bond is obtained.

Tetrakis (carboxylamidate) dirhodium(II) is dinuclear with a pseudo fourfold symmetry configuration that consists of a Rh-Rh metal core surrounded by four carboxylamide bridging ligands. In most carboxamidates the two nitrogen atoms and two oxygen atoms are bound to each rhodium in a *cis*-(2,2) orientation, but recently the *trans*-(2,2) isomers have been reported by our group and others.⁴¹ The interactions between the μ -bridging amide ligand and the Rh-Rh core fall into a special category of metal complex bond formation. The molecular orbitals are changed.

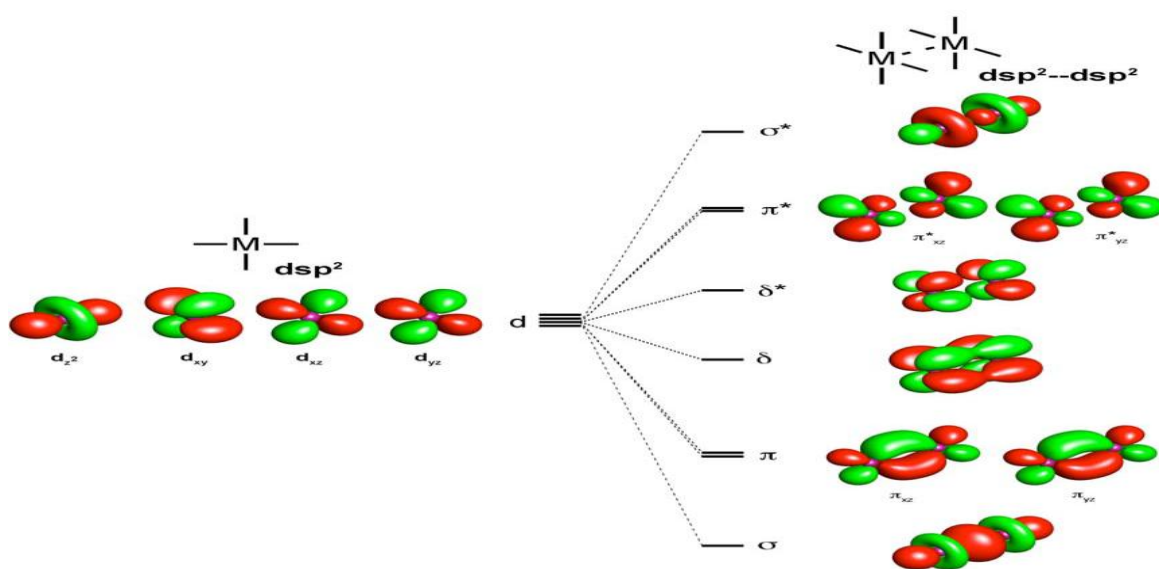


Figure 10: A combination of Atomic Orbitals showing Metal-Metal bonding-antibonding interactions²⁰

For the carboxylamides the interactions between the metals and the ligands cause a reorientation of the π^* and δ^* Molecular orbitals (MOs). This was demonstrated by Bear and co-workers in a series of complexes with the general formula $\text{Rh}_2(\text{OAc})_m(\text{acam})_n$ (acam = carboxylamidate), ($m=0-4$; $n=4-m$).²² Their research showed that as the number of the

equatorial acam ligands increased, the (HOMO) changed from π^* to δ^* . This inversion can be explained as an interaction between the π -orbitals of the donor acam ligands and the δ^* orbital of the Rh-Rh core. When the four non-bonding π -orbitals (π^2) of the μ -bridging carboxamidate ligands are combined, the ligand MOs shown in Figure 11 is given. In-phase mixing between these MOs and $\delta^*(\text{Rh-Rh})$ leads to M-L bonding interactions and the out-of-phase mixing raises the energy of the $\delta^*(\text{Rh-Rh})$ MO above that of the $\pi^*(\text{Rh-Rh})$ MOs. Thus, the electronic configuration for the $\text{Rh}_2(\text{acam})_4$ is better assigned as $\sigma^2\pi^4\delta^2\pi^{*4}\delta^{*2}$.²³

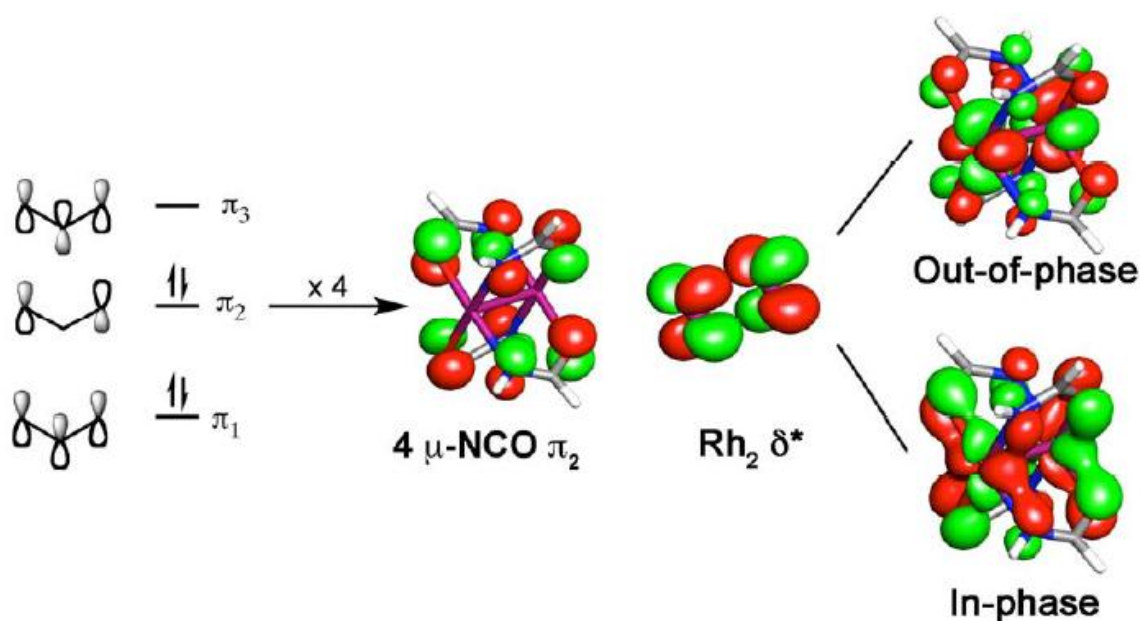
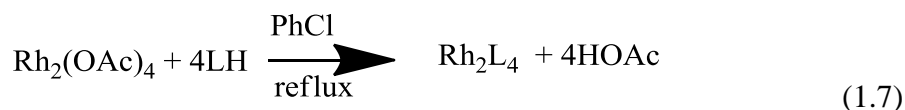


Figure 11: Metal-Ligand interactions in MO of tetrakis(carboxylamidate) dirhodium(II)²⁰

Preparation and Classification of Tetrakis (carboxylamidate) Dirhodium (II)

The key development in the successful synthesis of the tetrakis(carboxylamidate) dirhodium(II) was the methodology for the semi-automated synthesis of tetrakis(carboxylamidate) dirhodium(II).²⁵ Prior to this, the synthesis of $\text{Rh}_2(\text{acam})_4$ involved dissolving $\text{Rh}_2(\text{OAc})_4$ in molten acetamide for several days.²⁴ The harsh reaction conditions precluded the use of many carboxylamides. The semi-automated protocol allows for the use

of much less carboxylamide at lower temperatures and results in higher yields. The advantage of this method is that the preparation of the catalyst involves reacting $\text{Rh}_2(\text{OAc})_4$ with an excess of neutral carboxamidate ligand in boiling chlorobenzene. The reaction is driven to completion by the use of a soxhlet continuous extractor in which the inner thimble is filled with a sodium carbonate/sand mixture which traps the evolved acetic acid.²⁵



The crude product is separated from chlorobenzene via distillation and then purified by flash column chromatography.²⁵

The use of X-ray crystallography to probe structural information of coordination compounds is very useful to many coordination chemists. The difficulty in this area of characterization however lies mainly in how to get the accurate structural data. It is very difficult to follow the chemistry of these important compounds without the accurate structural data. It is therefore very important that accurate structural characterization of these compounds be done in order to study their chemistry.

The goals of this thesis were two-fold; the first one was to synthesize and determine the structural properties of a stable tri-methyl carboxamidate analogue of dirhodium(II) carboxylate. The second goal was to use X-ray crystallography to investigate the structural properties of an iron-oxo complex. Emphasis was on determining the coordinating modes of the various chelating ligands through solving the crystal structures of these complexes as accurately as possible.

In order to achieve these goals, three main objectives were set: 1) to synthesize a novel Rh_2L_4 complex (where L = carboxylamide), 2) to synthesize an axial adduct of a novel

dirhodium carboxamidate complex and determine its crystal structure using X-ray diffraction.; and 3) to determine the crystal and molecular structure of a complicated di-iron complex having a N-Hydroxyethyl-ethylenediaminetriacetic acid (HEDTA) ligand that can have different coordination numbers in the solid and in solution states.

CHAPTER 2

EXPERIMENTAL

Reagents

Chlorobenzene

Chlorobenzene (PhCl) was with dried magnesium sulfate (MgSO_4) for at least 48 hours before use. Both PhCl and MgSO_4 were acquired from Fisher Scientific Inc.

Pyridine

Pyridine (> 99.80 %) was purchased from Fisher Scientific and further dried with MgSO_4 before use.

Benzene

Benzene (> 99.93 %) was purchased from Fisher Scientific and distilled from sodium metal.

$\text{RhCl}_3 \cdot 3 \text{H}_2\text{O}$

$\text{RhCl}_3 \cdot 3 \text{H}_2\text{O}$ salts were used as supplied as precious metal loans from Johnson Matthey.

Synthesis of Starting Materials

Preamble: Most of the starting materials for the synthesis of the Tetrakis (carboxylamidate) Dirhodium(II) complex were synthesized in house.

Sodium Acetate Trihydrate

The procedure used to synthesize sodium acetate trihydrate during this work was a slight modification of the procedure reported by J. Ahmad.²⁶ For the modified procedure, sodium acetate (70g, 0.853 mol) was weighed into a 125 mL Erlenmeyer flask. 40 mL of distilled water was measured and transferred into the Erlenmeyer flask containing the sodium acetate. The contents of the flask were heated at 105 °C until dissolution occurred.

The solution was then allowed to cool for approximately 2 hours for crystals to form. The crystals were filtered by vacuum and dried for 2 days. A 79.27 g (68.27 % yield) of $\text{NaCO}_2\text{CH}_3 \cdot 3\text{H}_2\text{O}$ was recovered.

Tetrakis (carboxylate) Dirhodium (II)

A modification of the procedure reported by Wilkinson *et al.*²⁷ was used in the synthesis of tetrakis(carboxylate) dirhodium during the course of this work. For this work sodium acetate trihydrate (10 g, 0.0735 mol) was weighed out on an analytical balance (APX 153 Denver Inst) and transferred into 500 mL round bottom flask.

$\text{RhCl}_3 \cdot 3\text{H}_2\text{O}$ (5 g, 0.0189 mol) was weighed and transferred into the flask. A 100 mL aliquot of glacial acetic acid (100 g, 1.665 mol) was measured with a graduated cylinder and added to the contents of the round bottom flask. A 100 mL aliquot of absolute Ethanol (78.9 g, 1.713 mol) was measured and added to the mixture in the round bottom flask thus forming a reddish brown color. The contents were set to equilibrate while being stirred by a magnetic stirrer under a nitrogen blanket for 15 minutes. After 15 minutes the contents of the flask were refluxed for about an hour and the reddish brown color changed to emerald green. The emerald green product was allowed to cool. The crude product was isolated by vacuum filtration and further dried by passing nitrogen over it. The crude crystals were washed in

methanol and filtered by vacuum filtration and placed in a vacuum oven at 50 °C and 28" Hg under ambient pressure for an hour. A total mass of 3.378 g (80.62 % yield) of product was recovered from a total of five recrystallizations from methanol.

N-(2, 4, 6-trimethylphenyl) Acetamide

N-(2,4,6-trimethylphenyl) acetamide was synthesized, as published, in collaboration with Landon Zink. A 7.5 mL aliquot (0.0537 mol) of 2,4,6-trimethylaniline was dissolved in 75 mL of toluene. A 1.91 mL aliquot (0.0269 mol) of acetyl chloride was added to the 2,4,6-trimethylaniline solution drop wise whilst stirring the solution. The solution was then refluxed for 2 hours with stirring. The reaction mixture was then allowed to cool and the crude product and the filtrate were separated by vacuum filtration.³¹

The crude product was washed with 100 mL of distilled water. The product, N-(2,4,6-trimethylphenyl) acetamide, was recovered through liquid-liquid extraction by adding 25 mL of diethyl ether to the water solution with stirring. This mixture was then placed in a separatory funnel and the aqueous layer was removed. The organic layer was saved to combine with the filtrate from the reaction mixture.³¹

The filtrate from the reaction mixture was recovered by rotary evaporation and the solid that was recovered was redissolved in 75 mL of diethyl ether. This was then combined with the diethyl ether from above in a separatory funnel. This solution was then washed with 5 mL of distilled water, 12.5 mL of 5% HCl, 12.5 mL of 5% NaOH, and an additional 5 mL of DI water. The diethyl ether was then removed via rotary evaporation. The final product was purified via sublimation.³¹

The final product was purified via sublimation. A mass of 4.48 g of the product was synthesized giving a percent yield of 94.12%. The product was a white crystalline solid that

had a melting point of 219 °C. The synthesized product was characterized by IR, and NMR analysis was used to confirm the identity.³¹

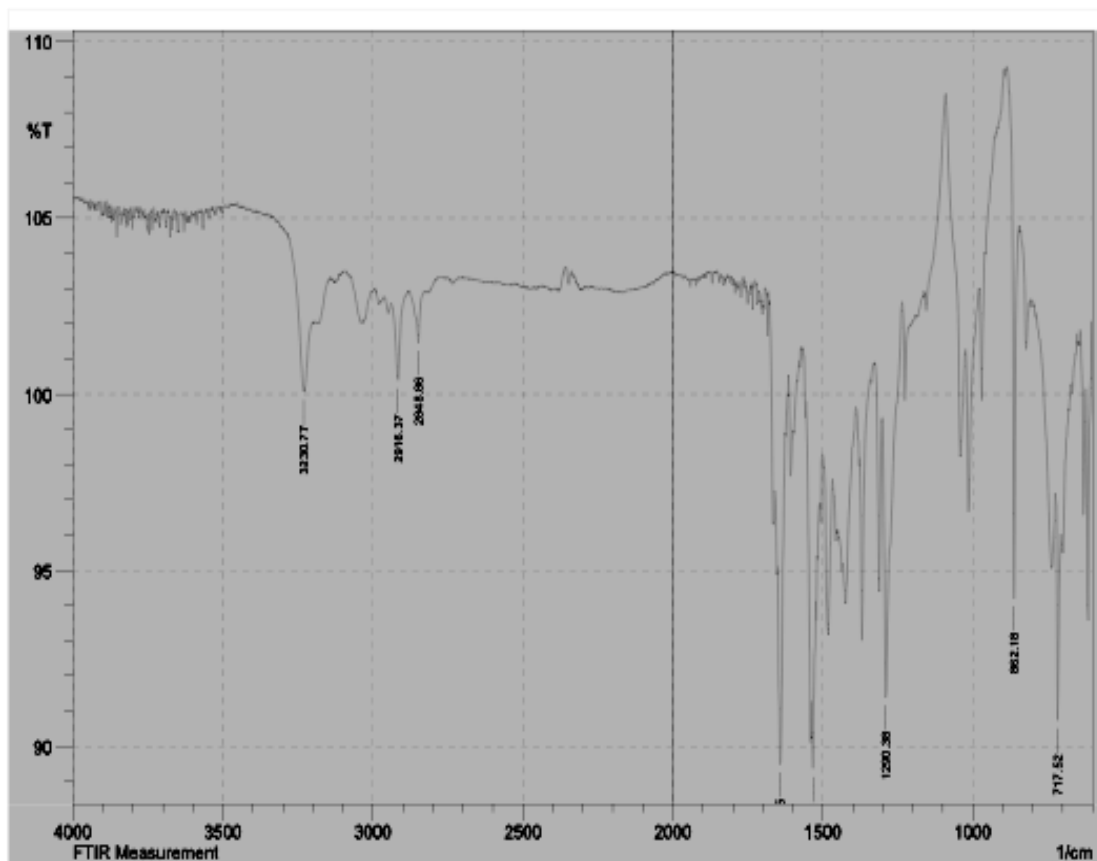
The IR spectrum as shown in figure 12 below gave peaks at 3230 cm⁻¹ for N-H stretch, 2916 cm⁻¹ for C-H aromatic stretch, 1643 cm⁻¹ for C=O stretch, 1533 cm⁻¹ for C=C aromatic stretch, 1290 cm⁻¹ for C-N stretch, and 717 cm⁻¹ for C-H aromatic out of plane bend.

The proton NMR (CDCl₃) spectrum is shown in figure 13a below. The spectrum showed peaks at δ 6.92 ppm (d, 2H), 6.75 ppm (s, 1H), 6.64 ppm (s, 1H), 2.25 ppm (m, 9H), and 1.70 ppm (d, 3H). Figure 13b shows the carbon-13 NMR spectrum of the compound. This gives peaks at δ 168 ppm, 137 ppm, 136 ppm, 135 ppm, 131 ppm, 129 ppm, 23 ppm, 21 ppm, and 18 ppm. These experimental data are very consistent and comparable to the data reported in literature.²⁸

Literature melting point for the product is 218-219 °C.²⁹ The literature values for the proton NMR spectrum showed peaks at δ 6.86 ppm for *p*-hydrogen, 6.70 ppm for N-H, and 2.05 ppm for alkyl hydrogens. The carbon NMR spectrum showed peaks at δ 168 ppm, 137 ppm, 136 ppm, 128 ppm, 23 ppm, 21 ppm, and 18 ppm. The IR spectrum showed peaks at 3236 cm⁻¹ for N-H stretch, 3042 cm⁻¹ for C-H aromatic stretch, 1646 cm⁻¹ for C=O stretch, 1541 cm⁻¹ for C=C aromatic stretch, 1291 cm⁻¹ for C-N stretch, and 717 cm⁻¹ for C-H aromatic out of plane bend.²⁹

This is most notable in the multiplet that was observed from 2.3 to 2.1 ppm. However, Moriyasu *et al.*³⁰ showed that *E*- and *Z*-forms of acetanilides are likely to separate at low temperatures due to the *o*-methyl restricting the carbonyl – nitrogen bond. The carbonyl – nitrogen bond is restricted further when methyl groups at both *o*-positions are added, and hence this causes the *E*- and *Z*-forms to separate at a higher temperature. The NMR data were all taken at -20 °C, which is shown to be sufficiently low to cause splitting of the peaks. Peaks

for proton NMR of the ligand are as follows: alkyl H at 1.70 (3H), aromatic methyl at 2.25 (9H), N-H at 6.64 and 6.75 (1H), and aromatic H at 6.92 (2H).³¹



No.	Peak	Intensity	Corr. Intensity	Base (H)	Base (L)	Area	Corr. Area
1	717.52	90.743	5.986	725.23	705.95	0.477	0.188
2	862.18	94.21	12.43	887.26	844.82	-0.797	0.455
3	1290.38	91.403	8.511	1301.95	1236.37	0.738	1.01
4	1533.41	89.361	1.66	1535.34	1523.76	0.44	0.034
5	1643.35	89.496	6.772	1651.07	1625.99	0.761	0.427
6	2848.86	101.469	1.45	2879.72	2829.57	-0.525	0.102
7	2916.37	100.393	2.313	2939.52	2879.72	-0.538	0.165
8	3230.77	100.072	2.927	3288.63	3196.05	-0.921	0.388

Figure 12: IR of N-(2,4,6-trimethylphenyl) Acetamide

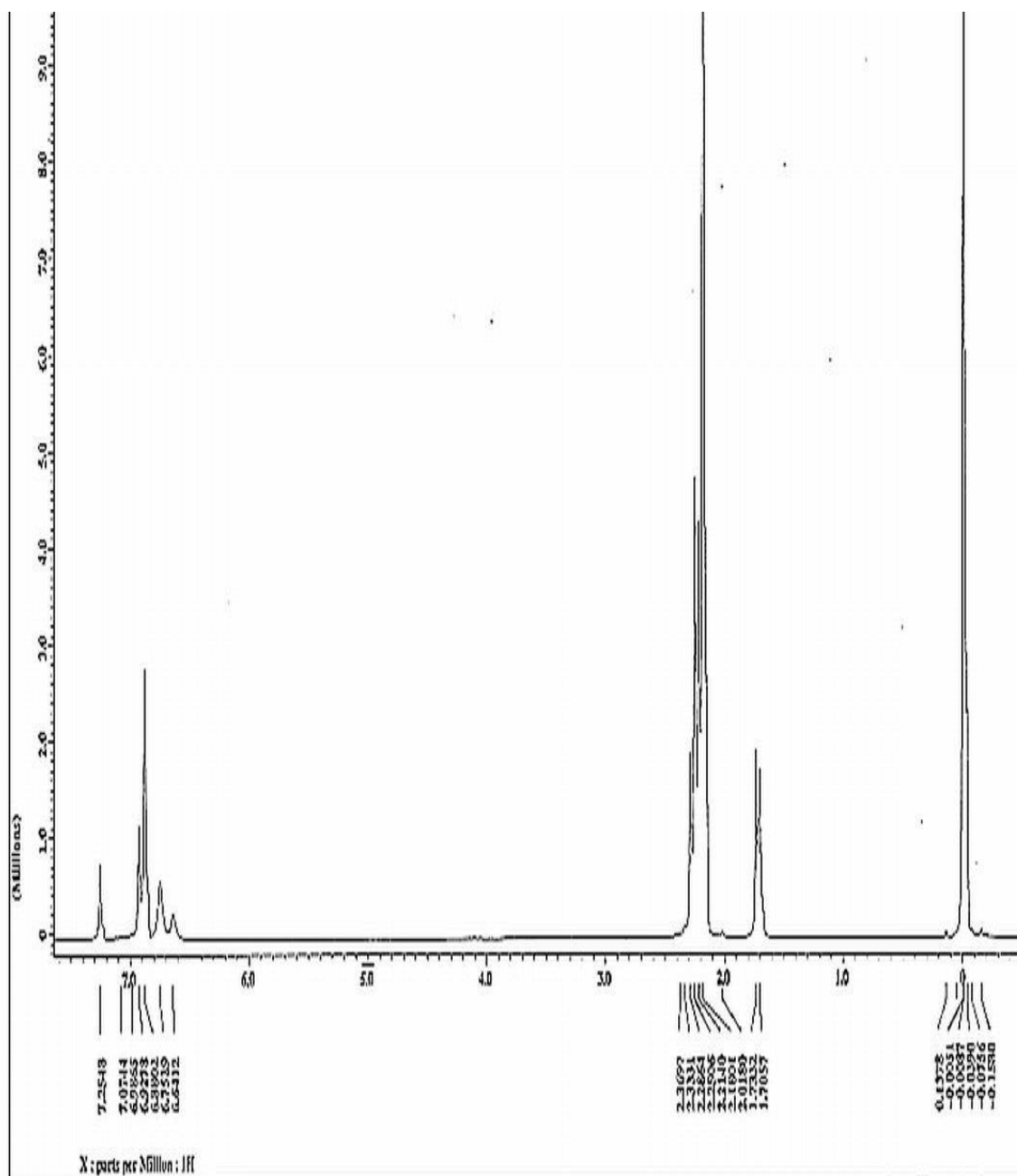


Figure 13a: ^1H NMR spectrum of 2,4,6-trimethylphenyl acetamide

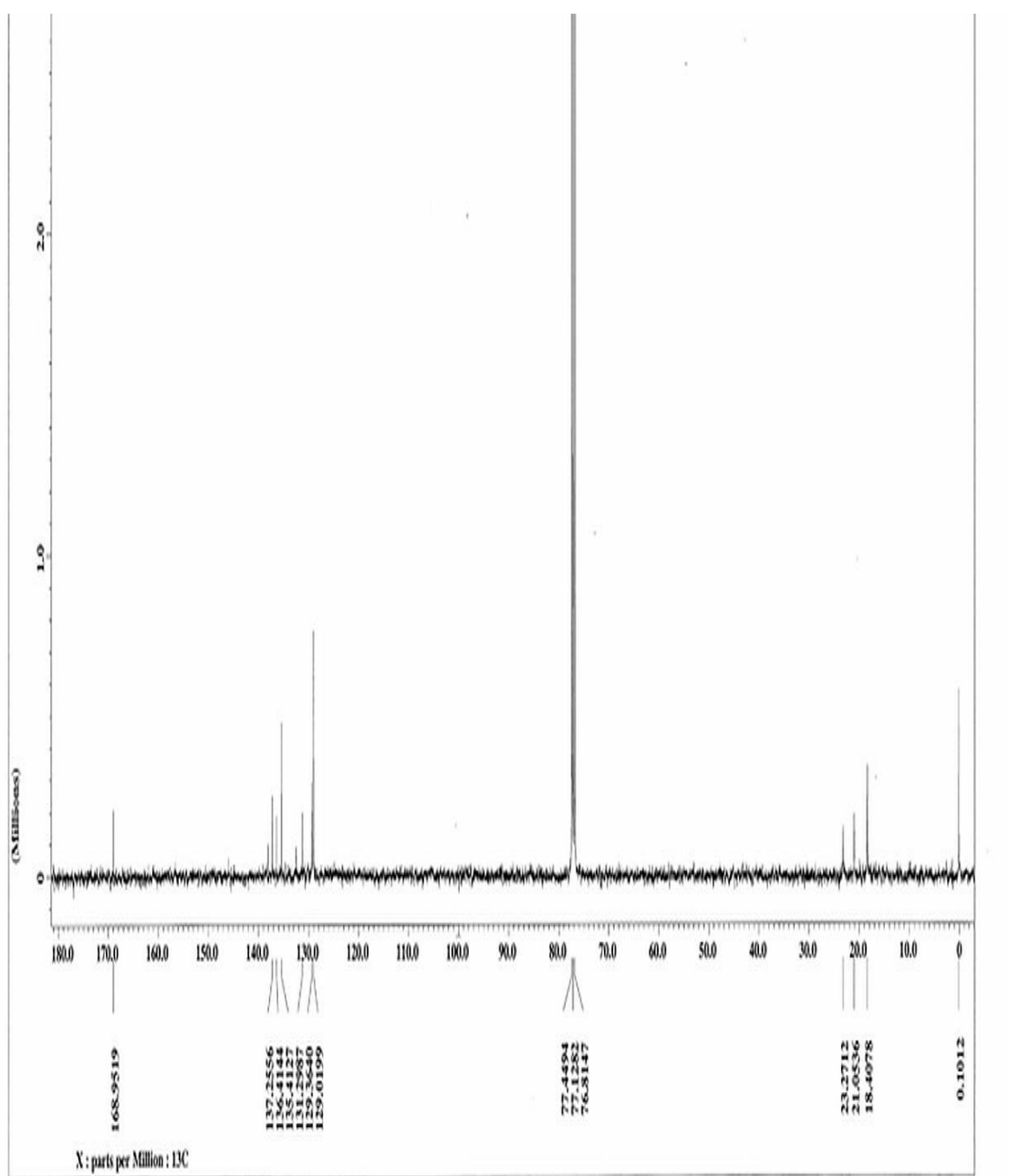


Figure13b: ^{13}C NMR spectrum of 2,4,6-trimethylphenyl acetamide

Tetrakis [μ -(N-{2, 4,6-trimethylphenyl} Acetamidato- κ N: κ O)] Dirhodium (II), [$\text{Rh}_2(\text{N-}\{2,4,6\text{-CH}_3\}\text{C}_6\text{H}_2\text{COCH}_3)_4$]

All glassware needed for the synthesis was washed with glassware cleaning detergent and rinsed with tap water and distilled water. They were further rinsed with acetone. The glassware was oven-dried at a temperature of 120°C for 24 hours.

A mixture of sand and sodium carbonate was prepared (ratio: 50:50). The sand was washed with chlorobenzene and dried prior to the preparation of the mixture. Ceramic thimbles were cleaned with acetone and dried. Then they were filled with the sand/sodium carbonate mixture about two-thirds full. (The mixture was further topped with sand to pack it firmly). The packed thimbles were oven dried for 24 hours. A mass of 5 g (0.026 mol) of N-2,4,6-trimethylphenyl acetamide (ligand) was weighed out and mixed with 0.5 g (0.001 mol) of $\text{Rh}_2(\text{OAc})_4$ in a 250mL round bottom flask. A 200 mL aliquot of PhCl was used as reaction solvent.

The reaction was driven to completion by use of a Soxhlet continuous extractor in which the inner ceramic thimble filled with the mixture of sodium carbonate and sand trapped the acetic acid produced during the reaction.



The thimbles were replaced every 24 hours and more chlorobenzene was added as necessary to account for evaporation. The reaction was done under nitrogen to minimize the decomposition of Rh_2L_4 .

After 7 days, thin layer chromatography was performed on the product mixture to determine if the desired rhodium containing products had been synthesized, and the reaction

had come to completion. This was done by spotting the ligand, reaction mixture, and Rh_2OAc_4 separately on one thin layer chromatography (TLC) plate. The TLC plate was developed in a solvent chamber containing 30% ethyl acetate (EtOAc) and 70% hexanes.

The disappearance of the Rh_2OAc_4 spot from the reaction mixture and the appearance of colored spots indicated the completion of the reaction. After it was observed that the reaction had come to a completion, the chlorobenzene used for the Soxhlet extraction was removed by vacuum distillation. The resulting product mixture was further dried under vacuum. Flash column chromatography was performed on the product mixture to separate and isolate the rhodium containing products.

Flash Column Chromatography

Column chromatography of this product mixture was facilitated by the fact that Rh_2L_4 complexes are colored. Fractions of the same color and refractive index (R_f) were also called bands.

A column of dimensions 5 cm diameter by a height of 30 cm was used. The column was packed with glass wool first then with some sand. After this, a slurry of flash silica gel and 100 % hexane was prepared and added to the column. The packing was done by applying some pressure from a N_2 cylinder. Some more sand was added on top of the silica gel to make it compact. The column was eluted with hexane to ensure that there were no air bubbles in the packed column.

The crude tetrakis[μ -(N-{2, 4,6-trimethylphenyl} acetamidato- κN : κO)] dirhodium(II), dissolved in 15 mL PhCl, was added and about 85 mL of 100% hexane was used to elute it. The purpose was to remove any residual chlorobenzene (PhCl). Fractions 1-4 were eluted and thin layer chromatography (TLC) was performed on them against the

reaction mixture. A 30% ethyl acetate/hexane solvent system was used to develop the TLC plate. They were shown to have PhCl only.

About 85 mL of 10% Ethyl acetate/hexane was prepared and used to elute the column. Fractions 5-10 showed no spots via TLC. This showed that all the chlorobenzene had been removed. The elution continued with the 10% Ethyl Acetate/hexane mixture and fractions 11-16 were collected. These were of a light blue-green color and had the same R_f as the spot with the largest R_f in the reaction mixture when analyzed by TLC. The fractions were combined and the solvent was removed by rotary evaporation.

About 500 mL of 20% Ethyl acetate/hexane was prepared and used to elute the column. Fractions 17-20 showed no spots by TLC analysis. About 500 mL of 30% Ethyl acetate/hexane was prepared and used to elute the column. Fractions 21-35 collected were blue in color and had the same R_f as the second colored band of the reaction mixture. The fractions were combined and the solvent was removed by rotary evaporation.

Fractions 36 to 37 showed a light blue-green color. They had the same R_f as fractions 21-35. The fractions were combined and the solvent was removed by rotary evaporation. No colored bands were recovered when fractions 38 to 45 were collected. The solvent system was changed to 40% EtOAc in hexanes. Fractions 46 to 50 showed no spots when analyzed by TLC.

Upon elution of the column with a 500 mL solvent of 50% ethyl acetate/hexane, fractions 51-57 showed a deep blue color and when spotted against the reaction mixture showed the third colored band. The fractions were combined and the solvent was removed by rotary evaporation and then stored for characterization. Elution with 60% to 100% solvent of ethyl acetate yielded no spots when spotted against the reaction mixture.

A 100% solvent of methanol was used to flush the column and to remove any unreacted or decomposed $\text{Rh}_2(\text{OAc})_4$. The column was unpacked and properly cleaned.

Characterization of Tetrakis (trimethylphenylacetamidate) Dirhodium(II)

Nuclear Magnetic Resonance (NMR) Analysis

About 25 milligrams of each of the various fractions of the tetrakis (trimethyl phenylacetamidate) dirhodium(II) complex collected from flash column chromatography were dissolved in deuterated chloroform (CDCl_3) containing 1% tetramethylsilane (TMS), and identified using nuclear magnetic resonance spectroscopy (NMR). The (CDCl_3) was obtained from ACROS. A 400 MHz JEOL NMR instrument was used for all NMR spectroscopic analyses.

Both ^1H and ^{13}C NMR analyses gave spectra with peaks of chemical shifts characteristic of three fractions obtained from the column chromatography, and the spectra are shown in figures 14a, 15a, and 16a for the proton NMR, and figures 14b, 15b, and 16b for the carbon-13 NMR respectively.

The proton NMR (CDCl_3) spectra for the fractions showed chemical shifts ranging from δ 6.86 ppm - 6.83 ppm (d, 2H), 2.37 ppm – 2.21 ppm (m, 9H), and 1.72 ppm – 1.68 ppm (d, 3H), and the carbon NMR showed peaks at δ 179 ppm, 144 ppm, 134 ppm, 133 ppm, 129 ppm, 129 ppm, 21 ppm, 20 ppm, and 19 ppm.

The proton NMR for the first deep-green colored fraction is shown in figure 14a below, and in the spectrum, the chemical shift at 6.86 ppm is characteristic of the two aromatic protons on each of the equatorial mesityl phenyl rings of the dirhodium complex. The chemical shifts at 2.37- 2.09 ppm are indicative of protons on the methyl groups of the

phenyl rings, with the chemical shifts at 1.89-1.34 ppm showing the methyl protons on the acetamide ring.

The spectrum in figure 14b shows the carbon-13 NMR for the first fraction. The chemical shifts at 19-21 ppm indicate the methyl carbon on the acetamide ring, while the peaks at 129-135 ppm show aromatic carbons. The peak at 144 ppm is indicative of the aromatic carbon bearing the nitrogen from the acetamide ring.

The chemical shifts from figures 15a, 15b, 16a, and 16b have similar values as those discussed above because the fractions are isomers of the same compound. From the NMR spectra, the preliminary assignments were that the first fraction, (deep green color) was the 2,2-*trans* isomer, the second fraction, (blue color) was the 2,2-*cis* isomer, and the third fraction, (light green) was the 3,1 isomer. FTIR spectroscopic analyses of these fractions were inconclusive.

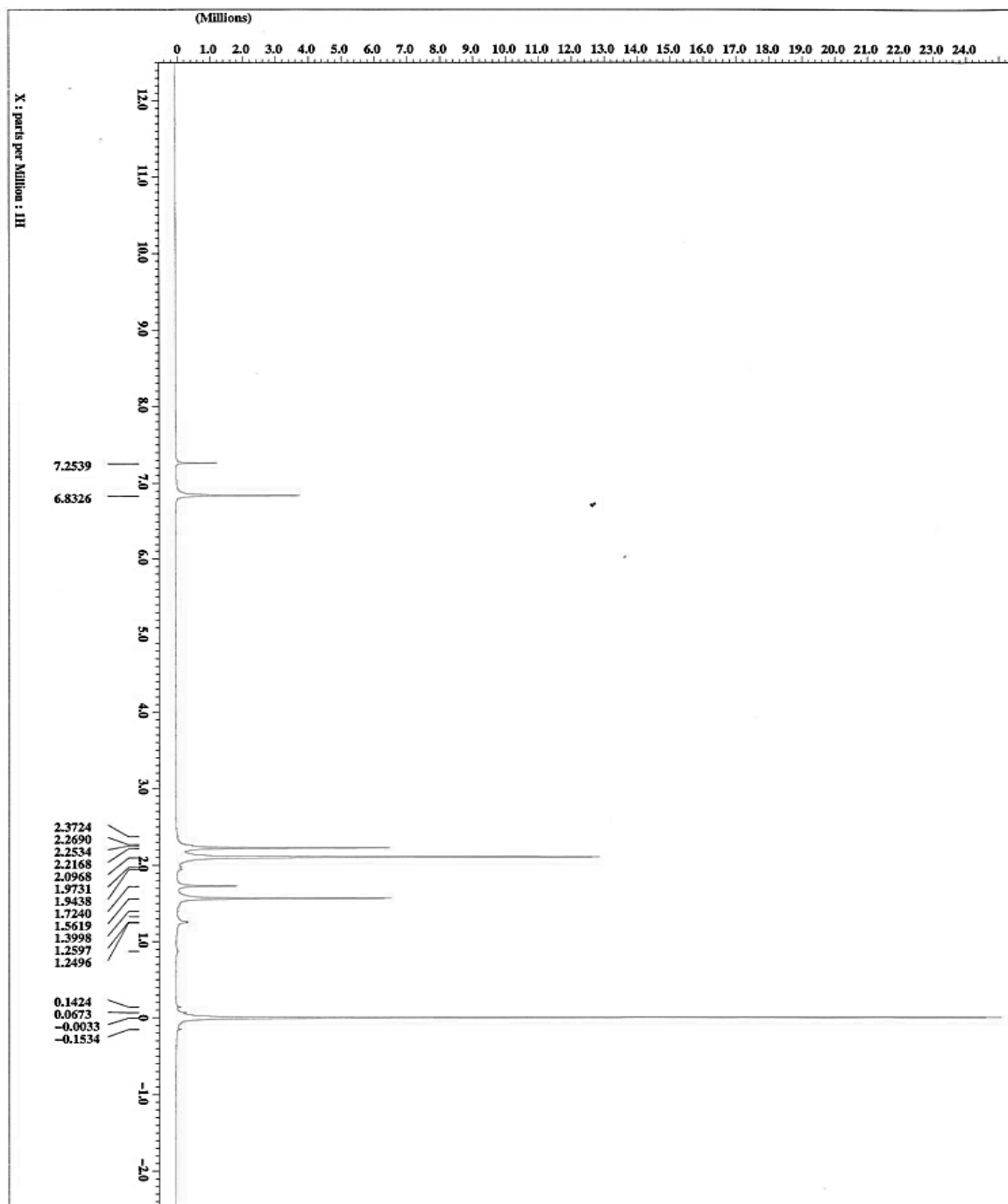


Figure 14a: ^1H NMR of the 2,2-*trans* isomer of $[\text{Rh}_2(\text{N}-\{2,4,6\text{-CH}_3\}\text{C}_6\text{H}_2)\text{COCH}_3)_4]$

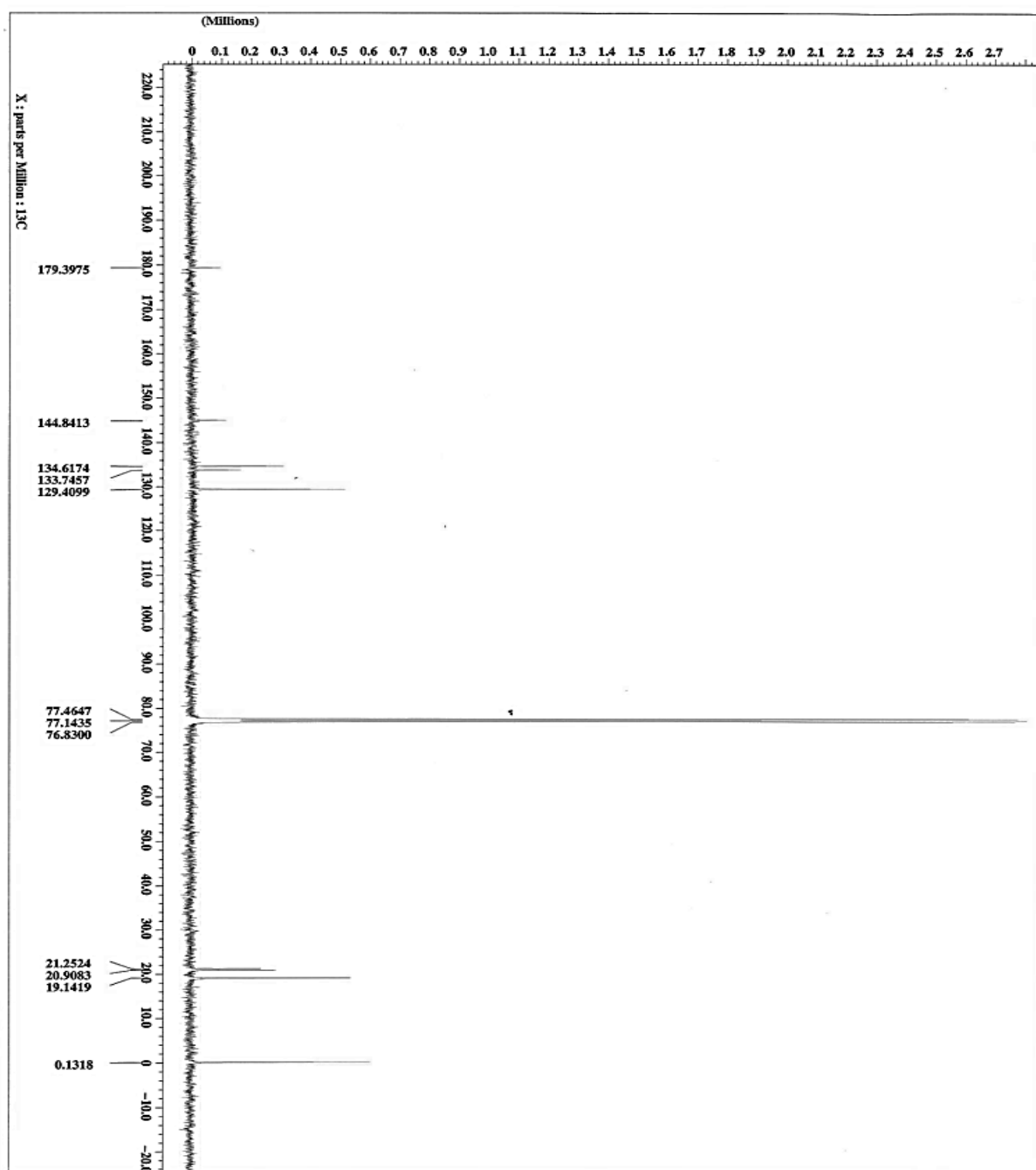


Figure 14b: ^{13}C NMR of the 2,2-*trans* isomer of $[\text{Rh}_2(\text{N}-\{2,4,6\text{-CH}_3\}\text{C}_6\text{H}_2)\text{COCH}_3)_4]$

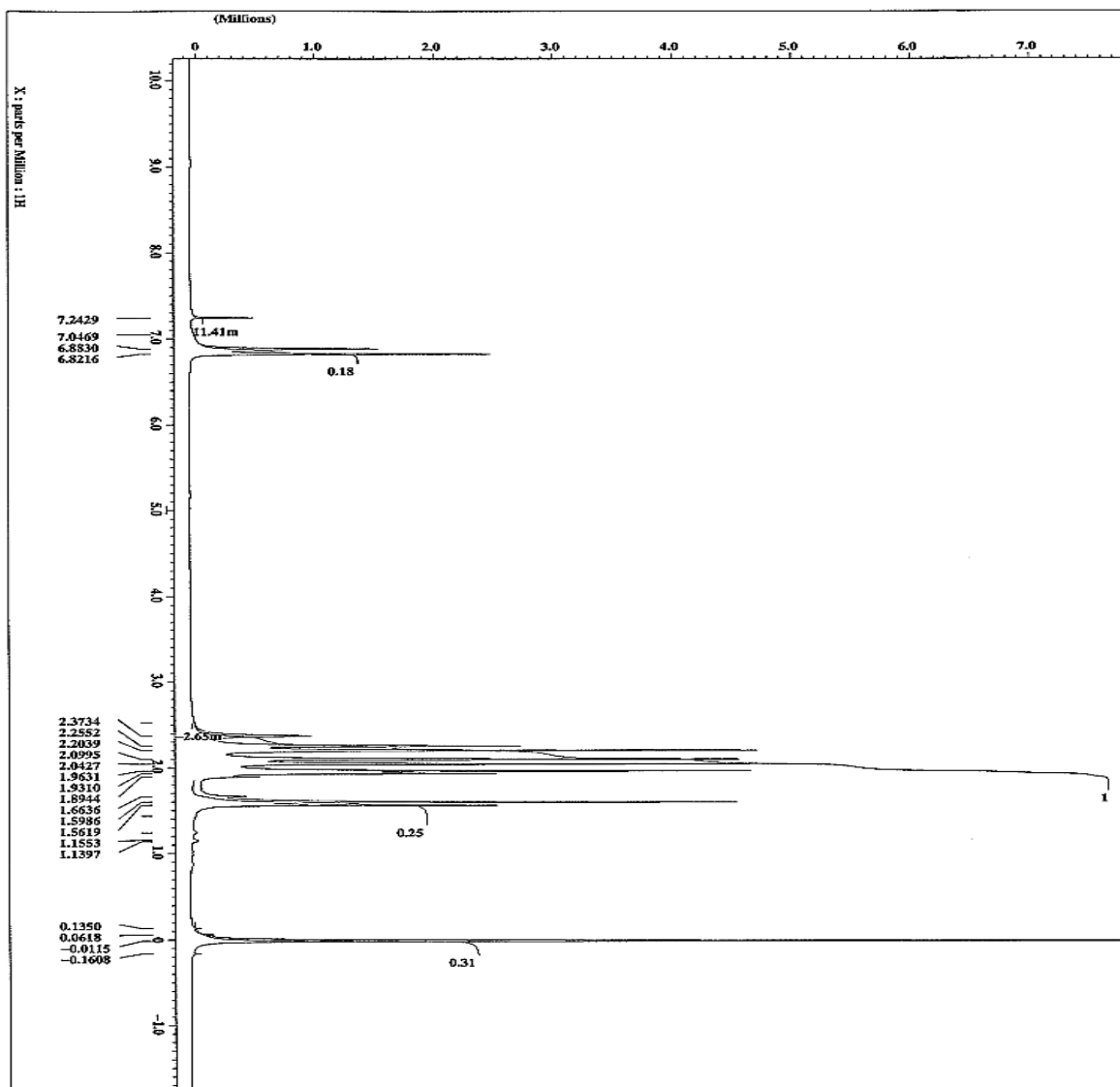


Figure 15a: ^1H NMR of the 2,2-*cis* isomer of $[\text{Rh}_2(\text{N}-\{2,4,6\text{-CH}_3\}\text{C}_6\text{H}_2)\text{COCH}_3)_4]$

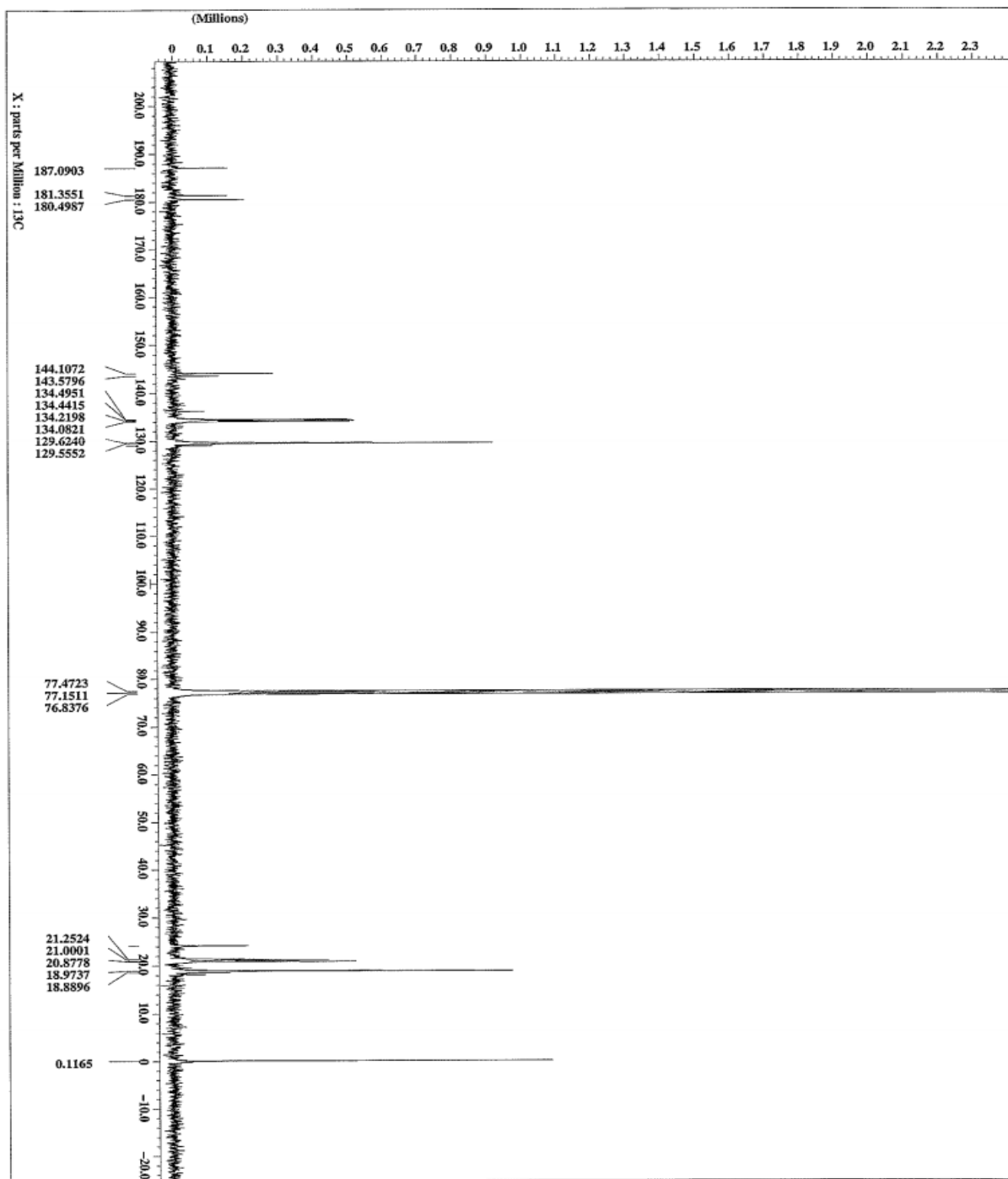


Figure 15b: ^{13}C NMR of the 2,2-*cis* isomer of $[\text{Rh}_2(\text{N}-\{2,4,6\text{-CH}_3\}\text{C}_6\text{H}_2)\text{COCH}_3)_4]$

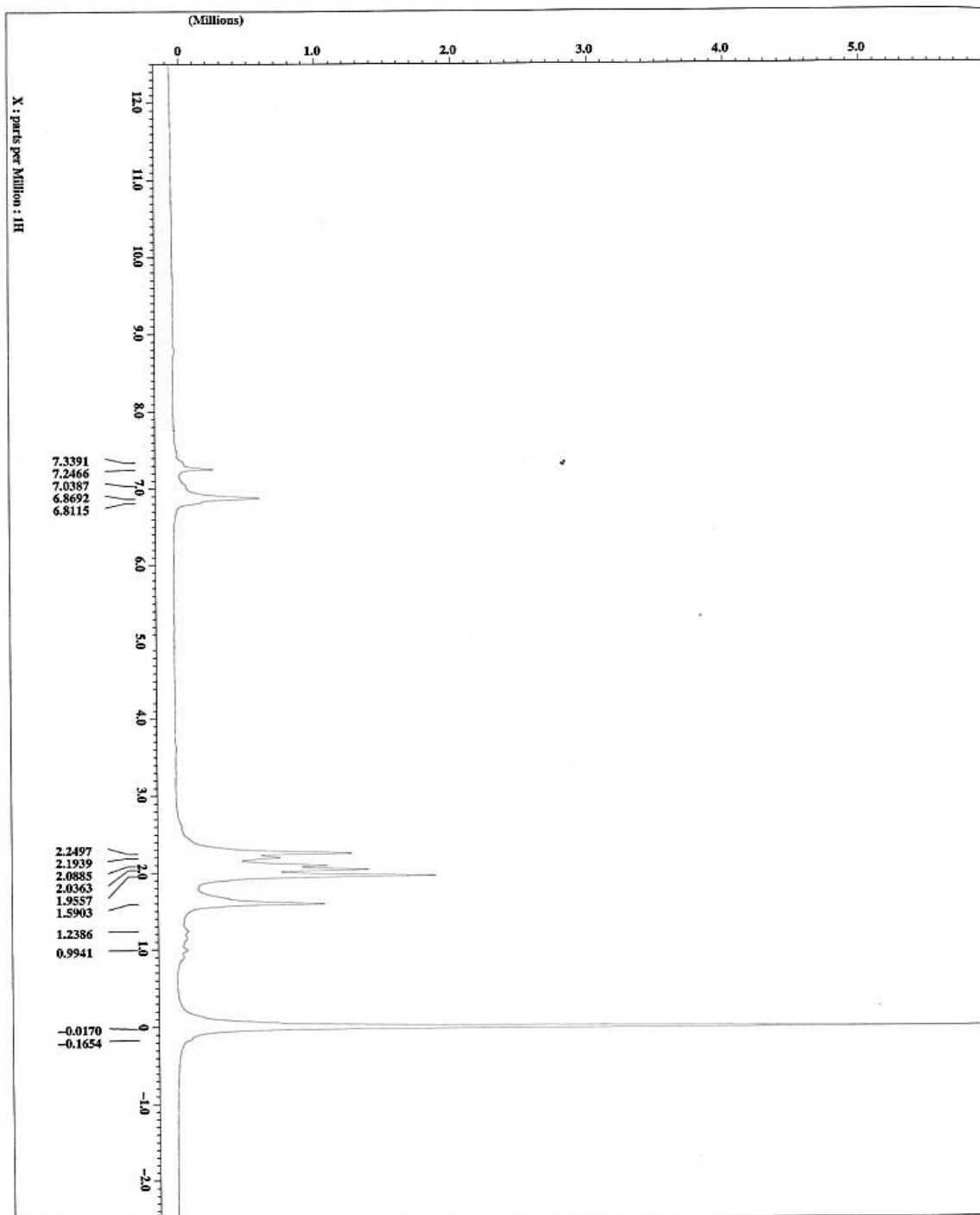


Figure 16a: ¹H NMR of the 3,1 isomer of [Rh₂(N-{2,4,6-CH₃}C₆H₂)COCH₃)₄]

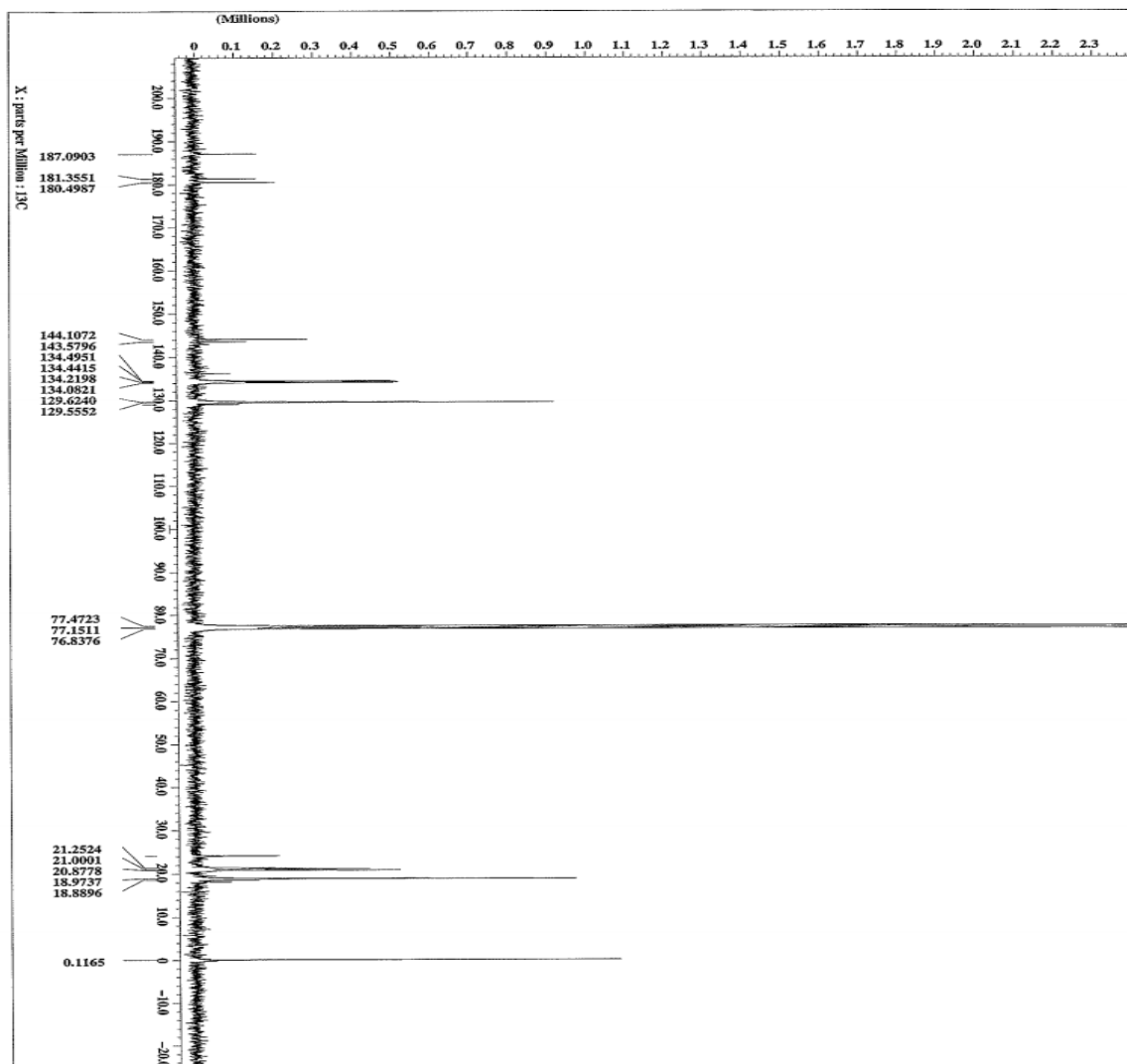


Figure 16b: ^{13}C NMR of the 3,1 isomer of $[\text{Rh}_2(\text{N}-\{2,4,6\text{-CH}_3\}\text{C}_6\text{H}_2)\text{COCH}_3)_4]$

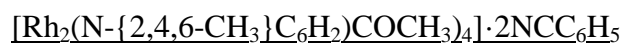
Synthesis of $[\text{Rh}_2(\text{N}-\{2,4,6\text{-CH}_3\}\text{C}_6\text{H}_2)\text{COCH}_3)_4]\cdot 2\text{NCC}_6\text{H}_5$ by Vapor Diffusion Method

Approximately 10 mg of the first fraction from the column chromatography (deep green-colored) (2,2-*trans*-tetrakis[μ -(N-{2,4,6-trimethylphenyl})acetamidato- $\kappa\text{N}:\kappa\text{O}$]]dirhodium)(II) was dissolved in 5 mL of dichloromethane forming a green solution. Approximately 2.29 μL of benzonitrile was added to the solution via a gas tight syringe causing the color to become blue. This change in color is indicative of coordination of the benzonitrile ligand at the axial site of the rhodium atom. This coordination is possibly due to the $d\pi$ electrons that the rhodium atom has, that enables $d\pi$ - $p\pi^*$ type bonding between the rhodium atom and the nitrile. The bis benzonitrile adduct was likely formed through this type of bonding mechanism.

Vapor diffusion was carried out by transferring about 1 mL $[\text{Rh}_2(\text{N}-\{2,4,6\text{-CH}_3\}\text{C}_6\text{H}_2)\text{COCH}_3)_4]\cdot 2\text{NCC}_6\text{H}_5$ into a small vial. The vial was then placed into a larger vial that contained about 2 mL of acetonitrile. The outer vial was then capped tightly. During crystallization vapor from the solvent of the outer vial diffused into the solution in the inner vial caused and crystal formation. Care was taken to prevent the vertical surfaces of the inner vial from touching the outer vial to keep the outer solvent from rising by capillary action and filling the inner vial. The crystals of the bis benzonitrile adduct were obtained after a week.

X-ray Crystallographic Studies

All data were collected on a Rigaku Mercury 375R/M CCD XtaLAB mini diffractometer (manufactured in May 2011). The X-ray source was Molybdenum $K\alpha$ radiation, $\lambda = 0.71075 \text{ \AA}$. The crystal-to-detector distance was 50.00 mm. The relevant and detailed crystallographic data on all compounds can be found in appendix A and B respectively.



Data Collection

A blue prism crystal of $[\text{Rh}_2(\text{N}-\{2,4,6\text{-CH}_3\}\text{C}_6\text{H}_2)\text{COCH}_3)_4] \cdot 2\text{NCC}_6\text{H}_5$ having approximate dimensions of 0.18 x 0.13 x 0.07 mm was mounted on a Mitogen loop by using a mounting pin and securing the crystal onto the goniometer.

Cell constants and an orientation matrix for data collection corresponded to a primitive tetragonal cell (Laue class: 4/mmm) with dimensions: $a = 10.9928(19) \text{ \AA}$, $c = 21.4549(19) \text{ \AA}$, $V = 2592.6(7) \text{ \AA}^3$. For $Z = 2$ and F.W. = 1117.01 g/mol, the calculated density was 1.431 g/cm^3 . The reflection conditions of: $h00: h = 2n$; $hhl: l = 2n$ uniquely determined the space group to be: P-421c (#114).

The data were collected at a temperature of $25 \pm 1^\circ\text{C}$ to a maximum 2θ value of 55.0° . A total of 1080 oscillation images were collected. A sweep of data was done using ω scans from -60.0 to 120.0° in 1.0° step, at $\chi=54.0^\circ$ and $\phi = 0.0^\circ$. The exposure rate was 16.0 sec./° . The detector swing angle was 29.50° . A second sweep was performed using ω scans from -60.0 to 120.0° in 1.0° step, at $\chi=54.0^\circ$ and $\phi = 120.0^\circ$. The exposure rate was 16.0 sec./° . The detector swing angle was 29.50° .

Another sweep was performed using ω scans from -60.0 to 120.0° in 1.0° step, at $\chi=54.0^\circ$ and $\phi = 240.0^\circ$. The exposure rate was 16.0 sec./° . The detector swing angle was 29.50° . Another sweep was performed using ω scans from -60.0 to 120.0° in 1.0° step, at $\chi=54.0^\circ$ and $\phi= 240.0^\circ$. The exposure rate was 16.0 sec./° . The detector swing angle was 29.50° . Another sweep was performed using ω scans from -60.0 to 120.0° in 1.0° step, at $\chi=54.0^\circ$ and $\phi = 120.0^\circ$. The exposure rate was 16.0 sec./° . The detector swing angle was 29.50° . Another sweep was performed using ω scans from -60.0 to 120.0° in 1.0° step, at

$\chi=54.0^\circ$ and $\varphi = 0.0^\circ$. The exposure rate was 16.0 sec./ $^\circ$. The detector swing angle was 29.50° .

Data Reduction

Of the 48 863 reflections that were collected, 2970 were unique ($R_{int} = 0.1045$); equivalent reflections were merged. Data were collected and processed using CrystalClear (Rigaku).³² The linear absorption coefficient, μ , for Mo-K α radiation is 6.879 cm^{-1} . An empirical absorption correction was applied that resulted in transmission factors ranging from 0.618 to 0.953. The data were corrected for Lorentz and polarization effects.

Structure Solution and Refinement

The structure was solved by direct methods³² and expanded using Fourier techniques. The non-hydrogen atoms were refined anisotropically. Hydrogen atoms were included but not refined. The final cycle of full-matrix least-squares refinement³² on F^2 was based on 2969 observed reflections and 165 variable parameters and converged (largest parameter shift was 0.00 times its esd) with unweighted and weighted agreement factors of:

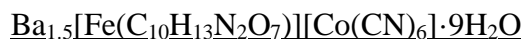
$$R1 = \Sigma ||F_o| - |F_c|| / \Sigma |F_o| = 0.0360 \quad (2.2)$$

$$wR2 = [\Sigma (w (F_o^2 - F_c^2)^2) / \Sigma w (F_o^2)^2]^{1/2} = 0.0744 \quad (2.3)$$

The standard deviation of an observation of unit weight³³ was 1.04. Unit weights were used. The maximum and minimum peaks on the final difference Fourier map corresponded to 0.64 and $-0.70 \text{ e}^-/\text{\AA}^3$, respectively. The absolute structure was deduced based on Flack parameter, 0.01(7), using 1291 Friedel pairs.³⁴

Neutral atom scattering factors were taken from Cromer and Waber³⁵. Anomalous dispersion effects were included in F_{calc} ³⁶; the values for $\Delta f'$ and $\Delta f''$ were those of Creagh

and McAuley³⁷. The values for the mass attenuation coefficients are those of Creagh and Hubbell³⁸. All calculations were performed using the CrystalStructure³⁹ crystallographic software package except for refinement, that was performed using SHELXL-97.⁴⁰



Data Collection

A yellow prism crystal of $\text{C}_{16}\text{H}_{31}\text{Ba}_{1.50}\text{CoFeN}_8\text{O}_{16}$ having approximate dimensions of 0.260 x 0.250 x 0.060 mm was mounted on a Mitogen loop by using a mounting pin and securing the crystal onto the goniometer.

The data were collected at a temperature of $25 \pm 1^\circ\text{C}$ to a maximum 2θ value of 55.0° . A total of 540 oscillation images were collected. A sweep of data was done using ω oscillations from -60.0 to 120.0° in 1.0° steps. The exposure rate was 30.0 sec./° . The detector swing angle was 30.00° . A second sweep was performed using ω oscillations from -60.0 to 120.0° in 1.0° steps. The exposure rate was 30.0 sec./° . The detector swing angle was 30.00° .

Another sweep was performed using ω oscillations from -60.0 to 120.0° in 1.0° steps. The exposure rate was 30.0 sec./° . The detector swing angle was 30.00° . Another sweep was performed using ω oscillations from -60.0 to 120.0° in 1.0° steps. The exposure rate was 30.0 sec./° . The detector swing angle was 30.00° . Another sweep was performed using ω oscillations from -60.0 to 120.0° in 1.0° steps. The exposure rate was 30.0 sec./° . The detector swing angle was 30.00° . Another sweep was performed using ω oscillations from -60.0 to 120.0° in 1.0° steps. The exposure rate was 30.0 sec./° . The detector swing angle was 30.00° .

Data Reduction

Of the 33 318 reflections that were collected, 14 487 were unique ($R_{\text{int}} = 0.0372$); equivalent reflections were merged. Data were collected and processed using CrystalClear (Rigaku). The linear absorption coefficient, μ , for Mo-K α radiation is 28.878 cm⁻¹. An empirical absorption correction was applied that resulted in transmission factors ranging from 0.542 to 0.841. The data were corrected for Lorentz and polarization effects.

Structure Solution and Refinement

The structure was solved by direct methods³² and expanded using Fourier techniques. The non-hydrogen atoms were refined anisotropically. Hydrogen atoms were refined using the riding model. The final cycle of full-matrix least-squares refinement³³ on F^2 was based on 14477 observed reflections and 770 variable parameters and converged (largest parameter shift was 0.00 times its esd) with unweighted and weighted agreement factors of:

$$R1 = \Sigma ||F_o| - |F_c|| / \Sigma |F_o| = 0.0438 \quad (2.4)$$

$$wR2 = [\Sigma (w (F_o^2 - F_c^2)^2) / \Sigma w(F_o^2)^2]^{1/2} = 0.1308 \quad (2.5)$$

The standard deviation of an observation of unit weight³⁴ was 0.97. Unit weights were used. The maximum and minimum peaks on the final difference Fourier map corresponded to 2.09 and -1.63 e⁻/Å³, respectively.

Neutral atom scattering factors were taken from Cromer and Waber³⁵. Anomalous dispersion effects were included in F_{calc} ³⁶; the values for $\Delta f'$ and $\Delta f''$ were those of Creagh and McAuley³⁷. The values for the mass attenuation coefficients are those of Creagh and Hubbell³⁸. All calculations were performed using the CrystalStructure³⁹ crystallographic software package except for refinement that was performed using SHELXL-97⁴⁰.

CHAPTER 3

RESULTS AND DISCUSSION

Preamble

During this project the novel isomers of Tetrakis[μ -(N-{2,4,6-trimethylphenyl} acetamidato- κ N: κ O)] dirhodium(II) were synthesized based on a method published by Eagle *et al.*³³ Various analytical methods were used to characterize and confirm the identity and purity of the starting ligands and the compounds. NMR was used to confirm the type, orientation, and environment of hydrogen and carbons in the compounds. X-ray crystallography was used to determine the crystal structure of benzonitrile axial adducts of one of the isomers.

As part of the research conducted, the crystal structure of a complicated di-iron cobalt(III) complex was determined using X-ray crystallography. The results are reported in this chapter.

N-(2,4,6-trimethylphenyl) Acetamide

N-(2,4,6-trimethylphenyl) acetamide was synthesized, as published, in collaboration with Landon Zink as discussed in Chapter 2.³¹

[Rh₂(N-{2,4,6-CH₃}C₆H₂)COCH₃)₄].2NCC₆H₅

The solving of the crystal structure of the above 2,2-*trans* isomer presented several crystallographic challenges.

Some of these challenges were (1) determining the difference between nitrogen and oxygen and, (2) determining the special atomic positions for various atoms because only a fourth of the structure appeared in the asymmetric unit cell. The other three-quarters parts were generated by symmetry. The need to assign special atomic positions and the percentage

occupancy assigned to that atom before refinement became important to the successful determination of the structure.

These challenges were resolved by assigning the Rh1, N1, C1, C2, and C5, atoms special anisotropic displacement parameters (ADP) of 10.25 each and setting them to 25% occupancy. After the percentage occupancies were set, the anisotropic displacement parameters were allowed to refine.

The Oak Ridge thermal ellipsoid plot (ORTEP) of the 2,2-*trans* isomer of $[\text{Rh}_2(\text{N}\{-2,4,6\text{-CH}_3\}\text{C}_6\text{H}_2)\text{COCH}_3)_4]\cdot 2\text{NCC}_6\text{H}_5$ is shown in figure 17. In the ORTEP, the 2,2-*trans* isomer has tetragonal symmetry (space group = P-42₁c). It contains a dinuclear Rh complex of four bar symmetry. There is a Rh—Rh unit and two benzonitrile ligands located in special positions along the twofold axis passing through the fourfold. Four symmetry equivalent mesitylacetamidato ligands bridge the Rh —Rh unit. Thus, each rhodium has an approximately octahedral coordination by one Rh (Rh—Rh = 2.4289 (6) Å), that is comparable to the range of bond lengths observed in tetrakis(carboxylamidate) dirhodium(II).

Two acetamidato O atoms *trans* to each other (Rh—O = 2.044 (3) Å), two acetamidato N atoms *trans* to each other (Rh—N = 2.090 (4) Å), and a benzonitrile N atom *trans* to Rh (Rh—N = 2.222 (3) Å). The structure is held together by weak van der Waals forces. It is the mesitylacetamidato analogue of the previously published phenylacetamidato compound, $\text{Rh}_2[\text{N}(\text{C}_6\text{H}_5)\text{C}(\text{O})\text{CH}_3]_4\cdot 2\text{NCC}_6\text{H}_5$,⁴¹ both having the 2,2-*trans* stereochemistry in the complex-core, that is one out of four possible isomers shown in figure 8.

The highest molecular symmetry that these two complexes can adopt is fourfold symmetry (-42m) with two mirror planes through the carboxylamidate chelate ring pairs and twofold axes in bisecting positions. While in the crystal structure of

$\text{Rh}_2[\text{N}(\text{C}_6\text{H}_5)\text{C}(\text{O})\text{CH}_3]_4 \cdot 2\text{NCC}_6\text{H}_5$, the Rh complex has point symmetry 1 and adopts a considerably twisted conformation in the core and one benzonitrile ligand (significantly bent off from the Rh—Rh axis), the complex of this structure is more regular and has fourfold symmetry, not far from 4_2m if the axial benzonitrile ligands are disregarded. This difference in conformation is probably due to steric considerations as a result of the bulky nature of the mesitylacetamidato equatorial ligands in this novel 2,2-*trans* isomer as compared to the previously published $\text{Rh}_2[\text{N}(\text{C}_6\text{H}_5)\text{COCH}_3]_4 \cdot 2\text{NCC}_6\text{H}_5$ analogue. This explanation may be more plausible because of the symmetry imposed on the structure by such a conformation.

In $\text{Rh}_2[\text{N}(\text{C}_6\text{H}_5)\text{COCH}_3]_4 \cdot 2\text{NCC}_6\text{H}_5$, the four N—Rh—Rh—O dihedral angles (where N and O are atoms of the bridging carboxylamidate ligands) range from 9.03 to 11.89°. Due to symmetry constraints in this novel 2,2-*trans* isomer, the same dihedral angle is only 1.12°. The inclination angle of the mesityl phenyl rings to the Rh—Rh-bond in the novel 2,2-*trans* isomer is about 26°; it is 34° in the phenylacetamidato complex.

This makes the space between adjacent mesityl rings narrow and forces the benzonitrile phenyl rings into a more inclined orientation than in $\text{Rh}_2[\text{N}(\text{C}_6\text{H}_5)\text{COCH}_3]_4 \cdot 2\text{NCC}_6\text{H}_5$, where they are not far from perpendicular to the carboxylamidate phenyl rings.

Packing diagrams of the structure as shown in figures 18 and 19 reveal that the molecules are held together by weak van der Waals forces, which is not surprising in view of the 16 CH_3 groups on the outer surface of the Rh complex.

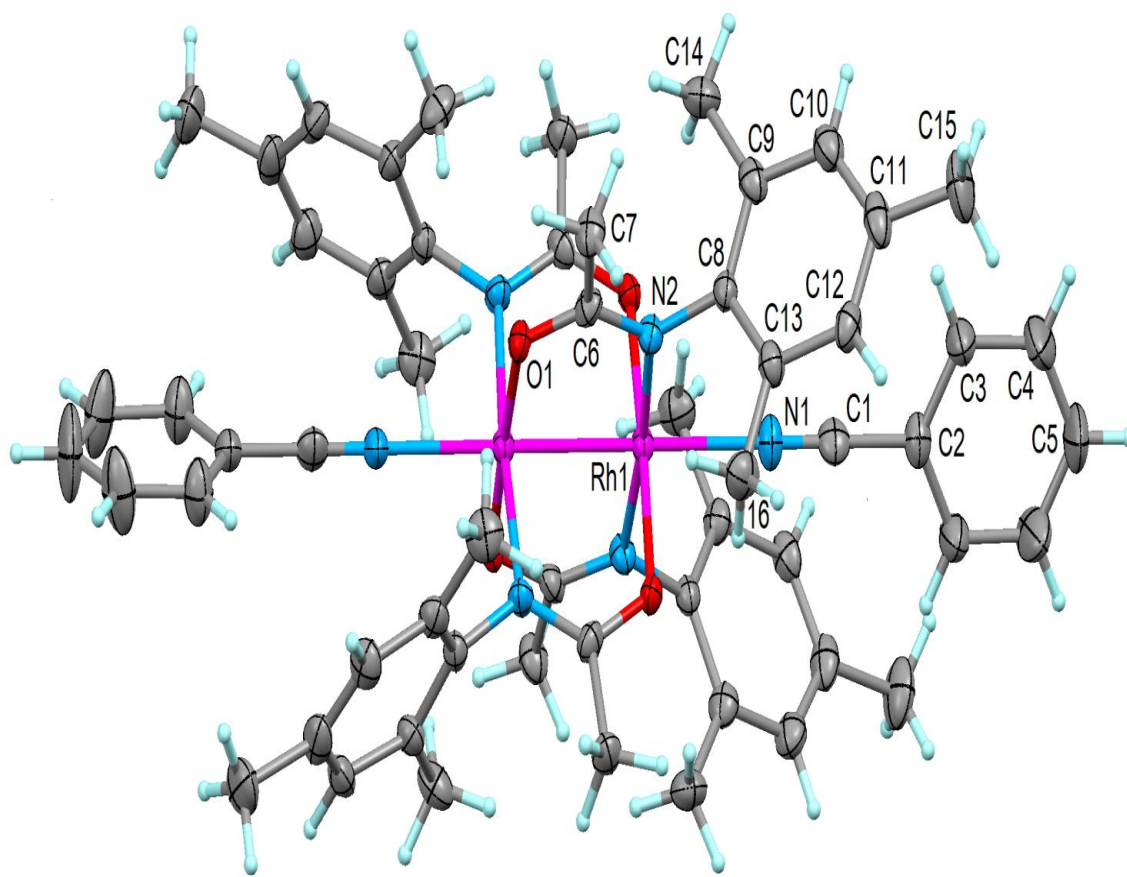


Figure 17: ORTEP⁴² of Bis(benzonitrile)-2,2-trans-tetrakis[μ -(N-{2,4,6-trimethylphenyl}Acetamidato- κ N: κ O)] dirhodium(II) with thermal ellipsoids at 30% probability and hydrogen atoms arbitrarily small

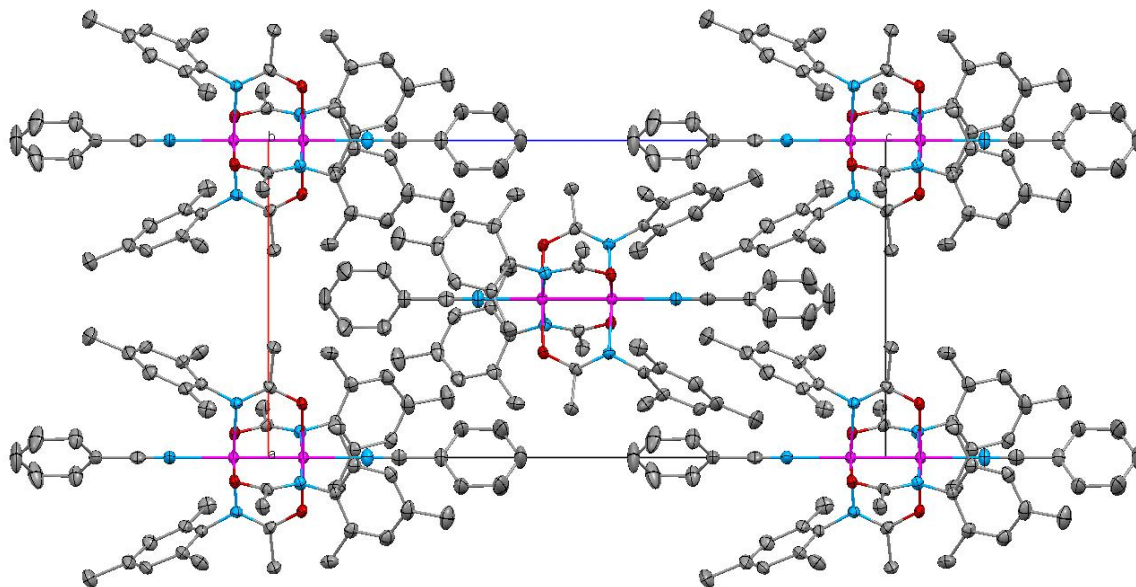


Figure 18: Packing diagram of the Bis(benzonitrile)-2,2-trans-tetrakis[μ -(N-{2,4,6-Trimethylphenyl}Acetamido- κ N: κ O)] dirhodium(II) viewed along the *a*-axis. H-atoms omitted for clarity

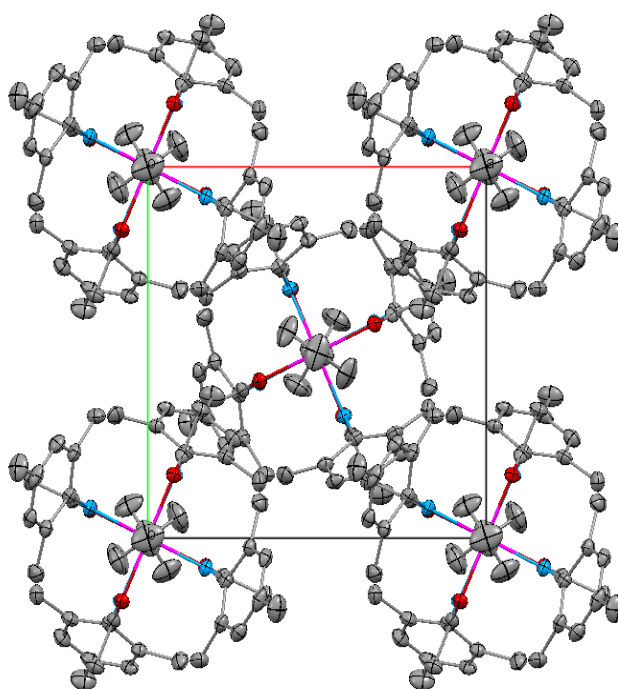
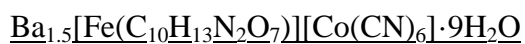


Figure 19: Packing diagram of the Bis(benzonitrile)-2,2-trans-tetrakis[μ -(N-{2,4,6-Trimethylphenyl}Acetamido- κ N: κ O)] dirhodium(II) viewed along the *c*-axis to emphasize the pseudo fourfold symmetry orientation. H-atoms omitted for clarity



A set of yellow crystals were provided by Dr. Jeff Wardeska of the Chemistry Department of the East Tennessee State University for structure determination. Dr. Wardeska also provided data on the elemental analysis as shown in table 1 below together with the molecular formula of the compound. Table 1 shows reliable agreement between the calculated and measured percentage of each element in the compound.

Table 1 Elemental analysis of $\text{Ba}_{1.5}[\text{Fe}(\text{C}_{10}\text{H}_{13}\text{N}_2\text{O}_7)][\text{Co}(\text{CN})_6] \cdot 9\text{H}_2\text{O}$

Element	Calculated % by weight	Measured % by weight
C	22.24	21.76
H	3.79	3.54
N	12.39	12.70
Fe	6.18	6.33
Co	6.51	6.68

1) Molecular formula: $\text{KBaFeCoC}_{16}\text{H}_{31}\text{N}_8\text{O}_{16}$ (Weight loss by drying. Calculated $9\text{H}_2\text{O}$)

After data collection, it was observed that there are several crystallographic challenges to the solution of this structure beyond straightforward modeling. This was because the solution software used to solve the structure failed. The challenges were: (1) atomic positions; (2) bonding between Fe and Co as metals and ligands; determining the difference between nitrogen and oxygen; (3) the existence of multiple H_2O molecules in the compound; (4) disordered oxygen atoms; and (5) the ambiguity that arises in assigning thermal parameters to

potassium (K) and Barium (Ba). The model that was constructed based on the information Dr. Wardeska provided was inconsistent with the data collected.

Knowledge of the chemical properties of the system (bonding characteristics, familiarity with similar structure and related literature) was necessary to determine which coordinated metal atoms were Fe and which ones were cobalt. According to Howard *et al*⁴⁶ and Meier and Lippard *et al*,⁴⁵ complexes of this type reveal the presence of a coordination number of seven. The coordination polyhedron of these complexes is a distorted pentagonal bipyramid as found for all the salts of these kinds of complexes that have been structurally determined to date.⁴⁶

Attempts to put potassium into the model of the structure resulted in the structure's inability to refine (the R1 value increased). The thermal parameters suggested the presence of a heavy metal; however, refinement suggested an atom heavier than potassium. When the atom identity was changed to barium, the model refined well and the R1 value decreased. Thus, a model was used with three barium atoms in the unit cell.

However, one of the barium atoms had an isotropic displacement parameter inconsistent with the other two. At this point the presence of disorder was considered. Upon the suggestions of Dr. Lee Daniels,⁴³ the barium atom was given a fixed isotropic thermal displacement parameter, and one of the barium atoms was set at X, (where X is 80% occupancy), and another barium atom (previously thought to be oxygen) set at 100%-X and as a free variable (FVAR).

This percentage occupancy was allowed to refine. The barium atom refined to 82.6% and then the thermal parameter was allowed to refine. The thermal parameter then refined

consistent with the other two barium atoms. Another challenge with the structure was how the ligand ethylenediaminetriacetic acid (HEDTA) bonds to the metals.

Extensive review of literature^{45,46} provided the answer about the possible orientations that the chelating ligand (HEDTA) can bind to metals. This knowledge coupled with communications with Dr. Jeff Wardeska,⁴⁴ helped in determining the crystal structure of $\text{Ba}_{1.5}[\text{Fe}(\text{C}_{10}\text{H}_{13}\text{N}_2\text{O}_7)][\text{Co}(\text{CN})_6]\cdot 9\text{H}_2\text{O}$.

The crystal structure is made up of (ethylenediaminetriacetato) iron (III) complexes packed so as to enable two of the carboxyl oxygen atoms to bond with the barium atoms. Figure 20 shows ORTEP of the asymmetric unit of the structure. The barium-oxygen bond distance averaged to be 2.780 Å. The barium-nitrogen bond distance averaged to be 2.88 Å. The bond lengths and contact distances are listed in Table 16 (See Appendix B). In the ethylenediaminetriacetic acid-iron (III) complex, the Fe-N bond length averaged to be 2.20 Å, while the Fe-O bond distance averaged to be 1.97 Å. The values are consistent with data published by Meier *et al.*⁴⁵ Bond angles are listed in Table 18 in appendix B.

The packing diagrams of the coordination complex as shown in figures 21 and 22 show a pentagonal bipyramid (PB) as found for all the salts of $[\text{Fe}(\text{EDTA})(\text{H}_2\text{O})]$ and $[\text{Fe}(\text{DTPA})]^{2-}$ that have been structurally characterized to date.⁴⁶

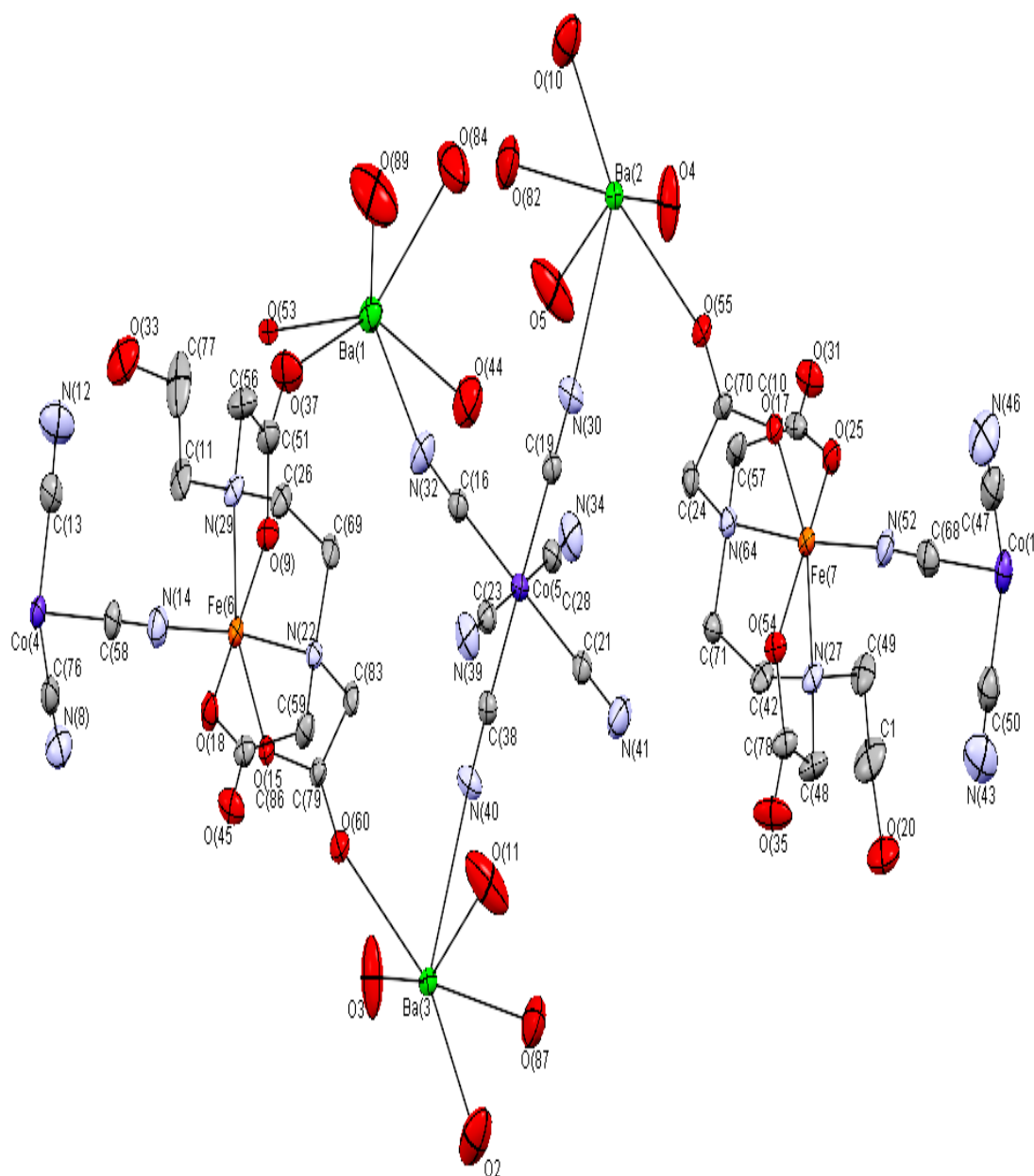


Figure 20: ORTEP⁴² of Ba_{1.5}[Fe(HEDTA)][Co(CN)₆]·9H₂O showing thermal ellipsoids at 30% probability and hydrogen atoms arbitrarily small

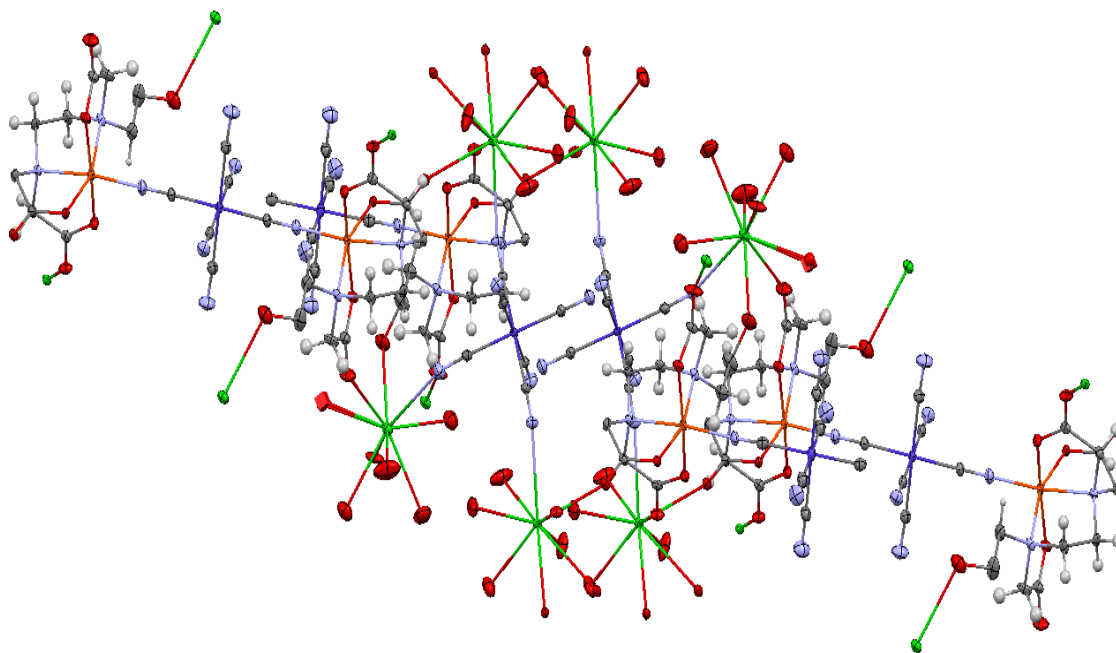


Figure 21: A symmetry extension diagram of Ba_{1.5}[Fe(HEDTA)][Co(CN)₆]·9H₂O

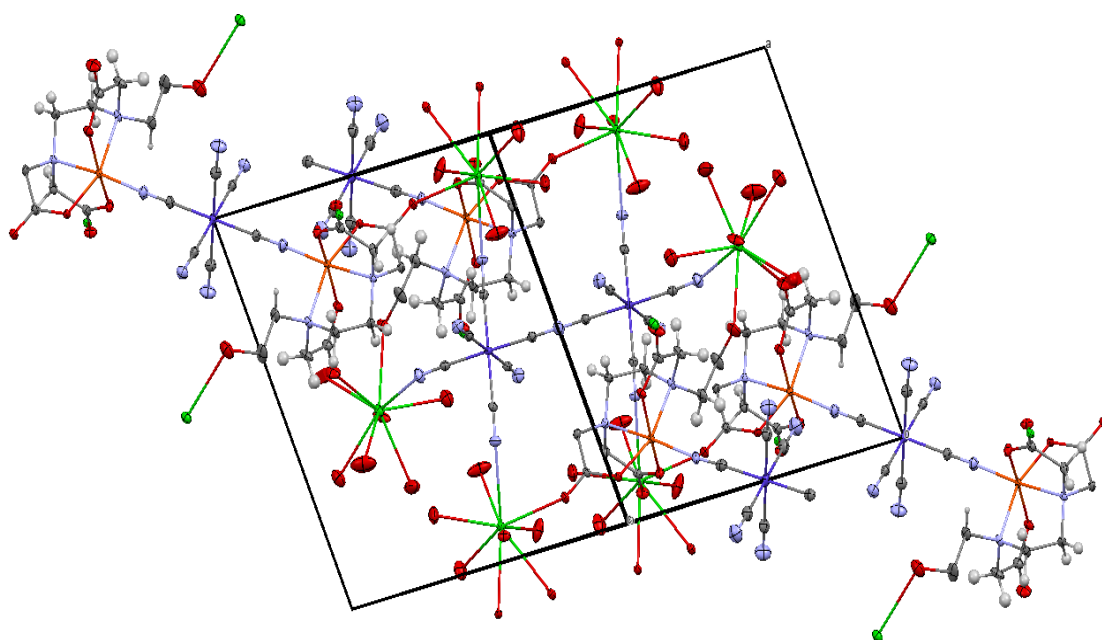


Figure 22: Packing diagram of Ba_{1.5}[Fe(HEDTA)][Co(CN)₆]·9H₂O viewed along the *a*-axis.

H-atoms omitted for clarity

CHAPTER 4

CONCLUSION

Three isomers (*2,2-trans*, *2,2-cis*, and *3,1*) of $[\text{Rh}_2(\text{N}-\{2,4,6\text{-CH}_3\}\text{C}_6\text{H}_2)\text{COCH}_3)_4] \cdot 2\text{NCC}_6\text{H}_4$ were successfully synthesized and identified by NMR spectroscopy. The crystal structure of the *2,2-trans* isomer was successfully determined using X-ray crystallography.

There were several crystallographic challenges faced when solving the crystal structure of $[\text{Rh}_2(\text{N}-\{2,4,6\text{-CH}_3\}\text{C}_6\text{H}_2)\text{COCH}_3)_4]$ such as determining the difference between nitrogen and oxygen, determining the special atomic positions for various atoms because only a fourth of the structure appeared in the asymmetric unit cell. The other three-quarters parts were generated by symmetry. The need to assign special atomic positions and the percentage occupancy assigned to which atom before refinement become important to the successful determination of the structure. These challenges were resolved by applying various refinement methods in x-ray diffraction studies and using knowledge of the bonding and reactivity of Rh_2L_4 compounds from previously published data.⁴¹ The final structure had an R1 value of 3.6%.

The X-ray crystal structure of $\text{Ba}_{1.5}[\text{Fe}(\text{C}_{10}\text{H}_{13}\text{N}_2\text{O}_7)][\text{Co}(\text{CN})_6] \cdot 9\text{H}_2\text{O}$ was also successfully solved. The challenges that were associated with solving the crystal structure such as 1) atomic positions; 2) bonding between Fe and Co as metals and ligands; determining the difference between nitrogen and oxygen; 3) the existence of multiple H_2O molecules in the compound; 4) disordered oxygen atoms; and 5) the ambiguity that arises in assigning thermal parameters to potassium (K) and Barium (Ba), were successfully resolved, and the final structure had an R1 value of 4.3%.

These goals were generally achieved by careful and thoughtful application of various techniques as described in this thesis. The structural information obtained from the crystal structures of these compounds will enable us study further the chemical reactivity, electronics, and other properties of these compounds. The data and methods used in this thesis will find useful application in solving structural problems of similar coordination compounds.

REFERENCES

1. Sands, D. E. *Introduction to Crystallography*; Dover Publications, Inc: Mineola, NY, 1994; 2, 11, 55-61, 88-92, 127.
2. Sands, D. E. *Introduction to Crystallography*; Dover Publications, Inc: Mineola, N.Y, 1994; 2, 11, pp 55-61, 88-92, 139.
3. Clark; C. M.; Dutrow B. L.; Single-Crystal X-ray Diffraction. http://serc.carleton.edu/research_education/geochemsheets/techniques/SXD.html. (Accessed on June 14, 2012).
4. Lattice planes and Bragg's law. <http://www.mrl.ucsb.edu/centralfacilities/x-ray/basics>. (Accessed on July 13, 2012)
5. Miller indices. 2012. *Encyclopædia Britannica Online*. Retrieved 15 July, 2012, from <http://www.britannica.com/EBchecked/topic/382843/Miller-indices>.
6. Hexagonal system. 2012. *Encyclopædia Britannica Online*. Retrieved 13 July, 2012, from <http://www.britannica.com/EBchecked/topic/264583/hexagonal-system>.
7. Jesperen, N. D.; Brady, J. E.; Hyslop, A. X-ray Diffraction of Solids. *Chemistry: The Molecular Nature of Matter*; 6th ed.; John Wiley & Sons: Hoboken, N.J, 2012; Chapter 12.
8. Doyle, M. P.; Ren, T. The Influence of Ligands on Dirhodium (II) on Reactivity and Selectivity in Metal Carbene Reactions. In *Progress in Inorganic Chemistry*, Karlin, K., Ed. Wiley: New York, 2001; 49, 113-168.
9. Chifotides, H.T.; Dunbar, K.R. Interactions of Metal—Metal-Bonded Antitumor Active Complexes with DNA Fragments and DNA. *Acc. Chem. Res.* **2005**, 38, 146-156.
10. Patty K.-L.; Fu, P. M. B.; Turro, C. DNA Photo cleavage by Photogenerated $\text{Rh}_2(\text{O}_2\text{CCH}_2)_4$. *Inorg. Chem.* **2001**, 40, 2476-2477.
11. Heyduk, A. F.; Nocera, D. G. Hydrogen Produced from Hydrohalic Acid Solutions by a Two-Electron Mixed-Valence Photocatalyst. *Science* **2001**, 293, 1639.
12. Doyle, M. P. Perspective on Dirhodium carboxamidates as catalysts. *J. Org. Chem.* **2006**, 71, 9253-9260.
13. Doyle, M.P. Chiral Dirhodium Carboxamidates: Catalysts for highly Enantioselective Synthesis of Lactones and Lactams. *Aldrichim. Acta* **1996**, 29, 3-11.
14. Lebel, H.; Charette, A. B.; Marcoux, J.-F.; Molinaro, C. Stereoselective Cyclopropanation Reactions *Chem. Rev.* **2003**, 103, 977-1050.

15. Doyle, M. P. Perspective on Dirhodium carboxamidates as catalysts. *J. Org. Chem.* **2006**, *71*, 9253-9260.
16. Charette, A. B.; Wurz, R. P. Progress towards Asymmetric Intermolecular and Intramolecular Cyclopropanations Using α -Nitro- α -diazo Carbonyl Substrates. *J. Mol. Catal. A: Chem.* **2003**, *196*, 83-91.
17. Davies, H.M.L.; Beckwith, R.E.J. Catalytic Enantioselective C–H Activation by Means of Metal–Carbenoid-Induced C–H Insertion. *Chem. Rev.* **2003**, *103*, 2861-2904.
18. Crabtree R. H. and Mingos, D. M. P. *Comprehensive Organometallic Chemistry III*, Eds. Elsevier, Oxford **2007**, 699-723.
19. Korp, J.D.; Dennis A. M.; Bernal, I.; Howard R. A.; Bear J. L. Crystal and molecular structure of the bis(pyridine) adduct of a dinuclear rhodium(II) complex with trifluoroacetamido bridging ligands. *Inorg. Chem.* **1983**, *22*, 1522-1529.
20. Nichols J. The Redox Chemistry of Dirhodium Carboxamidates: from fundamental Structures to Catalytic Functions. PhD Thesis, University of Maryland, MD, 2008, <http://hdl.handle.net/1903/8051>
21. Doyle, M. P.; High, K. G.; Bagheri, V.; Pieters, R. J.; Lewis, P. J.; Pearson, M. M. Rhodium (II) perfluorobutyrate catalyzed silane alcoholysis: A highly selective route to silyl ethers. *J. Org. Chem.* **1990**, *55*, 6082-6086.
22. Doyle, M. P.; Devora, G. A.; Nefedov, A. O.; High, K. G. Addition/elimination in the rhodium (II) perfluorobutyrate catalyzed hydrosilylation of 1-alkenes: Rhodium hydride promoted isomerization and hydrogenation. *Organometallics* **1992**, *11*, 549-555.
23. Doyle, M. P.; McKervey, M. A.; Ye, T. *Modern Catalytic Methods for Organic Synthesis with Diazo Compounds: From Cyclopropanes to Ylides*. Wiley: New York, 1998.
24. Duncan, J.; Malinski, T.; Zhu, Z. S.; Hu, T. P.; Kadish, K. M.; Bear, J. L. Characterization of novel rhodium(II) dimers with N-phenylacetamido bridging ligands. *J. Am. Chem. Soc.* **1982**, *104*, 5507-5509
25. Doyle, M. P.; Brandes, B. D.; Kazala, A. P.; Pieters, R. J.; Jarstfer, M. B.; Watkins, L. M.; Eagle, C. T. Chiral Rhodium(II) Carboxamides. A New Class of Catalysts for Enantioselective Cyclopropanation Reactions. *Tetrahedron Lett.* **1990**, *31*, 6613-6616.
26. Ahmad, J. Crystallization from a Supersaturated Solution of Sodium Acetate. *J. Chem. Educ.*, **2000**, *77* (11), 1446.
27. Rempel, G. A.; Legzdins, P.; Smith, H.; Wilkinson, G.; Ucko, D. A. Tetrakis (Acetato) Dirhodium (II) and Similar Carboxylato Compounds. *Inorganic Syntheses*. **1972**, *13*, 90.

28. Gowda, B. T.; Usha K. M.; Jyothi, K. Z. Infrared, ¹H and ¹³C NMR Spectral Studies on Di- and Tri-substituted N-Aryl Amides, 2,6-X₂C₆H₃NHCOCH₃-iXi and 2,4,6-X₃C₆H₂NHCOCH₃ - iXi (X = Cl or CH₃ and i = 0, 1, 2 or 3). *Naturforsch.* **2004**, *59*, 69-76.
29. Greer, F.; Pearson, D. E. The Beckmann Rearrangement. VII. The Isolation and Rearrangement of 2,4,6-Trimethylacetophenone Oxime. *J. Am. Chem. Soc.* **1955**, *77*, 6649-6650.
30. Moriyasu, M.; Kawanishi, K.; Kato, A.; Hashimoto, Y.; Sugiura, M. Kinetic studies of fast equilibrium by means of high-performance liquid chromatography. X: Separation of rotamers of acetanilides. *The Chemical Society of Japan.* **1985**, *58*, 2581-2585.
31. Zink, L. C. Synthesis of N-(substituted phenyl) acetamides. Honor Thesis, East Tennessee State University, Johnson City, TN, 2012.
32. Pflugrath, J. W. The finer things in X-ray diffraction data collection (CrystalClear Software User's Guide, Molecular Structure Corporation.). *Acta Cryst.* **1999**, *D55*, 1718-1725.
33. Least Squares function minimized: (SHELXL97) $\sum w (F_o - F_c)^2$ where w = Least Squares weights. Standard deviation of an observation of unit weight: $[\sum w (F_o - F_c)^2 / (N_o - N_v)]^{1/2}$ where, N_o = number of observations N_v = number of variables.
34. Flack, H. D. On enantiomorph-polarity estimation. *Acta Cryst.* **1983**, *A39*, 876-881.
35. Cromer, D. T.; Waber, J. T.; International Tables for X-ray Crystallography. **1974**, *Vol. IV*, The Kynoch Press, Birmingham, England, Table 2.2 A.
36. Ibers, J. A.; Hamilton, W. C. Dispersion corrections and crystal structure refinements. *Acta Cryst.*, **1964**, *17*, 781.
37. Creagh, D. C.; McAuley, W. J. *International Tables for Crystallography; Vol C*, (A.J.C. Wilson, ed.), Kluwer Academic Publishers, Boston, 1992; *Table 4.2.6.8*, pp 219-222.
38. Creagh, D. C. & Hubbell, J.H.; *International Tables for Crystallography; Vol C*, (A.J.C. Wilson, ed.), Kluwer Academic Publishers, Boston, 1992; *Table 4.2.4.3*, pp 200-206
39. CrystalStructure 4.0: Crystal Structure Analysis Package, Rigaku and Rigaku Americas 9009 New Trails Dr. The Woodlands, TX. **2000-2010**.
40. SHELX97: Sheldrick, G.M. **1997**.
41. Eagle, C. T.; Farrar, D. G.; Holder G. N.; Pennington, W. T.; Bailey R. D. Structural and Electronic Properties of (2,2-trans)-Dirhodium(II) Tetrakis(N-phenylacetamidate). *J. Organomet Chem*, **2000**, *596*, 90-94.
42. Burnett, M. N.; Johnson, C. K. ORTEP-III: Oak Ridge Thermal Ellipsoid Plot Program for Crystal Structure Illustrations, Oak Ridge National Laboratory Report ORNL-6895, **1996**.

43. Daniels, L. M. Director, Small-Molecule Products, Rigaku Americas Corporation, 9009 New Trails Drive, The Woodlands TX. Private Communications, 2011-2012.
44. Wardeska, J. Chemistry department East Tennessee State University, Johnson City, TN. Private Communications, 2012.
45. Meier, R.; Bedell, S. A.; Henkel, G. Structure of the seven-coordinate aqua-(*N*-hydroxyethyl)ethylenediaminetriacetato iron(III) complex and solution coexistence between six- and seven-coordinate species. *Inorganica Chimica Acta*, **2002**, 337, 337-343.
46. (a) Howard, W.L. and Wilson, D.A. *Kirk-Othmer Encyclopedia of Chemical Technology*; vol. 5, 4th ed., John Wiley & Sons, Inc, New York, 1993; 764.
- (b) Hart, J.R. in: Gerhartz, W. ; Yamamoto, Y.S; Kaudy, L. ; Rounsaville, J.F. and Schulz, G. (Eds.), *Ullmann's Encyclopedia of Industrial Chemistry*, Vol. A10, 5th revised ed., Photography to Plastics, Processing, VCH, Weinheim, **1992**, 95-100.
- (c) Lippard, S.J.; Schugar, H.J. and Walling, C. 'Crystal and molecular structure of an oxo-bridged binuclear iron(III) complex' *Inorg. Chem.* **1967**, 6, 1825-1831.
- (d) Schugar, H.J.; Walling, C.; Jones, R.B.; Gray, H.B. The structure of iron(III) in aqueous solution. *J. Am. Chem. Soc.* **1967**, 89, 3712-3720.

APPENDICES

Appendix A

Crystallographic Report for [Rh₂(N-{2,4,6-CH₃}C₆H₂)COCH₃)₄].2NCC₆H₄

Experimental details

A. Crystal Data

Empirical Formula	C ₅₈ H ₆₆ N ₆ O ₄ Rh ₂
Formula Weight	1117.01g/mol
Crystal Color, Habit	blue, prism
Crystal Dimensions	0.18 X 0.13 X 0.07 mm
Crystal System	tetragonal
Lattice Type	Primitive
Lattice Parameters	a = 10.9928 (19) Å c = 21.4549 (19) Å V = 2592.6 (7) Å ³
Space Group	P-42 ₁ c (#114)
Z value	2
D _{calc}	1.431 g/cm ³
F ₀₀₀	1156.00
μ(MoKα)	6.879 cm ⁻¹

B. Intensity Measurements

Diffractionmeter	Rigaku Mercury375R/M CCD (XtaLABmini)
Radiation	MoKα (λ = 0.71075 Å)

Temperature	4.0°C
Detector Aperture	75 mm (diameter)
Data Images	1069 exposures
ω oscillation Range ($\chi=54.0$, $\varphi=0.0$)	-60.0 - 120.0°
Exposure Rate	16.0 sec./°
Detector Swing Angle	29.50°
ω oscillation Range ($\chi=54.0$, $\varphi=120.0$)	-60.0 - 120.0°
Exposure Rate	16.0 sec./°
Detector Swing Angle	29.50°
ω oscillation Range ($\chi=54.0$, $\varphi=240.0$)	-60.0 - 120.0°
Exposure Rate	16.0 sec./°
Detector Swing Angle	29.50°
ω oscillation Range ($\chi=54.0$, $\varphi=240.0$)	-60.0 - 120.0°
Exposure Rate	16.0 sec./°
Detector Swing Angle	29.50°
ω oscillation Range ($\chi=54.0$, $\varphi=120.0$)	-60.0 - 120.0°
Exposure Rate	16.0 sec./°
Detector Swing Angle	29.50°
ω oscillation Range ($\chi=54.0$, $\varphi=0.0$)	-60.0 - 120.0°
Exposure Rate	16.0 sec./°
Detector Swing Angle	29.50°

Detector Position	50.00 mm
Pixel Size	0.073 mm
$2\theta_{\max}$	55.0°
No. of Reflections Measured	Total: 48863 Unique: 2969 ($R_{\text{int}} = 0.1045$) Friedel pairs: 1291
Corrections	Lorentz-polarization Absorption (trans. factors: 0.618 - 0.953)

C. Structure Solution and Refinement

Structure Solution	Direct Methods
Refinement	Full-matrix least-squares on F^2
Function Minimized	$\Sigma w (F_o^2 - F_c^2)^2$
Least Squares Weights	$w = 1 / [\sigma^2(F_o^2) + (0.0214 \cdot P)^2 + 2.1722 \cdot P]$ where $P = (\text{Max}(F_o^2, 0) + 2F_c^2)/3$
$2\theta_{\max}$ cutoff	55.0°
Anomalous Dispersion	All non-hydrogen atoms
No. Observations (All reflections)	2969
No. Variables	165
Reflection/Parameter Ratio	17.99
Residuals: R1 ($I > 2.00\sigma(I)$)	0.0360
Residuals: R (All reflections)	0.0729
Residuals: wR2 (All reflections)	0.0744
Goodness of Fit Indicator	1.038

Flack Parameter (Friedel pairs = 1291)	0.01(7)
Max Shift/Error in Final Cycle	0.000
Maximum peak in Final Diff. Map	0.64 e ⁻ /Å ³
Minimum peak in Final Diff. Map	-0.70 e ⁻ /Å ³

Table 2: Atomic coordinates and B_{iso}/B_{eq} and occupancy

atom	x	y	z	B _{eq}	occ
Rh(1)	0.5000	0.5000	0.5566	2.44	1/2
O(1)	0.6695(3)	0.4237(3)	0.44533(15)	2.71(8)	
N(1)	0.5000	0.5000	0.6602	3.51	1/2
N(2)	0.6716(3)	0.4187(3)	0.55161(19)	2.76(9)	
C(1)	0.5000	0.5000	0.7117	3.87	1/2
C(2)	0.5000	0.5000	0.7799	3.76	1/2
C(3)	0.5590(5)	0.4097(5)	0.8123(2)	5.26(14)	
C(4)	0.5563(7)	0.4117(6)	0.8766(2)	7.84(20)	
C(5)	0.5000	0.5000	0.9084	9.26	1/2
C(6)	0.7216(3)	0.3988(3)	0.4976(3)	2.97(8)	
C(7)	0.8471(3)	0.3447(4)	0.4908(2)	3.76(11)	
C(8)	0.7316(4)	0.3860(4)	0.60847(17)	2.76(8)	
C(9)	0.7176(4)	0.2700(4)	0.63429(19)	3.53(11)	
C(10)	0.7689(4)	0.2470(5)	0.6922(2)	4.26(11)	
C(11)	0.8301(5)	0.3331(6)	0.7260(2)	4.61(13)	
C(12)	0.8475(4)	0.4460(5)	0.6986(2)	3.71(11)	
C(13)	0.8015(4)	0.4747(4)	0.63931(18)	3.29(9)	
C(14)	0.6525(5)	0.1712(4)	0.5992(2)	4.55(13)	
C(15)	0.8818(5)	0.3099(6)	0.7896(2)	6.29(17)	
C(16)	0.8313(5)	0.5948(4)	0.6110(2)	4.61(13)	

Table 3: Atomic coordinates and B_{iso} and occupancy involving hydrogen atoms

atom	x	y	z	B _{iso}	occ
H(3)	0.6000	0.3483	0.7913	6.32	
H(4)	0.5948	0.3498	0.8985	9.40	
H(5)	0.5000	0.5000	0.9517	11.13	1/2
H(7)	0.8642	0.3312	0.4475	4.50	
H(7)	0.8508	0.2688	0.5128	4.50	
H(7)	0.9062	0.3998	0.5078	4.50	
H(10)	0.7613	0.1692	0.7089	5.13	
H(12)	0.8911	0.5049	0.7203	4.50	

H(14)	0.6891	0.1614	0.5589	5.45
H(14)	0.5685	0.1928	0.5944	5.45
H(14)	0.6585	0.0962	0.6220	5.45
H(15)	0.8394	0.2432	0.8086	7.50
H(15)	0.8724	0.3814	0.8148	7.50
H(15)	0.9666	0.2902	0.7860	7.50
H(16)	0.7601	0.6453	0.6111	5.53
H(16)	0.8585	0.5830	0.5689	5.53
H(16)	0.8945	0.6333	0.6347	5.53

Table 4: Anisotropic displacement parameters

atom	U ₁₁	U ₂₂	U ₃₃	U ₁₂	U ₁₃	U ₂₃
Rh(1)	0.0331(3)	0.0354(3)	0.02435(15)	0.0013(5)	0.0000	0.0000
O(1)	0.037(2)	0.041(2)	0.0251(18)	0.0021(19)	0.0032(18)	-
0.0048(18)						
N(1)	0.037(4)	0.066(5)	0.0302(19)	-0.005(7)	0.0000	0.0000
N(2)	0.031(2)	0.041(3)	0.033(2)	0.006(2)	-0.002(2)	-0.003(2)
C(1)	0.037(4)	0.057(5)	0.053(3)	0.014(7)	0.0000	0.0000
C(2)	0.040(5)	0.068(6)	0.035(2)	-0.002(10)	0.0000	0.0000
C(3)	0.093(4)	0.062(4)	0.045(3)	0.024(3)	-0.003(3)	0.000(2)
C(4)	0.154(7)	0.087(5)	0.057(3)	0.049(4)	-0.030(4)	0.005(3)
C(5)	0.206(13)	0.116(9)	0.030(3)	0.036(15)	0.0000	0.0000
C(6)	0.0385(19)	0.0371(19)	0.0373(19)	0.0014(16)	0.009(3)	-0.007(3)
C(7)	0.038(2)	0.061(3)	0.044(3)	0.0102(19)	0.003(2)	-0.005(3)
C(8)	0.036(2)	0.040(2)	0.029(2)	0.006(2)	-0.0010(17)	-
0.0026(18)						
C(9)	0.037(3)	0.052(3)	0.045(2)	0.0103(19)	-0.003(2)	0.005(2)
C(10)	0.056(3)	0.056(3)	0.050(2)	0.013(2)	-0.003(3)	0.008(3)
C(11)	0.049(3)	0.084(4)	0.042(3)	0.025(3)	-0.003(2)	0.007(3)
C(12)	0.039(3)	0.060(3)	0.042(2)	0.007(2)	-0.011(2)	-0.011(2)
C(13)	0.037(2)	0.048(3)	0.040(2)	0.0028(19)	-0.0055(18)	0.002(2)
C(14)	0.065(4)	0.037(3)	0.071(3)	0.003(3)	0.001(3)	0.004(3)
C(15)	0.071(4)	0.119(6)	0.049(3)	0.009(4)	-0.016(3)	0.015(4)
C(16)	0.056(4)	0.052(3)	0.067(3)	-0.007(3)	-0.019(3)	-0.005(3)

Table 5: Bond lengths (Å)

atom	atom	distance	atom	atom	distance
Rh(1)	Rh(1) ¹	2.4289(2)	Rh(1)	O(1) ¹	2.044(3)
Rh(1)	O(1) ²	2.044(3)	Rh(1)	N(1)	2.222(3)
Rh(1)	N(2)	2.090(3)	Rh(1)	N(2) ³	2.090(3)

O(1)	C(6)	1.289(7)	N(1)	C(1)	1.106(5)
N(2)	C(6)	1.301(7)	N(2)	C(8)	1.433(5)
C(1)	C(2)	1.463(6)	C(2)	C(3)	1.374(6)
C(2)	C(3) ³	1.374(6)	C(3)	C(4)	1.380(6)
C(4)	C(5)	1.338(7)	C(6)	C(7)	1.509(5)
C(8)	C(9)	1.399(6)	C(8)	C(13)	1.407(6)
C(9)	C(10)	1.388(6)	C(9)	C(14)	1.503(6)
C(10)	C(11)	1.369(8)	C(11)	C(12)	1.387(8)
C(11)	C(15)	1.500(6)	C(12)	C(13)	1.405(6)
C(13)	C(16)	1.490(6)			

Symmetry Operators:

(1) Y,-X+1,-Z+1
 (3) -X+1,-Y+1,Z

(2) -Y+1,X,-Z+1

Table 6: Bond lengths involving hydrogens (Å)

atom	atom	distance	atom	atom	distance
C(3)	H(3)	0.928(5)	C(4)	H(4)	0.929(6)
C(5)	H(5)	0.929(6)	C(7)	H(7)	0.959(4)
C(7)	H(7)	0.959(4)	C(7)	H(7)	0.960(4)
C(10)	H(10)	0.931(5)	C(12)	H(12)	0.930(5)
C(14)	H(14)	0.960(5)	C(14)	H(14)	0.959(5)
C(14)	H(14)	0.961(4)	C(15)	H(15)	0.960(6)
C(15)	H(15)	0.960(6)	C(15)	H(15)	0.960(6)
C(16)	H(16)	0.960(5)	C(16)	H(16)	0.960(4)

C(16) H(16) 0.959(5)

Table 7: Bond angles ($^{\circ}$)

atom	atom	atom	angle	atom	atom	atom	angle
Rh(1) ¹	Rh(1)	O(1) ¹	88.84(9)	Rh(1) ¹	Rh(1)	O(1) ²	88.84(9)
Rh(1) ¹	Rh(1)	N(1)	180	Rh(1) ¹	Rh(1)	N(2)	87.06(11)
Rh(1) ¹	Rh(1)	N(2) ³	87.06(11)	O(1) ¹	Rh(1)	O(1) ²	177.672(17)
O(1) ¹	Rh(1)	N(1)	91.16(9)	O(1) ¹	Rh(1)	N(2)	88.83(13)
O(1) ¹	Rh(1)	N(2) ³	91.05(13)	O(1) ²	Rh(1)	N(1)	91.16(9)
O(1) ²	Rh(1)	N(2)	91.05(13)	O(1) ²	Rh(1)	N(2) ³	88.83(13)
N(1)	Rh(1)	N(2)	92.94(11)	N(1)	Rh(1)	N(2) ³	92.94(11)
N(2)	Rh(1)	N(2) ³	174.122(16)	Rh(1) ¹	O(1)	C(6)	120.7(3)
Rh(1)	N(1)	C(1)	180	Rh(1)	N(2)	C(6)	119.9(3)
Rh(1)	N(2)	C(8)	118.6(3)	C(6)	N(2)	C(8)	121.4(3)
N(1)	C(1)	C(2)	180	C(1)	C(2)	C(3)	120.4(2)
C(1)	C(2)	C(3) ³	120.4(2)	C(3)	C(2)	C(3) ³	119.2(3)
C(2)	C(3)	C(4)	118.9(5)	C(3)	C(4)	C(5)	122.1(6)
C(4)	C(5)	C(4) ³	118.7(5)	O(1)	C(6)	N(2)	123.5(3)
O(1)	C(6)	C(7)	113.9(5)	N(2)	C(6)	C(7)	122.6(5)
N(2)	C(8)	C(9)	121.0(4)	N(2)	C(8)	C(13)	118.6(4)
C(9)	C(8)	C(13)	120.4(4)	C(8)	C(9)	C(10)	118.4(4)
C(8)	C(9)	C(14)	120.9(4)	C(10)	C(9)	C(14)	120.7(4)
C(9)	C(10)	C(11)	123.2(5)	C(10)	C(11)	C(12)	117.5(4)
C(10)	C(11)	C(15)	123.4(5)	C(12)	C(11)	C(15)	119.1(5)
C(11)	C(12)	C(13)	122.4(4)	C(8)	C(13)	C(12)	117.8(4)
C(8)	C(13)	C(16)	122.9(4)	C(12)	C(13)	C(16)	119.3(4)

Symmetry Operators:

(1) Y,-X+1,-Z+1

(2) -Y+1,X,-Z+1

(3) -X+1,-Y+1,Z

Table 8: Bond angles involving hydrogens ($^{\circ}$)

atom	atom	atom	angle	atom	atom	atom	angle
C(2)	C(3)	H(3)	120.6(4)	H(3)	C(3)	C(4)	120.5(5)
C(3)	C(4)	H(4)	119.0(6)	H(4)	C(4)	C(5)	119.0(5)
C(4)	C(5)	H(5)	120.7(3)	C(4) ¹	C(5)	H(5)	120.7(3)
C(6)	C(7)	H(7)	109.5(4)	C(6)	C(7)	H(7)	109.5(3)
C(6)	C(7)	H(7)	109.5(4)	H(7)	C(7)	H(7)	109.5(4)

H(7)	C(7)	H(7)	109.4(4)	H(7)	C(7)	H(7)	109.5(4)
C(9)	C(10)	H(10)	118.4(5)	H(10)	C(10)	C(11)	118.4(4)
C(11)	C(12)	H(12)	118.8(4)	H(12)	C(12)	C(13)	118.8(5)
C(9)	C(14)	H(14)	109.4(4)	C(9)	C(14)	H(14)	109.5(4)
C(9)	C(14)	H(14)	109.4(4)	H(14)	C(14)	H(14)	109.6(4)
H(14)	C(14)	H(14)	109.5(4)	H(14)	C(14)	H(14)	109.5(5)
C(11)	C(15)	H(15)	109.4(5)	C(11)	C(15)	H(15)	109.4(5)
C(11)	C(15)	H(15)	109.5(4)	H(15)	C(15)	H(15)	109.5(5)
H(15)	C(15)	H(15)	109.5(6)	H(15)	C(15)	H(15)	109.6(5)
C(13)	C(16)	H(16)	109.4(5)	C(13)	C(16)	H(16)	109.4(4)
C(13)	C(16)	H(16)	109.5(4)	H(16)	C(16)	H(16)	109.5(4)
H(16)	C(16)	H(16)	109.5(4)	H(16)	C(16)	H(16)	109.4(5)

Symmetry Operators:

(1) -X+1,-Y+1,Z

Table 9: Torsion Angles($^{\circ}$)
(Those having bond angles > 160 degrees are excluded.)

atom1	atom2	atom3	atom4	angle	atom1	atom2	atom3	atom4	angle
Rh(1) ¹	Rh(1)	O(1) ¹	C(6) ¹	-0.7(2)	O(1) ¹	Rh(1)	Rh(1) ¹	O(1) ²	90
O(1) ¹	Rh(1)	Rh(1) ¹	O(1)	-90	O(1) ¹	Rh(1)	Rh(1) ¹	N(2) ¹	1.12(9)
Rh(1) ¹	Rh(1)	O(1) ³	C(6) ³	-0.7(2)	O(1) ³	Rh(1)	Rh(1) ¹	O(1) ²	-90
O(1) ³	Rh(1)	Rh(1) ¹	O(1)	90	O(1) ³	Rh(1)	Rh(1) ¹	N(2) ³	1.12(9)
Rh(1) ¹	Rh(1)	N(2)	C(6)	1.9(2)	N(2)	Rh(1)	Rh(1) ¹	O(1)	-1.12(9)
N(2)	Rh(1)	Rh(1) ¹	N(2) ¹	90	N(2)	Rh(1)	Rh(1) ¹	N(2) ³	-90
Rh(1) ¹	Rh(1)	N(2) ²	C(6) ²	1.9(2)	N(2) ²	Rh(1)	Rh(1) ¹	O(1) ²	-1.12(9)
N(2) ²	Rh(1)	Rh(1) ¹	N(2) ¹	-90	N(2) ²	Rh(1)	Rh(1) ¹	N(2) ³	90
O(1) ¹	Rh(1)	N(2)	C(6)	90.8(2)	O(1) ¹	Rh(1)	N(2)	C(8)	-89.2(2)
N(2)	Rh(1)	O(1) ¹	C(6) ¹	-87.8(3)	O(1) ¹	Rh(1)	N(2) ²	C(6) ²	-86.9(2)
O(1) ¹	Rh(1)	N(2) ²	C(8) ²	93.2(2)	N(2) ²	Rh(1)	O(1) ¹	C(6) ¹	86.3(3)
O(1) ³	Rh(1)	N(2)	C(6)	-86.9(2)	O(1) ³	Rh(1)	N(2)	C(8)	93.2(2)
N(2)	Rh(1)	O(1) ³	C(6) ³	86.3(3)	O(1) ³	Rh(1)	N(2) ²	C(6) ²	90.8(2)
O(1) ³	Rh(1)	N(2) ²	C(8) ²	-89.2(2)	N(2) ²	Rh(1)	O(1) ³	C(6) ³	-87.8(3)
N(1)	Rh(1)	N(2)	C(8)	1.9(2)	N(1)	Rh(1)	N(2) ²	C(8) ²	1.9(2)
Rh(1) ¹	O(1)	C(6)	N(2)	0.6(5)	Rh(1)	N(2)	C(6)	O(1)	-1.9(5)
Rh(1)	N(2)	C(8)	C(9)	91.8(4)	Rh(1)	N(2)	C(8)	C(13)	-85.8(4)
C(6)	N(2)	C(8)	C(9)	-88.2(5)	C(6)	N(2)	C(8)	C(13)	94.2(4)
C(8)	N(2)	C(6)	C(7)	-2.3(5)	C(3)	C(2)	C(3) ²	C(4) ²	0.6083(9)
C(3) ²	C(2)	C(3)	C(4)	0.6083(9)	C(2)	C(3)	C(4)	C(5)	-1.3(9)
C(3)	C(4)	C(5)	C(4) ²	0.6(3)	N(2)	C(8)	C(9)	C(14)	7.9(6)
N(2)	C(8)	C(13)	C(16)	-9.5(6)	C(9)	C(8)	C(13)	C(12)	-5.2(6)
C(13)	C(8)	C(9)	C(10)	3.2(6)	C(8)	C(9)	C(10)	C(11)	1.6(6)
C(9)	C(10)	C(11)	C(12)	-4.2(7)	C(10)	C(11)	C(12)	C(13)	2.1(7)

C(11) C(12) C(13) C(8) 2.5(6)

Symmetry Operators:

(1) Y,-X+1,-Z+1

(2) -X+1,-Y+1,Z

(3) -Y+1,X,-Z+1

Table 10: Intramolecular contacts less than 3.60 Å

atom	atom	distance	atom	atom	distance
Rh(1)	C(6) ¹	2.962(4)	Rh(1)	C(6) ²	2.920(4)
Rh(1)	C(8) ¹	3.048(4)	O(1)	C(6) ³	3.592(5)
O(1)	C(6) ²	3.576(5)	O(1)	C(8)	3.590(5)
O(1)	C(14) ²	3.210(6)	O(1)	C(16) ³	3.161(6)
N(1)	C(3)	3.473(6)	N(1)	C(3) ¹	3.473(6)
N(1)	C(8)	3.047(5)	N(1)	C(8) ¹	3.047(5)
N(1)	C(9)	3.525(4)	N(1)	C(9) ¹	3.525(4)
N(1)	C(13)	3.356(4)	N(1)	C(13) ¹	3.356(4)
N(2)	C(6) ³	3.534(5)	N(2)	C(6) ²	3.578(5)
N(2)	C(14)	2.914(6)	N(2)	C(16)	2.907(6)
C(1)	C(8)	3.600(5)	C(1)	C(8) ¹	3.600(5)
C(2)	C(4) ¹	2.373(6)	C(2)	C(5)	2.757(8)
C(3)	C(4) ¹	2.714(8)	C(6)	C(9)	3.257(7)
C(6)	C(13)	3.273(7)	C(6)	C(14)	3.404(7)
C(6)	C(16)	3.466(7)	C(7)	C(8)	2.862(6)
C(7)	C(9)	3.490(6)	C(7)	C(13)	3.528(6)
C(8)	C(11)	2.805(6)	C(9)	C(12)	2.772(7)

C(10) C(13) 2.772(7)

Symmetry Operators:

(1) -X+1,-Y+1,Z

(2) -Y+1,X,-Z+1

(3) Y,-X+1,-Z+1

Table 11: Intramolecular contacts less than 3.60 Å involving hydrogens

atom	atom	distance	atom	atom	distance
Rh(1)	H(14)	3.5537(6)	Rh(1)	H(14) ¹	3.5537(6)
Rh(1)	H(16)	3.4776(5)	Rh(1)	H(16) ¹	3.4776(5)
O(1)	H(7)	2.370(3)	O(1)	H(7)	2.994(3)
O(1)	H(7)	2.939(3)	O(1)	H(14) ²	3.461(3)
O(1)	H(14) ²	2.356(3)	O(1)	H(16) ³	2.370(3)
O(1)	H(16) ³	3.259(3)	N(1)	H(3)	3.451(3)
N(1)	H(3) ¹	3.451(3)	N(1)	H(16)	
N(1)	3.4400(12)		N(2)	H(7)	3.224(4)
N(1)	H(16) ¹	3.4400(12)	N(2)	H(7)	2.753(3)
N(2)	H(7)	2.700(3)	N(2)	H(14)	2.880(3)
N(2)	H(14)	2.839(3)	N(2)	H(16)	2.761(3)
N(2)	H(16)	2.963(3)	C(1)	H(3) ¹	2.628(3)
C(1)	H(3)	2.628(3)	C(2)	H(4)	3.207(3)
C(2)	H(3) ¹	2.0123(6)	C(3)	H(3) ¹	3.215(6)
C(2)	H(4) ¹	3.207(3)	C(3)	H(15)	3.586(6)
C(3)	H(5)	3.217(4)	H(3)	H(4)	2.3007(2)
C(3)	H(15)	3.460(6)	H(3)	C(10)	3.034(5)
H(3)	C(5)	3.210(5)	H(3)	C(11)	2.896(5)
H(3)	H(10)	3.1852(4)			

H(3)	C(12)	3.537(4)	H(3)	C(15)	3.127(6)
H(3)	H(15)	2.8980(5)	H(3)	H(15)	3.0583(5)
C(4)	H(4) ¹	3.139(7)	H(4)	H(5)	2.2616(3)
H(4)	H(15)	3.5105(4)	H(4)	H(15)	3.5578(5)
C(6)	H(14)	2.944(4)	C(6)	H(14)	3.503(5)
C(6)	H(14) ²	2.874(5)	C(6)	H(16) ³	3.032(5)
C(6)	H(16)	2.950(4)	C(6)	H(16) ³	3.515(4)
C(7)	H(14)	3.035(4)	C(7)	H(14) ²	3.096(4)
C(7)	H(16) ³	3.321(4)	C(7)	H(16)	3.112(4)
H(7)	H(14)	3.5919(4)	H(7)	H(14) ²	2.8294(4)
H(7)	H(16) ³	2.8945(4)	H(7)	C(8)	2.755(4)
H(7)	C(9)	2.990(4)	H(7)	C(13)	3.575(4)
H(7)	C(14)	3.056(5)	H(7)	H(14)	2.3520(3)
H(7)	H(16) ³	3.5029(3)	H(7)	C(8)	2.893(4)
H(7)	C(13)	3.157(4)	H(7)	H(14) ²	3.5657(5)
H(7)	H(14) ²	3.0711(3)	H(7)	C(16)	3.190(4)
H(7)	H(16)	2.4595(3)	C(8)	H(10)	3.229(4)
C(8)	H(12)	3.246(4)	C(8)	H(14)	2.729(4)
C(8)	H(14)	2.796(4)	C(8)	H(14)	3.298(4)

Table 11: Intramolecular contacts less than 3.60 Å involving hydrogens (continued)

atom	atom	distance	atom	atom	distance
C(8)	H(16)	2.868(4)	C(8)	H(16)	2.712(4)
C(8)	H(16)	3.304(4)	C(10)	H(12)	3.195(5)

C(10)	H(14)	3.136(4)	C(10)	H(14)	3.100(4)
C(10)	H(14)	2.547(5)	C(10)	H(15)	2.615(4)
C(10)	H(15)	3.224(5)	C(10)	H(15)	3.000(4)
H(10)	C(12)	3.195(5)	H(10)	C(14)	2.640(5)
H(10)	H(14)	3.3158(3)	H(10)	H(14)	3.2548(3)
H(10)	H(14)	2.32317(20)	H(10)	C(15)	2.673(5)
H(10)	H(15)	2.44425(19)	H(10)	H(15)	3.4778(4)
H(10)	H(15)	3.0982(4)	C(12)	H(15)	3.248(5)
C(12)	H(15)	2.607(4)	C(12)	H(15)	2.857(5)
C(12)	H(16)	3.041(5)	C(12)	H(16)	3.166(5)
C(12)	H(16)	2.527(5)	H(12)	C(15)	2.611(6)
H(12)	H(15)	3.4911(4)	H(12)	H(15)	2.4487(2)
H(12)	H(15)	2.8716(4)	H(12)	C(16)	2.628(4)
H(12)	H(16)	3.1536(3)	H(12)	H(16)	3.3789(3)
H(12)	H(16)	2.31658(20)	H(14)	H(16) ³	2.9877(2)
H(14)	H(16) ³	3.5523(3)			

Symmetry Operators:

(1) -X+1,-Y+1,Z

(2) -Y+1,X,-Z+1

(3) Y,-X+1,-Z+1

Table 12: Intermolecular contacts less than 3.60 Å involving hydrogens

atom	atom	distance	atom	atom	distance
O(1)	H(15) ¹	3.181(3)	N(1)	H(15) ²	3.2732(9)
N(1)	H(15) ³	3.2732(9)	N(1)	H(15) ²	
	3.4127(13)				
N(1)	H(15) ³	3.4127(13)	C(1)	H(15) ²	3.2332(8)

C(1)	$H(15)^3$	3.2332(8)	C(1)	$H(15)^2$	3.2115(6)
C(1)	$H(15)^3$	3.2115(6)	C(2)	$H(10)^2$	3.2253(6)
C(2)	$H(10)^3$	3.2253(6)	C(2)	$H(15)^2$	
C(2)	$H(15)^3$	3.5087(18)	C(3)	$H(10)^2$	3.500(6)
C(3)	$H(10)^3$	3.416(6)	C(3)	$H(15)^3$	3.211(5)
C(3)	$H(16)^4$	3.284(5)	H(3)	$C(11)^3$	3.594(6)
H(3)	$C(15)^3$	3.434(6)	H(3)	$H(15)^3$	2.6868(3)
H(3)	$C(16)^4$	3.568(4)	H(3)	$H(16)^4$	3.4249(4)
H(3)	$H(16)^4$	2.8478(3)	C(4)	$H(7)^5$	3.423(7)
C(4)	$H(16)^4$	3.566(7)	C(4)	$H(16)^4$	3.117(7)
H(4)	$C(7)^5$	3.387(4)	H(4)	$H(7)^5$	2.8078(4)
H(4)	$H(7)^3$	3.5378(4)	H(4)	$H(7)^5$	3.1101(3)
H(4)	$C(16)^4$	2.926(5)	H(4)	$H(16)^4$	2.7641(5)
H(4)	$H(16)^4$	3.0585(5)	H(4)	$H(16)^4$	2.4870(4)
C(5)	$H(5)^6$	3.002(6)	H(5)	$C(5)^6$	3.002(6)
H(5)	$H(5)^6$	2.07254(18)	H(5)	$H(7)^2$	3.4643(6)
H(5)	$H(7)^3$	3.4643(6)	C(7)	$H(4)^1$	3.387(4)
H(7)	$C(4)^1$	3.423(7)	H(7)	$H(4)^1$	2.8078(4)
H(7)	$C(14)^7$	3.525(4)	H(7)	$H(14)^7$	3.2776(6)
H(7)	$H(14)^7$	2.9564(4)	H(7)	$C(15)^1$	3.485(4)
H(7)	$H(15)^1$	3.2647(3)	H(7)	$H(15)^1$	2.8891(2)
H(7)	$H(4)^8$	3.5378(4)	H(7)	$H(4)^1$	3.1101(3)
H(7)	$H(5)^8$	3.4643(6)	H(7)	$H(7)^9$	3.0176(5)

H(7)	H(14) ⁷	3.2974(5)	H(7)	H(14) ⁷	3.5396(3)
H(7)	H(16) ⁹	2.9060(4)	H(7)	H(16) ⁹	3.5135(3)
C(9)	H(15) ³	3.313(4)	C(10)	H(15) ³	3.381(4)
H(10)	C(2) ⁸	3.2253(6)	H(10)	C(3) ⁴	3.500(6)
H(10)	C(3) ⁸	3.416(6)	H(10)	C(12) ⁴	3.375(5)
H(10)	H(12) ⁴	2.8941(4)	H(10)	H(15) ⁴	3.5253(6)
H(10)	H(15) ³	3.2720(6)	C(11)	H(3) ⁸	3.594(6)
C(11)	H(12) ⁹	3.547(6)	C(12)	H(10) ²	3.375(5)
C(12)	H(12) ⁹	2.961(4)	C(12)	H(16) ⁹	3.269(4)
H(12)	H(10) ²	2.8941(4)	H(12)	C(11) ⁹	3.547(6)
H(12)	C(12) ⁹	2.961(4)	H(12)	H(12) ⁹	2.3967(4)
H(12)	H(14) ²	3.5710(3)	H(12)	C(15) ⁹	3.548(6)
H(12)	H(15) ⁹	3.5259(4)	H(12)	H(15) ⁹	3.0834(4)
H(12)	H(16) ⁹	3.3520(4)	C(13)	H(15) ²	3.516(4)
C(13)	H(16) ⁹	3.548(4)	C(14)	H(7) ¹⁰	3.525(4)
C(14)	H(15) ³	3.228(5)	H(14)	H(7) ¹⁰	3.2776(6)
H(14)	H(7) ¹⁰	3.2974(5)	H(14)	C(15) ³	3.226(5)
H(14)	H(15) ³	3.3420(4)	H(14)	H(15) ³	3.0178(3)
H(14)	H(15) ³	2.8061(2)	H(14)	H(7) ¹⁰	2.9564(4)
H(14)	H(7) ¹⁰	3.5396(3)	H(14)	H(12) ⁴	3.5710(3)
H(14)	H(15) ⁴	2.7440(4)	H(14)	H(15) ³	3.4337(5)
H(14)	H(15) ³	3.1473(3)	C(15)	H(3) ⁸	3.434(6)
C(15)	H(7) ⁵	3.485(4)	C(15)	H(12) ⁹	3.548(6)

C(15)	H(14) ⁸	3.226(5)	C(15)	H(16) ⁴	3.201(5)
H(15)	O(1) ⁵	3.181(3)	H(15)	N(1) ⁸	3.2732(9)
H(15)	C(1) ⁸	3.2332(8)	H(15)	H(7) ⁵	3.2647(3)
H(15)	C(13) ⁴	3.516(4)	H(15)	H(14) ⁸	3.3420(4)
H(15)	C(16) ⁴	3.026(5)	H(15)	H(16) ⁴	2.3071(2)
H(15)	H(16) ⁴	3.0904(5)	H(15)	H(7) ⁵	2.8891(2)
H(15)	H(10) ²	3.5253(6)	H(15)	H(12) ⁹	3.5259(4)
H(15)	H(14) ⁸	3.0178(3)	H(15)	H(14) ²	2.7440(4)
H(15)	H(14) ⁸	3.4337(5)	H(15)	H(16) ⁴	3.3742(5)
H(15)	N(1) ⁸	3.4127(13)	H(15)	C(1) ⁸	3.2115(6)
H(15)	C(2) ⁸	3.5087(18)	H(15)	C(3) ⁸	3.211(5)
H(15)	H(3) ⁸	2.6868(3)	H(15)	C(9) ⁸	3.313(4)
H(15)	C(10) ⁸	3.381(4)	H(15)	H(10) ⁸	3.2720(6)
H(15)	H(12) ⁹	3.0834(4)	H(15)	C(14) ⁸	3.228(5)
H(15)	H(14) ⁸	2.8061(2)	H(15)	H(14) ⁸	3.1473(3)
C(16)	H(3) ²	3.568(4)	C(16)	H(4) ²	2.926(5)
C(16)	H(15) ²	3.026(5)	H(16)	H(3) ²	3.4249(4)
H(16)	C(4) ²	3.566(7)	H(16)	H(4) ²	2.7641(5)
H(16)	C(15) ²	3.201(5)	H(16)	H(15) ²	2.3071(2)
H(16)	H(15) ²	3.3742(5)	H(16)	H(4) ²	3.0585(5)
H(16)	H(7) ⁹	2.9060(4)	H(16)	C(3) ²	3.284(5)
H(16)	H(3) ²	2.8478(3)	H(16)	C(4) ²	3.117(7)
H(16)	H(4) ²	2.4870(4)	H(16)	H(7) ⁹	3.5135(3)

H(16)	$C(12)^9$	3.269(4)	H(16)	$H(12)^9$	3.3520(4)
H(16)	$C(13)^9$	3.548(4)	H(16)	$H(15)^2$	3.0904(5)

Symmetry Operators:

- | | |
|---------------------------------|-----------------------------------|
| (1) $Y+1/2, X+1/2-1, Z+1/2-1$ | (2) $-X+1/2+1, Y+1/2, -Z+1/2+1$ |
| (3) $X+1/2-1, -Y+1/2, -Z+1/2+1$ | (4) $-X+1/2+1, Y+1/2-1, -Z+1/2+1$ |
| (5) $Y+1/2, X+1/2-1, Z+1/2$ | (6) $Y, -X+1, -Z+2$ |
| (7) $Y+1, -X+1, -Z+1$ | (8) $X+1/2, -Y+1/2, -Z+1/2+1$ |
| (9) $-X+2, -Y+1, Z$ | (10) $-Y+1, X-1, -Z+1$ |

Appendix B

Crystallographic Report for Ba_{1.5}[Fe(C₁₀H₁₃N₂O₇)] [Co(CN)₆]·9H₂O

Experimental Details

A. Crystal Data

Empirical Formula	C ₁₆ H ₃₁ Ba _{1.50} CoFeN ₈ O ₁₆
Formula Weight	912.24 g/mol
Crystal Color, Habit	yellow, prism
Crystal Dimensions	0.260 X 0.25 X 0.060 mm
Crystal System	triclinic
Lattice Type	Primitive
Lattice Parameters	a = 13.634 (2) Å b = 13.768 (2) Å c = 17.254(2) α = 84.795 (6)° β = 87.863 (6)° γ = 78.908 (6)° V = 2592.6 (7) Å ³
Space Group	P-1 (#2)
Z value	4
D _{calc}	1.915 g/cm ³
F ₀₀₀	1792.00
μ(MoKα)	28.878 cm ⁻¹

B. Intensity Measurements

Diffractometer	Rigaku Mercury375R/M CCD (XtaLAB mini)
Radiation	MoKα (λ = 0.71075 Å)

Temperature	25.0°C
Detector Aperture	75 mm (diameter)
Data Images	540 exposures
ω oscillation Range ($\chi=54.0$, $\varphi=0.0$)	-60.0 - 120.0°
Exposure Rate	16.0 sec./°
Detector Swing Angle	29.50°
ω oscillation Range ($\chi=54.0$, $\varphi=120.0$)	-60.0 - 120.0°
Exposure Rate	16.0 sec./°
Detector Swing Angle	29.50°
ω oscillation Range ($\chi=54.0$, $\varphi=240.0$)	-60.0 - 120.0°
Exposure Rate	16.0 sec./°
Detector Swing Angle	29.50°
ω oscillation Range ($\chi=54.0$, $\varphi=240.0$)	-60.0 - 120.0°
Exposure Rate	30.0 sec./°
Detector Swing Angle	30.00°
ω oscillation Range ($\chi=54.0$, $\varphi=120.0$)	-60.0 - 120.0°
Exposure Rate	30.0 sec./°
Detector Swing Angle	30.00°
ω oscillation Range ($\chi=54.0$, $\varphi=0.0$)	-60.0 - 120.0°
Exposure Rate	30.0 sec./°
Detector Swing Angle	30.00°

Detector Position	50.00 mm
Pixel Size	0.146 mm
$2\theta_{\max}$	55.0°
No. of Reflections Measured	Total: 33318 Unique: 14477 ($R_{\text{int}} = 0.0372$)
Corrections	Lorentz-polarization Absorption (trans. factors: 0.542 - 0.841)

C. Structure Solution and Refinement

Structure Solution	Direct Methods
Refinement	Full-matrix least-squares on F^2
Function Minimized	$\Sigma w (F_o^2 - F_c^2)^2$
Least Squares Weights	$w = 1 / [\sigma^2(F_o^2) + (0.0677 \cdot P)^2 + 10.6494 \cdot P]$ where $P = (\text{Max}(F_o^2, 0) + 2F_c^2) / 3$
$2\theta_{\max}$ cutoff	55.0°
Anomalous Dispersion	All non-hydrogen atoms
No. Observations (All reflections)	14477
No. Variables	770
Reflection/Parameter Ratio	18.80
Residuals: R1 ($I > 2.00\sigma(I)$)	0.0438
Residuals: R (All reflections)	0.0571
Residuals: wR2 (All reflections)	0.1308
Goodness of Fit Indicator	0.974
Max Shift/Error in Final Cycle	0.001

Maximum peak in Final Diff. Map $2.09 \text{ e}^-/\text{\AA}^3$

Minimum peak in Final Diff. Map $-1.63 \text{ e}^-/\text{\AA}^3$

Table 13: Atomic coordinates and $B_{\text{ISO}}/B_{\text{EQ}}$ and occupancy

atom	x	y	z	B_{eq}	occ
Ba(1a)	0.56057(2)	0.06310(2)	0.25453(2)	1.557(7)	0.826(1)
Ba(1b)	0.4415(2)	-0.0729(2)	0.2490(2)	3.15(5)	0.174(1)
Ba(2)	0.91642(2)	0.36872(2)	0.21312(2)	1.573(7)	1
Ba(3)	0.08962(2)	0.62990(2)	0.28396(2)	1.615(7)	1
Co(4)	0.0000	0.0000	0.0000	1.65(2)	1/2
Co(5)	0.50265(4)	0.49448(4)	0.25029(3)	1.50(2)	1
Co(10)	1.0000	1.0000	0.5000	2.21(2)	1/2
Fe(6)	0.18741(5)	0.26662(5)	0.05298(3)	1.43(1)	1
Fe(7)	0.82169(5)	0.72963(5)	0.44449(3)	1.47(2)	1
O(9)	0.2921(3)	0.1860(3)	0.1194(2)	2.15(6)	1
O(15)	0.1167(3)	0.3272(3)	0.1449(2)	1.77(5)	1
O(17)	0.8868(3)	0.6729(3)	0.3501(2)	1.79(5)	1
O(18)	0.1053(3)	0.3529(3)	-0.0282(2)	2.23(6)	1
O(20)	0.6308(4)	0.8895(4)	0.6803(3)	4.3(1)	1
O(25)	0.9070(3)	0.6400(3)	0.5216(2)	2.15(6)	1
O(31)	0.9399(3)	0.4930(3)	0.5892(2)	2.66(7)	1
O(33)	0.3120(4)	0.1194(4)	-0.2249(3)	4.6(1)	1
O(35)	0.5754(3)	0.9302(4)	0.3872(3)	3.87(9)	1

O(36)	0.6211(5)	0.0985(5)	0.5382(4)	5.9(2)	1
O(37)	0.4399(3)	0.0845(4)	0.1274(3)	3.76(9)	1
O(44)	0.5807(4)	0.1704(4)	0.3829(3)	4.7(1)	1
O(45)	0.0593(3)	0.5049(3)	-0.0871(2)	2.61(7)	1
O(54)	0.7112(3)	0.8126(3)	0.3835(2)	1.99(6)	1
O(55)	0.8960(3)	0.5566(3)	0.2688(2)	2.14(6)	1
O(60)	0.1094(3)	0.4403(3)	0.2287(2)	2.11(6)	1
O(82)	0.8426(4)	0.2803(4)	0.0950(3)	4.6(1)	1
O(84)	0.7605(4)	0.0404(5)	0.2962(4)	6.2(2)	1
O(87)	0.1568(4)	0.7218(4)	0.4021(3)	4.9(1)	1
O(88)	0.3564(4)	0.6994(4)	0.4415(3)	4.5(1)	1
O(89)	0.6747(5)	0.0893(6)	0.1165(4)	8.0(2)	1
O(100)	0.9868(4)	0.1650(4)	0.2323(3)	4.5(1)	1
O(103)	0.3594(4)	0.6968(5)	0.9460(3)	5.4(2)	1
O(105)	0.0201(5)	0.8332(4)	0.2645(3)	5.1(1)	1
O(107)	0.0503(5)	0.6700(4)	0.1279(3)	5.4(2)	1
O(109)	0.9517(5)	0.3266(4)	0.3706(3)	4.9(2)	1
O(113)	0.2383(4)	0.7108(5)	0.2014(4)	6.5(2)	1
O(115)	0.7680(4)	0.2828(5)	0.2920(4)	6.6(2)	1
O(117)	1.2494(6)	1.0057(8)	0.2257(6)	12.1(4)	1
N(8)	-0.1022(4)	0.0028(4)	0.1604(3)	3.17(9)	1
N(12)	0.1636(4)	-0.1675(5)	0.0636(4)	4.3(2)	1
N(14)	0.1106(4)	0.1563(4)	0.0409(3)	2.61(8)	1

N(22)	0.2519(3)	0.3989(3)	0.0543(2)	1.54(6)	1
N(27)	0.7103(3)	0.7652(3)	0.5385(2)	1.89(7)	1
N(29)	0.3066(3)	0.2278(3)	-0.0356(2)	1.82(7)	1
N(30)	0.7158(3)	0.4779(4)	0.1857(3)	2.55(8)	1
N(32)	0.5094(4)	0.2823(4)	0.2081(3)	3.31(9)	1
N(34)	0.5798(4)	0.4030(4)	0.4097(3)	3.30(9)	1
N(39)	0.4246(4)	0.5843(4)	0.0902(3)	3.03(9)	1
N(40)	0.2881(3)	0.5168(4)	0.3129(3)	2.38(8)	1
N(41)	0.5008(4)	0.7015(4)	0.2992(3)	3.40(9)	1
N(43)	0.8352(5)	1.1631(5)	0.4311(4)	4.5(2)	1
N(46)	1.1026(5)	0.9996(5)	0.3400(3)	4.5(2)	1
N(52)	0.8979(4)	0.8413(4)	0.4561(3)	2.46(8)	1
N(64)	0.7539(3)	0.5990(3)	0.4431(3)	1.73(6)	1
C(13)	0.1034(4)	-0.1024(4)	0.0399(3)	2.47(9)	1
C(16)	0.5046(4)	0.3634(4)	0.2234(3)	2.02(8)	1
C(19)	0.6350(4)	0.4855(4)	0.2097(3)	1.85(8)	1
C(21)	0.5020(4)	0.6236(4)	0.2794(3)	2.00(8)	1
C(23)	0.4548(4)	0.5493(4)	0.1503(3)	1.98(8)	1
C(24)	0.7574(4)	0.5778(4)	0.3609(3)	1.93(8)	1
C(26)	0.3495(4)	0.3197(4)	-0.0529(3)	2.21(8)	1
C(28)	0.5507(4)	0.4386(4)	0.3499(3)	2.06(8)	1
C(38)	0.3692(4)	0.5060(4)	0.2896(3)	1.74(7)	1
C(42)	0.6569(4)	0.6795(4)	0.5512(3)	2.26(9)	1

C(47)	1.0647(5)	1.0001(5)	0.4014(4)	3.0(1)	1
C(48)	0.6441(4)	0.8577(4)	0.5084(3)	2.7(1)	1
C(49)	0.7591(5)	0.7777(5)	0.6129(3)	2.9(1)	1
C(50)	0.8960(5)	1.1005(4)	0.4577(4)	2.8(1)	1
C(51)	0.3730(4)	0.1369(4)	0.0896(3)	2.33(9)	1
C(56)	0.3806(4)	0.1446(4)	0.0014(3)	2.9(1)	1
C(57)	0.8161(4)	0.5169(4)	0.4924(3)	2.03(8)	1
C(58)	0.0698(4)	0.0958(4)	0.0263(3)	2.05(8)	1
C(59)	0.1880(4)	0.4811(4)	0.0062(3)	1.96(8)	1
C(68)	0.9336(4)	0.8996(4)	0.4726(3)	2.56(9)	1
C(69)	0.3545(4)	0.3724(4)	0.0204(3)	2.03(8)	1
C(70)	0.8536(4)	0.6012(4)	0.3228(3)	1.58(7)	1
C(71)	0.6513(4)	0.6292(4)	0.4765(3)	1.98(8)	1
C(76)	-0.0638(4)	0.0008(4)	0.0992(3)	2.35(9)	1
C(77)	0.3445(6)	0.1766(6)	-0.1728(4)	4.3(2)	1
C(78)	0.6405(4)	0.8696(4)	0.4198(3)	2.23(8)	1
C(79)	0.1505(3)	0.3966(4)	0.1739(3)	1.53(7)	1
C(83)	0.2477(4)	0.4205(4)	0.1369(3)	1.75(7)	1
C(86)	0.1121(4)	0.4453(4)	-0.0404(3)	1.89(8)	1
C(104)	0.8929(4)	0.5503(4)	0.5383(3)	1.95(8)	1
C(114)	0.2665(5)	0.1996(5)	-0.1077(3)	2.7(1)	1
C(116)	0.6906(6)	0.7958(5)	0.6837(4)	3.8(2)	1

$$B_{eq} = 8/3 \pi^2 (U_{11}(aa^*)^2 + U_{22}(bb^*)^2 + U_{33}(cc^*)^2 + 2U_{12}(aa^*bb^*)\cos \gamma + 2U_{13}(aa^*cc^*)\cos \beta + 2U_{23}(bb^*cc^*)\cos \alpha)$$

Table 14: Atomic coordinates and B_{iso} involving hydrogen atoms

atom	x	y	z	B_{iso}	occ
H(11A)	0.2141	0.2534	-0.1271	3.24	1
H(11B)	0.2365	0.1416	-0.0946	3.24	1
H(11C)	0.6480	0.7466	0.6889	4.54	1
H(11D)	0.7310	0.7867	0.7298	4.54	1
H(24A)	0.7002	0.6180	0.3342	2.32	1
H(24B)	0.7550	0.5084	0.3573	2.32	1
H(26A)	0.3085	0.3644	-0.0908	2.65	1
H(26B)	0.4162	0.3022	-0.0753	2.65	1
H(42A)	0.5897	0.7028	0.5708	2.71	1
H(42B)	0.6914	0.6311	0.5903	2.71	1
H(48A)	0.6673	0.9139	0.5264	3.19	1
H(48B)	0.5771	0.8581	0.5294	3.19	1
H(49A)	0.7940	0.8329	0.6035	3.43	1
H(49B)	0.8091	0.7184	0.6255	3.43	1
H(56A)	0.4474	0.1537	-0.0148	3.48	1
H(56B)	0.3706	0.0827	-0.0170	3.48	1
H(57A)	0.8498	0.4671	0.4591	2.44	1
H(57B)	0.7725	0.4858	0.5282	2.44	1

H(59A)	0.2305	0.5141	-0.0293	2.35	1
H(59B)	0.1532	0.5295	0.0401	2.35	1
H(69A)	0.3976	0.3292	0.0579	2.44	1
H(69B)	0.3820	0.4320	0.0078	2.44	1
H(71A)	0.6209	0.5712	0.4878	2.38	1
H(71B)	0.6103	0.6747	0.4392	2.38	1
H(77A)	0.3564	0.2382	-0.2000	5.17	1
H(77B)	0.4070	0.1413	-0.1506	5.17	1
H(83A)	0.2498	0.4900	0.1405	2.10	1
H(83B)	0.3046	0.3805	0.1640	2.10	1

Table 15: Anisotropic displacement parameters

atom	U ₁₁	U ₂₂	U ₃₃	U ₁₂	U ₁₃	U ₂₃
Ba(1a)	0.0223(2)	0.0168(2)	0.0174(2)	0.0024(1)	-0.0002(1)	-
	0.0008(1)					
Ba(1b)	0.034(1)	0.039(2)	0.047(2)	-0.0023(8)	0.0006(9)	-
	0.0122(9)					
Ba(2)	0.0197(2)	0.0191(2)	0.0202(2)	-0.0018(1)	0.0010(1)	-
	0.0016(1)					
Ba(3)	0.0206(2)	0.0191(2)	0.0205(2)	-0.0013(1)	0.0003(1)	-
	0.0015(1)					
Co(4)	0.0237(5)	0.0171(5)	0.0231(5)	-0.0062(4)	-0.0002(4)	-
	0.0023(4)					
Co(5)	0.0165(3)	0.0195(3)	0.0200(3)	-0.0021(3)	0.0010(3)	-

0.0005(3)						
Co(10)	0.0349(5)	0.0232(5)	0.0277(5)	-0.0101(4)	-0.0037(4)	-
0.0011(4)						
Fe(6)	0.0205(3)	0.0166(3)	0.0175(3)	-0.0038(3)	0.0002(3)	-
0.0036(3)						
Fe(7)	0.0211(3)	0.0163(3)	0.0176(3)	-0.0014(3)	0.0002(3)	-
0.0025(3)						
O(9)	0.028(2)	0.030(2)	0.020(2)	0.002(2)	0.001(2)	-0.002(2)
O(15)	0.020(2)	0.024(2)	0.025(2)	-0.007(2)	0.004(2)	-0.008(2)
O(17)	0.022(2)	0.024(2)	0.023(2)	-0.006(2)	0.003(2)	-0.006(2)
O(18)	0.032(2)	0.023(2)	0.029(2)	-0.005(2)	-0.011(2)	0.000(2)
O(20)	0.056(3)	0.057(3)	0.046(3)	0.004(3)	0.018(3)	-0.014(3)
O(25)	0.029(2)	0.024(2)	0.028(2)	-0.003(2)	-0.006(2)	-0.002(2)
O(31)	0.032(2)	0.036(2)	0.027(2)	0.002(2)	-0.002(2)	0.011(2)
O(33)	0.073(4)	0.054(3)	0.043(3)	-0.003(3)	0.010(3)	-0.011(2)
O(35)	0.043(3)	0.050(3)	0.038(3)	0.022(2)	0.005(2)	0.013(2)
O(36)	0.078(4)	0.080(4)	0.070(4)	-0.021(3)	0.006(3)	-0.009(3)
O(37)	0.043(3)	0.048(3)	0.042(3)	0.012(2)	-0.009(2)	0.006(2)
O(44)	0.070(4)	0.057(3)	0.050(3)	-0.007(3)	-0.001(3)	-0.009(3)
O(45)	0.029(2)	0.038(2)	0.028(2)	-0.000(2)	-0.001(2)	0.007(2)
O(54)	0.028(2)	0.027(2)	0.018(2)	0.002(2)	0.000(2)	0.000(2)
O(55)	0.027(2)	0.027(2)	0.027(2)	-0.003(2)	0.002(2)	-0.009(2)
O(60)	0.025(2)	0.028(2)	0.027(2)	-0.004(2)	0.004(2)	-0.007(2)

O(82)	0.067(3)	0.051(3)	0.059(3)	-0.005(3)	-0.017(3)	-0.023(3)
O(84)	0.045(3)	0.121(6)	0.071(4)	-0.010(3)	0.006(3)	-0.030(4)
O(87)	0.068(4)	0.055(3)	0.065(3)	-0.003(3)	-0.017(3)	-0.030(3)
O(88)	0.064(3)	0.074(4)	0.031(3)	-0.005(3)	-0.006(2)	-0.003(3)
O(89)	0.069(4)	0.134(6)	0.084(5)	-0.004(4)	0.023(4)	0.037(4)
O(100)	0.077(4)	0.031(3)	0.057(3)	0.002(3)	-0.013(3)	-0.003(2)
O(103)	0.065(4)	0.096(5)	0.034(3)	0.004(3)	-0.002(3)	0.006(3)
O(105)	0.096(4)	0.029(3)	0.064(3)	0.005(3)	-0.017(3)	-0.001(2)
O(107)	0.101(4)	0.078(4)	0.040(3)	-0.055(4)	-0.030(3)	0.014(3)
O(109)	0.096(4)	0.067(4)	0.036(3)	-0.042(3)	-0.025(3)	0.007(3)
O(113)	0.038(3)	0.087(5)	0.107(5)	-0.005(3)	0.004(3)	0.059(4)
O(115)	0.036(3)	0.089(5)	0.110(5)	-0.008(3)	0.003(3)	0.059(4)
O(117)	0.065(5)	0.21(1)	0.144(8)	0.019(5)	0.026(5)	0.091(7)
N(8)	0.042(3)	0.044(3)	0.032(3)	-0.005(3)	0.008(2)	-0.003(2)
N(12)	0.047(3)	0.049(4)	0.057(4)	0.007(3)	-0.003(3)	0.010(3)
N(14)	0.036(3)	0.029(3)	0.037(3)	-0.012(2)	0.003(2)	-0.005(2)
N(22)	0.019(2)	0.021(2)	0.018(2)	-0.003(2)	0.001(2)	-0.004(2)
N(27)	0.030(2)	0.022(2)	0.019(2)	-0.002(2)	0.004(2)	-0.004(2)
N(29)	0.032(2)	0.020(2)	0.017(2)	-0.005(2)	0.003(2)	-0.004(2)
N(30)	0.023(2)	0.038(3)	0.032(3)	-0.001(2)	0.002(2)	0.003(2)
N(32)	0.051(3)	0.026(3)	0.049(3)	-0.006(2)	0.001(3)	-0.007(2)
N(34)	0.044(3)	0.048(3)	0.032(3)	-0.008(3)	-0.007(2)	0.003(2)
N(39)	0.037(3)	0.045(3)	0.032(3)	-0.010(2)	-0.005(2)	0.005(2)

N(40)	0.022(2)	0.036(3)	0.029(3)	-0.001(2)	0.003(2)	0.006(2)
N(41)	0.047(3)	0.031(3)	0.052(3)	-0.008(2)	0.005(3)	-0.011(3)
N(43)	0.051(4)	0.049(4)	0.062(4)	0.001(3)	-0.007(3)	0.012(3)
N(46)	0.067(4)	0.066(4)	0.035(3)	-0.011(3)	0.009(3)	-0.005(3)
N(52)	0.037(3)	0.027(3)	0.031(3)	-0.004(2)	-0.002(2)	-0.012(2)
N(64)	0.021(2)	0.021(2)	0.024(2)	-0.003(2)	0.002(2)	-0.003(2)
C(13)	0.031(3)	0.028(3)	0.033(3)	-0.004(2)	-0.001(3)	0.003(2)
C(16)	0.024(3)	0.026(3)	0.026(3)	-0.002(2)	0.000(2)	-0.001(2)
C(19)	0.023(3)	0.022(3)	0.025(3)	-0.003(2)	0.000(2)	-0.001(2)
C(21)	0.025(3)	0.025(3)	0.025(3)	-0.005(2)	0.003(2)	-0.003(2)
C(23)	0.022(3)	0.028(3)	0.026(3)	-0.006(2)	0.004(2)	-0.004(2)
C(24)	0.025(3)	0.026(3)	0.024(3)	-0.007(2)	-0.002(2)	-0.005(2)
C(26)	0.034(3)	0.024(3)	0.027(3)	-0.008(2)	0.011(2)	-0.004(2)
C(28)	0.022(3)	0.027(3)	0.028(3)	-0.003(2)	-0.000(2)	-0.002(2)
C(38)	0.022(3)	0.022(3)	0.021(2)	-0.002(2)	-0.001(2)	0.002(2)
C(42)	0.032(3)	0.030(3)	0.023(3)	-0.005(2)	0.011(2)	-0.003(2)
C(47)	0.045(4)	0.034(3)	0.036(3)	-0.008(3)	-0.003(3)	-0.001(3)
C(48)	0.039(3)	0.025(3)	0.030(3)	0.008(2)	0.011(3)	-0.002(2)
C(49)	0.042(3)	0.046(4)	0.019(3)	-0.000(3)	0.000(3)	-0.008(3)
C(50)	0.041(3)	0.031(3)	0.036(3)	-0.007(3)	-0.004(3)	-0.003(3)
C(51)	0.031(3)	0.025(3)	0.031(3)	0.000(2)	-0.001(2)	-0.002(2)
C(56)	0.038(3)	0.034(3)	0.031(3)	0.008(3)	0.009(3)	0.000(3)
C(57)	0.031(3)	0.018(3)	0.026(3)	-0.000(2)	-0.001(2)	0.000(2)

C(58)	0.031(3)	0.025(3)	0.024(3)	-0.009(2)	0.001(2)	-0.001(2)
C(59)	0.030(3)	0.019(3)	0.024(3)	-0.003(2)	-0.002(2)	-0.000(2)
C(68)	0.030(3)	0.036(3)	0.029(3)	-0.003(3)	-0.000(2)	-0.001(3)
C(69)	0.022(3)	0.030(3)	0.028(3)	-0.010(2)	0.009(2)	-0.008(2)
C(70)	0.023(2)	0.019(3)	0.017(2)	0.000(2)	-0.001(2)	-0.001(2)
C(71)	0.018(2)	0.023(3)	0.034(3)	-0.002(2)	0.006(2)	-0.004(2)
C(76)	0.028(3)	0.026(3)	0.036(3)	-0.008(2)	-0.004(3)	-0.002(2)
C(77)	0.070(5)	0.080(5)	0.025(3)	-0.037(4)	0.019(3)	-0.021(3)
C(78)	0.032(3)	0.021(3)	0.027(3)	0.004(2)	0.007(2)	0.002(2)
C(79)	0.020(2)	0.020(3)	0.017(2)	-0.002(2)	-0.002(2)	-0.003(2)
C(83)	0.023(3)	0.025(3)	0.020(2)	-0.006(2)	0.000(2)	-0.005(2)
C(86)	0.028(3)	0.023(3)	0.019(2)	-0.001(2)	0.002(2)	-0.002(2)
C(104)	0.022(3)	0.027(3)	0.022(3)	0.002(2)	0.003(2)	-0.003(2)
C(114)	0.044(3)	0.043(4)	0.018(3)	-0.014(3)	0.004(2)	-0.009(2)
C(116)	0.066(5)	0.050(4)	0.025(3)	-0.000(3)	0.008(3)	-0.009(3)

The general temperature factor expression: $\exp(-2\pi^2(a^2U_{11}h^2 + b^2U_{22}k^2 + c^2U_{33}l^2 + 2a*b*U_{12}hk + 2a*c*U_{13}hl + 2b*c*U_{23}kl))$

Table 16: Bond lengths (Å)

atom	atom	distance	atom	atom	distance
Ba(1a)	O(20) ¹	2.785(5)	Ba(1a)	O(33) ²	2.842(5)
Ba(1a)	O(35) ³	2.785(4)	Ba(1a)	O(37)	2.751(5)

Ba(1a)	O(44)	2.820(5)	Ba(1a)	O(84)	2.797(6)
Ba(1a)	O(89)	2.830(7)	Ba(2)	O(15) ⁴	2.906(3)
Ba(2)	O(45) ⁵	2.710(4)	Ba(2)	O(55)	2.800(4)
Ba(2)	O(82)	2.779(6)	Ba(2)	O(100)	2.778(5)
Ba(2)	O(109)	2.767(5)	Ba(2)	O(115)	2.788(6)
Ba(2)	N(30)	2.889(4)	Ba(3)	O(17) ⁶	2.925(3)
Ba(3)	O(31) ¹	2.709(4)	Ba(3)	O(60)	2.821(4)
Ba(3)	O(87)	2.767(6)	Ba(3)	O(105)	2.771(5)
Ba(3)	O(107)	2.751(5)	Ba(3)	O(113)	2.784(6)
Ba(3)	N(40)	2.886(4)	Co(4)	C(13)	1.892(5)
Co(4)	C(13) ⁷	1.892(5)	Co(4)	C(58)	1.865(6)
Co(4)	C(58) ⁷	1.865(6)	Co(4)	C(76)	1.890(6)
Co(4)	C(76) ⁷	1.890(6)	Co(5)	C(16)	1.899(6)
Co(5)	C(19)	1.896(5)	Co(5)	C(21)	1.889(6)
Co(5)	C(23)	1.905(5)	Co(5)	C(28)	1.903(5)
Co(5)	C(38)	1.901(5)	Co(10)	C(47)	1.887(6)
Co(10)	C(47) ⁸	1.887(6)	Co(10)	C(50)	1.897(5)
Co(10)	C(50) ⁸	1.897(5)	Co(10)	C(68)	1.894(6)
Co(10)	C(68) ⁸	1.894(6)	Fe(6)	O(9)	1.966(4)
Fe(6)	O(15)	1.990(3)	Fe(6)	O(18)	1.983(4)
Fe(6)	N(14)	2.033(5)	Fe(6)	N(22)	2.172(4)
Fe(6)	N(29)	2.211(4)	Fe(7)	O(17)	1.977(4)
Fe(7)	O(25)	1.978(4)	Fe(7)	O(54)	1.980(3)

Fe(7)	N(27)	2.202(4)	Fe(7)	N(52)	2.042(5)
Fe(7)	N(64)	2.177(5)	O(9)	C(51)	1.293(6)
O(15)	C(79)	1.284(6)	O(17)	C(70)	1.294(6)
O(18)	C(86)	1.291(6)	O(20)	C(116)	1.385(8)
O(25)	C(104)	1.290(7)	O(31)	C(104)	1.237(6)
O(33)	C(77)	1.384(10)	O(35)	C(78)	1.212(6)
O(37)	C(51)	1.219(6)	O(45)	C(86)	1.240(6)
O(54)	C(78)	1.299(6)	O(55)	C(70)	1.227(6)
O(60)	C(79)	1.226(6)	N(8)	C(76)	1.162(7)
N(12)	C(13)	1.149(7)	N(14)	C(58)	1.137(8)
N(22)	C(59)	1.494(6)	N(22)	C(69)	1.488(6)
N(22)	C(83)	1.479(6)	N(27)	C(42)	1.498(7)
N(27)	C(48)	1.475(6)	N(27)	C(49)	1.507(7)
N(29)	C(26)	1.496(7)	N(29)	C(56)	1.486(6)
N(29)	C(114)	1.490(7)	N(30)	C(19)	1.153(6)
N(32)	C(16)	1.159(8)	N(34)	C(28)	1.153(7)
N(39)	C(23)	1.159(7)	N(40)	C(38)	1.149(6)
N(41)	C(21)	1.152(8)	N(43)	C(50)	1.150(8)
N(46)	C(47)	1.162(8)	N(52)	C(68)	1.079(8)
N(64)	C(24)	1.471(6)	N(64)	C(57)	1.494(6)
N(64)	C(71)	1.490(6)	C(24)	C(70)	1.521(7)
C(26)	C(69)	1.525(8)	C(42)	C(71)	1.528(8)
C(48)	C(78)	1.525(7)	C(49)	C(116)	1.519(8)

C(51)	C(56)	1.517(8)	C(57)	C(104)	1.499(8)
C(59)	C(86)	1.513(8)	C(77)	C(114)	1.529(8)
C(79)	C(83)	1.530(7)			

Symmetry Operators:

- | | |
|--------------------|--------------------|
| (1) -X+1,-Y+1,-Z+1 | (2) -X+1,-Y,-Z |
| (3) X,Y-1,Z | (4) X+1,Y,Z |
| (5) -X+1,-Y+1,-Z | (6) X-1,Y,Z |
| (7) -X,-Y,-Z | (8) -X+2,-Y+2,-Z+1 |

Table 17: Bond lengths involving hydrogens (Å)

atom	atom	distance	atom	atom	distance
C(24)	H(24A)	0.970	C(24)	H(24B)	0.970
C(26)	H(26A)	0.970	C(26)	H(26B)	0.970
C(42)	H(42A)	0.970	C(42)	H(42B)	0.970
C(48)	H(48A)	0.970	C(48)	H(48B)	0.970
C(49)	H(49A)	0.970	C(49)	H(49B)	0.970
C(56)	H(56A)	0.970	C(56)	H(56B)	0.970
C(57)	H(57A)	0.970	C(57)	H(57B)	0.970
C(59)	H(59A)	0.970	C(59)	H(59B)	0.970
C(69)	H(69A)	0.970	C(69)	H(69B)	0.970
C(71)	H(71A)	0.970	C(71)	H(71B)	0.970
C(77)	H(77A)	0.970	C(77)	H(77B)	0.970
C(83)	H(83A)	0.970	C(83)	H(83B)	0.970

C(114)H(11A)	0.970	C(114)H(11B)	0.970
C(116)H(11C)	0.970	C(116)H(11D)	0.970

Table 18: Bond angles ^(o)

atom	atom	atom	angle	atom	atom	atom	angle
O(20) ¹	Ba(1a)	O(33) ²	133.31(15)	O(20) ¹	Ba(1a)	O(35) ³	78.62(13)
O(20) ¹	Ba(1a)	O(37)	77.12(13)	O(20) ¹	Ba(1a)	O(44)	74.43(15)
O(20) ¹	Ba(1a)	O(84)	139.86(16)	O(20) ¹	Ba(1a)	O(89)	143.02(15)
O(33) ²	Ba(1a)	O(35) ³	69.47(13)	O(33) ²	Ba(1a)	O(37)	98.87(13)
O(33) ²	Ba(1a)	O(44)	123.64(14)	O(33) ²	Ba(1a)	O(84)	63.26(18)
O(33) ²	Ba(1a)	O(89)	70.20(17)	O(35) ³	Ba(1a)	O(37)	131.04(14)
O(35) ³	Ba(1a)	O(44)	72.52(14)	O(35) ³	Ba(1a)	O(84)	76.26(16)
O(35) ³	Ba(1a)	O(89)	136.79(16)	O(37)	Ba(1a)	O(44)	137.47(13)
O(37)	Ba(1a)	O(84)	142.25(15)	O(37)	Ba(1a)	O(89)	70.27(16)
O(44)	Ba(1a)	O(84)	68.43(17)	O(44)	Ba(1a)	O(89)	120.04(19)
O(84)	Ba(1a)	O(89)	72.32(18)	O(15) ⁴	Ba(2)	O(45) ⁵	67.33(10)
O(15) ⁴	Ba(2)	O(55)	105.66(10)	O(15) ⁴	Ba(2)	O(82)	90.78(12)
O(15) ⁴	Ba(2)	O(100)	71.76(13)	O(15) ⁴	Ba(2)	O(109)	102.46(14)
O(15) ⁴	Ba(2)	O(115)	144.13(13)	O(15) ⁴	Ba(2)	N(30)	143.40(11)
O(45) ⁵	Ba(2)	O(55)	74.18(11)	O(45) ⁵	Ba(2)	O(82)	78.22(13)
O(45) ⁵	Ba(2)	O(100)	127.75(13)	O(45) ⁵	Ba(2)	O(109)	144.37(15)
O(45) ⁵	Ba(2)	O(115)	140.29(14)	O(45) ⁵	Ba(2)	N(30)	76.98(12)

O(55) Ba(2) O(82) 138.84(12)	O(55) Ba(2) O(100) 149.64(13)
O(55) Ba(2) O(109) 76.41(13)	O(55) Ba(2) O(115) 104.87(15)
O(55) Ba(2) N(30) 70.65(12)	O(82) Ba(2) O(100) 71.18(14)
O(82) Ba(2) O(109) 137.26(16)	O(82) Ba(2) O(115) 78.24(18)
O(82) Ba(2) N(30) 73.82(14)	O(100) Ba(2) O(109) 74.80(15)
O(100) Ba(2) O(115) 72.38(16)	O(100) Ba(2) N(30) 129.71(15)
O(109) Ba(2) O(115) 67.24(18)	O(109) Ba(2) N(30) 111.42(14)
O(115) Ba(2) N(30) 65.96(14)	O(17) ⁶ Ba(3) O(31) ¹ 66.48(9)
O(17) ⁶ Ba(3) O(60) 105.24(10)	O(17) ⁶ Ba(3) O(87) 89.71(13)
O(17) ⁶ Ba(3) O(105) 71.55(14)	O(17) ⁶ Ba(3) O(107) 100.37(14)
O(17) ⁶ Ba(3) O(113) 144.91(13)	O(17) ⁶ Ba(3) N(40) 143.29(10)
O(31) ¹ Ba(3) O(60) 74.81(11)	O(31) ¹ Ba(3) O(87) 78.17(14)
O(31) ¹ Ba(3) O(105) 126.47(14)	O(31) ¹ Ba(3) O(107) 143.09(16)
O(31) ¹ Ba(3) O(113) 141.97(14)	O(31) ¹ Ba(3) N(40) 77.41(11)
O(60) Ba(3) O(87) 140.25(12)	O(60) Ba(3) O(105) 149.77(13)
O(60) Ba(3) O(107) 76.11(14)	O(60) Ba(3) O(113) 103.33(15)
O(60) Ba(3) N(40) 69.87(12)	O(87) Ba(3) O(105) 69.79(15)
O(87) Ba(3) O(107) 138.02(17)	O(87) Ba(3) O(113) 81.02(18)
O(87) Ba(3) N(40) 76.21(14)	O(105) Ba(3) O(107) 75.04(16)
O(105) Ba(3) O(113) 73.49(17)	O(105) Ba(3) N(40) 130.80(16)
O(107) Ba(3) O(113) 67.38(19)	O(107) Ba(3) N(40) 112.84(14)

O(113)Ba(3) N(40) 66.85(14)	C(13) Co(4) C(13) ⁷ 180.0(4)
C(13) Co(4) C(58) 90.5(3)	C(13) Co(4) C(58) ⁷ 89.5(3)
C(13) Co(4) C(76) 89.6(2)	C(13) Co(4) C(76) ⁷ 90.4(2)
C(13) ⁷ Co(4) C(58) 89.5(3)	C(13) ⁷ Co(4) C(58) ⁷ 90.5(3)
C(13) ⁷ Co(4) C(76) 90.4(2)	C(13) ⁷ Co(4) C(76) ⁷ 89.6(2)
C(58) Co(4) C(58) ⁷ 180.0(3)	C(58) Co(4) C(76) 90.1(3)
C(58) Co(4) C(76) ⁷ 89.9(3)	C(58) ⁷ Co(4) C(76) 89.9(3)
C(58) ⁷ Co(4) C(76) ⁷ 90.1(3)	C(76) Co(4) C(76) ⁷ 180.0(4)
C(16) Co(5) C(19) 89.1(2)	C(16) Co(5) C(21) 178.6(2)
C(16) Co(5) C(23) 91.4(2)	C(16) Co(5) C(28) 88.1(2)
C(16) Co(5) C(38) 91.6(2)	C(19) Co(5) C(21) 90.9(2)
C(19) Co(5) C(23) 88.6(2)	C(19) Co(5) C(28) 91.3(2)
C(19) Co(5) C(38) 178.80(19)	C(21) Co(5) C(23) 90.0(2)
C(21) Co(5) C(28) 90.5(2)	C(21) Co(5) C(38) 88.4(2)
C(23) Co(5) C(28) 179.5(3)	C(23) Co(5) C(38) 90.41(19)
C(28) Co(5) C(38) 89.72(19)	C(47) Co(10)C(47) ⁸ 180.0(4)
C(47) Co(10)C(50) 88.7(3)	C(47) Co(10)C(50) ⁸ 91.3(3)
C(47) Co(10)C(68) 89.6(3)	C(47) Co(10)C(68) ⁸ 90.4(3)
C(47) ⁸ Co(10)C(50) 91.3(3)	C(47) ⁸ Co(10)C(50) ⁸ 88.7(3)
C(47) ⁸ Co(10)C(68) 90.4(3)	C(47) ⁸ Co(10)C(68) ⁸ 89.6(3)
C(50) Co(10)C(50) ⁸ 180.0(4)	C(50) Co(10)C(68) 91.0(3)

C(50) Co(10) C(68) ⁸ 89.0(3)	C(50) ⁸ Co(10) C(68) 89.0(3)
C(50) ⁸ Co(10) C(68) ⁸ 91.0(3)	C(68) Co(10) C(68) ⁸ 180.0(3)
O(9) Fe(6) O(15) 91.19(13)	O(9) Fe(6) O(18) 168.16(15)
O(9) Fe(6) N(14) 96.26(17)	O(9) Fe(6) N(22) 92.72(15)
O(9) Fe(6) N(29) 79.98(14)	O(15) Fe(6) O(18) 97.32(13)
O(15) Fe(6) N(14) 100.87(16)	O(15) Fe(6) N(22) 79.00(14)
O(15) Fe(6) N(29) 159.41(16)	O(18) Fe(6) N(14) 90.23(17)
O(18) Fe(6) N(22) 80.90(15)	O(18) Fe(6) N(29) 89.28(14)
N(14) Fe(6) N(22) 171.02(15)	N(14) Fe(6) N(29) 98.57(17)
N(22) Fe(6) N(29) 82.85(15)	O(17) Fe(7) O(25) 97.25(13)
O(17) Fe(7) O(54) 91.93(13)	O(17) Fe(7) N(27) 160.42(16)
O(17) Fe(7) N(52) 101.36(16)	O(17) Fe(7) N(64) 79.59(14)
O(25) Fe(7) O(54) 166.89(14)	O(25) Fe(7) N(27) 88.32(14)
O(25) Fe(7) N(52) 91.47(16)	O(25) Fe(7) N(64) 81.06(15)
O(54) Fe(7) N(27) 80.01(14)	O(54) Fe(7) N(52) 95.89(16)
O(54) Fe(7) N(64) 91.47(15)	N(27) Fe(7) N(52) 97.23(17)
N(27) Fe(7) N(64) 82.78(15)	N(52) Fe(7) N(64) 172.53(15)
Fe(6) O(9) C(51) 121.2(3)	Ba(2) ⁶ O(15) Fe(6) 139.53(16)
Ba(2) ⁶ O(15) C(79) 97.4(3)	Fe(6) O(15) C(79) 118.7(3)
Ba(3) ⁴ O(17) Fe(7) 136.88(16)	Ba(3) ⁴ O(17) C(70) 97.7(3)
Fe(7) O(17) C(70) 118.7(3)	Fe(6) O(18) C(86) 119.7(4)

Ba(1a) ¹ O(20) C(116) 125.7(4)	Fe(7) O(25) C(104) 119.9(3)
Ba(3) ¹ O(31) C(104) 141.0(4)	Ba(1a) ² O(33) C(77) 117.4(4)
Ba(1a) ⁹ O(35) C(78) 136.8(4)	Ba(1a) O(37) C(51) 147.2(4)
Ba(2) ⁵ O(45) C(86) 138.4(4)	Fe(7) O(54) C(78) 118.9(3)
Ba(2) O(55) C(70) 138.3(3)	Ba(3) O(60) C(79) 137.7(3)
Fe(6) N(14) C(58) 173.1(5)	Fe(6) N(22) C(59) 107.9(3)
Fe(6) N(22) C(69) 105.5(3)	Fe(6) N(22) C(83) 105.1(3)
C(59) N(22) C(69) 112.2(4)	C(59) N(22) C(83) 110.7(4)
C(69) N(22) C(83) 114.9(4)	Fe(7) N(27) C(42) 106.6(3)
Fe(7) N(27) C(48) 104.9(3)	Fe(7) N(27) C(49) 111.5(3)
C(42) N(27) C(48) 112.5(4)	C(42) N(27) C(49) 109.2(4)
C(48) N(27) C(49) 112.0(4)	Fe(6) N(29) C(26) 105.0(3)
Fe(6) N(29) C(56) 106.4(3)	Fe(6) N(29) C(114) 111.9(3)
C(26) N(29) C(56) 111.8(4)	C(26) N(29) C(114) 110.2(4)
C(56) N(29) C(114) 111.4(4)	Ba(2) N(30) C(19) 142.2(4)
Ba(3) N(40) C(38) 142.9(4)	Fe(7) N(52) C(68) 170.0(5)
Fe(7) N(64) C(24) 105.0(3)	Fe(7) N(64) C(57) 107.3(3)
Fe(7) N(64) C(71) 104.8(3)	C(24) N(64) C(57) 111.7(4)
C(24) N(64) C(71) 114.8(4)	C(57) N(64) C(71) 112.4(4)
Co(4) C(13) N(12) 177.0(6)	Co(5) C(16) N(32) 177.4(5)
Co(5) C(19) N(30) 178.5(5)	Co(5) C(21) N(41) 178.2(5)

Co(5) C(23) N(39) 178.6(5)	N(64) C(24) C(70) 109.2(4)
N(29) C(26) C(69) 111.4(4)	Co(5) C(28) N(34) 178.7(5)
Co(5) C(38) N(40) 177.4(5)	N(27) C(42) C(71) 112.1(4)
Co(10)C(47) N(46) 178.4(6)	N(27) C(48) C(78) 112.9(4)
N(27) C(49) C(116) 116.5(5)	Co(10)C(50) N(43) 177.8(6)
O(9) C(51) O(37) 124.4(5)	O(9) C(51) C(56) 115.9(4)
O(37) C(51) C(56) 119.7(5)	N(29) C(56) C(51) 113.0(4)
N(64) C(57) C(104) 113.8(4)	Co(4) C(58) N(14) 177.9(5)
N(22) C(59) C(86) 112.9(4)	Co(10)C(68) N(52) 178.1(5)
N(22) C(69) C(26) 108.9(4)	O(17) C(70) O(55) 122.1(5)
O(17) C(70) C(24) 115.4(4)	O(55) C(70) C(24) 122.5(5)
N(64) C(71) C(42) 109.6(4)	Co(4) C(76) N(8) 178.7(6)
O(33) C(77) C(114) 110.6(6)	O(35) C(78) O(54) 123.9(5)
O(35) C(78) C(48) 120.3(5)	O(54) C(78) C(48) 115.9(4)
O(15) C(79) O(60) 122.9(5)	O(15) C(79) C(83) 115.7(4)
O(60) C(79) C(83) 121.4(5)	N(22) C(83) C(79) 108.6(4)
O(18) C(86) O(45) 123.2(5)	O(18) C(86) C(59) 117.3(4)
O(45) C(86) C(59) 119.5(5)	O(25) C(104)O(31) 122.7(5)
O(25) C(104)C(57) 117.0(4)	O(31) C(104)C(57) 120.3(5)
N(29) C(114)C(77) 114.5(5)	O(20) C(116)C(49) 113.8(5)

Symmetry Operators:

- | | |
|----------------------|----------------------|
| (1) $-X+1,-Y+1,-Z+1$ | (2) $-X+1,-Y,-Z$ |
| (3) $X,Y-1,Z$ | (4) $X+1,Y,Z$ |
| (5) $-X+1,-Y+1,-Z$ | (6) $X-1,Y,Z$ |
| (7) $-X,-Y,-Z$ | (8) $-X+2,-Y+2,-Z+1$ |
| (9) $X,Y+1,Z$ | |

Table 19: Bond angles involving hydrogens ($^{\circ}$)

atom	atom	atom	angle	atom	atom	atom	angle
N(64)	C(24)	H(24A)	109.8	N(64)	C(24)	H(24B)	109.8
C(70)	C(24)	H(24A)	109.8	C(70)	C(24)	H(24B)	109.8
H(24A)	C(24)	H(24B)	108.3	N(29)	C(26)	H(26A)	109.3
N(29)	C(26)	H(26B)	109.4	C(69)	C(26)	H(26A)	109.4
C(69)	C(26)	H(26B)	109.4	H(26A)	C(26)	H(26B)	108.0
N(27)	C(42)	H(42A)	109.2	N(27)	C(42)	H(42B)	109.2
C(71)	C(42)	H(42A)	109.2	C(71)	C(42)	H(42B)	109.2
H(42A)	C(42)	H(42B)	107.9	N(27)	C(48)	H(48A)	109.0
N(27)	C(48)	H(48B)	109.0	C(78)	C(48)	H(48A)	109.0
C(78)	C(48)	H(48B)	109.0	H(48A)	C(48)	H(48B)	107.8
N(27)	C(49)	H(49A)	108.2	N(27)	C(49)	H(49B)	108.2
C(116)	C(49)	H(49A)	108.2	C(116)	C(49)	H(49B)	108.2
H(49A)	C(49)	H(49B)	107.3	N(29)	C(56)	H(56A)	109.0
N(29)	C(56)	H(56B)	109.0	C(51)	C(56)	H(56A)	109.0

C(51) C(56) H(56B)	109.0	H(56A)C(56) H(56B)	107.8
N(64) C(57) H(57A)	108.8	N(64) C(57) H(57B)	108.8
C(104)C(57) H(57A)	108.8	C(104)C(57) H(57B)	108.8
H(57A) C(57) H(57B)	107.7	N(22) C(59) H(59A)	109.0
N(22) C(59) H(59B)	109.0	C(86) C(59) H(59A)	109.0
C(86) C(59) H(59B)	109.0	H(59A) C(59) H(59B)	107.8
N(22) C(69) H(69A)	109.9	N(22) C(69) H(69B)	109.9
C(26) C(69) H(69A)	109.9	C(26) C(69) H(69B)	109.9
H(69A)C(69) H(69B)	108.3	N(64) C(71) H(71A)	109.8
N(64) C(71) H(71B)	109.8	C(42) C(71) H(71A)	109.7
C(42) C(71) H(71B)	109.8	H(71A) C(71) H(71B)	108.2
O(33) C(77) H(77A)	109.5	O(33) C(77) H(77B)	109.5
C(114)C(77) H(77A)	109.5	C(114)C(77) H(77B)	109.5
H(77A) C(77) H(77B)	108.1	N(22) C(83) H(83A)	110.0
N(22) C(83) H(83B)	110.0	C(79) C(83) H(83A)	110.0
C(79) C(83) H(83B)	110.0	H(83A) C(83) H(83B)	108.4
N(29) C(114)H(11A)	108.6	N(29) C(114)H(11B)	108.6
C(77) C(114)H(11A)	108.6	C(77) C(114)H(11B)	108.6
H(11A) C(114) H(11B)	107.6	O(20) C(116)H(11C)	108.8
O(20) C(116)H(11D)	108.8	C(49) C(116)H(11C)	108.8
C(49) C(116)H(11D)	108.8	H(11C) C(116) H(11D)	107.7

Table 20: Torsion Angles(°)

(Those having bond angles > 160 or < 20 degrees are excluded.)

atom1	atom2	atom3	atom4	angle	atom1	atom2	atom3	atom4	angle
O(20) ¹	Ba(1a)	O(33) ²	C(77) ²	63.2(4)	O(33) ²	Ba(1a)	O(20) ¹	C(116) ¹	-166.5(3)
O(20) ¹	Ba(1a)	O(35) ³	C(78) ³	-174.8(5)	O(35) ³	Ba(1a)	O(20) ¹	C(116) ¹	146.5(4)
O(20) ¹	Ba(1a)	O(37)	C(51)	53.6(6)	O(37)	Ba(1a)	O(20) ¹	C(116) ¹	-76.4(4)
O(44)	Ba(1a)	O(20) ¹	C(116) ¹	71.6(4)	O(84)	Ba(1a)	O(20) ¹	C(116) ¹	94.4(4)
O(89)	Ba(1a)	O(20) ¹	C(116) ¹	-47.9(5)	O(33) ²	Ba(1a)	O(35) ³	C(78) ³	39.9(5)
O(35) ³	Ba(1a)	O(33) ²	C(77) ²	113.2(4)	O(33) ²	Ba(1a)	O(37)	C(51)	-173.8(6)
O(37)	Ba(1a)	O(33) ²	C(77) ²	-17.4(3)	O(44)	Ba(1a)	O(33) ²	C(77) ²	163.8(3)
O(84)	Ba(1a)	O(33) ²	C(77) ²	-162.3(4)	O(89)	Ba(1a)	O(33) ²	C(77) ²	-82.6(3)
O(35) ³	Ba(1a)	O(37)	C(51)	115.7(5)	O(37)	Ba(1a)	O(35) ³	C(78) ³	123.7(4)
O(44)	Ba(1a)	O(35) ³	C(78) ³	-97.7(5)	O(84)	Ba(1a)	O(35) ³	C(78) ³	-26.4(5)
O(89)	Ba(1a)	O(35) ³	C(78) ³	17.8(6)	O(44)	Ba(1a)	O(37)	C(51)	4.6(7)
O(84)	Ba(1a)	O(37)	C(51)	-116.7(6)	O(89)	Ba(1a)	O(37)	C(51)	-108.7(6)
O(15) ⁴	Ba(2)	O(45) ⁵	C(86) ⁵	162.8(4)	O(45) ⁵	Ba(2)	O(15) ⁴	Fe(6) ⁴	-75.3(3)
O(45) ⁵	Ba(2)	O(15) ⁴	C(79) ⁴	78.57(17)	O(15) ⁴	Ba(2)	O(55)	C(70)	-146.9(3)
O(55)	Ba(2)	O(15) ⁴	Fe(6) ⁴	-140.2(2)	O(55)	Ba(2)	O(15) ⁴	C(79) ⁴	13.65(17)
O(82)	Ba(2)	O(15) ⁴	Fe(6) ⁴	1.6(3)	O(82)	Ba(2)	O(15) ⁴	C(79) ⁴	155.45(17)

O(100)Ba(2) O(15) ⁴ Fe(6) ⁴ 71.5(3) 134.68(19)	O(100)Ba(2) O(15) ⁴ C(79) ⁴ -
O(109)Ba(2) O(15) ⁴ Fe(6) ⁴ 140.6(3)	O(109)Ba(2) O(15) ⁴ C(79) ⁴ -65.51(19)
O(115)Ba(2) O(15) ⁴ Fe(6) ⁴ 72.4(4)	O(115)Ba(2) O(15) ⁴ C(79) ⁴ -133.8(3)
O(15) ⁴ Ba(2) N(30) C(19) 168.5(4)	N(30) Ba(2) O(15) ⁴ Fe(6) ⁴ -61.7(3)
N(30) Ba(2) O(15) ⁴ C(79) ⁴ 92.1(3)	O(45) ⁵ Ba(2) O(55) C(70) 152.8(4)
O(55) Ba(2) O(45) ⁵ C(86) ⁵ -82.2(4)	O(82) Ba(2) O(45) ⁵ C(86) ⁵ 66.9(4)
O(100)Ba(2) O(45) ⁵ C(86) ⁵ 121.6(4)	O(109)Ba(2) O(45) ⁵ C(86) ⁵ -117.7(4)
O(115)Ba(2) O(45) ⁵ C(86) ⁵ 12.2(5)	O(45) ⁵ Ba(2) N(30) C(19) -178.7(6)
N(30) Ba(2) O(45) ⁵ C(86) ⁵ -8.9(4)	O(82) Ba(2) O(55) C(70) 103.1(4)
O(100)Ba(2) O(55) C(70) -66.4(5)	O(109)Ba(2) O(55) C(70) -47.5(4)
O(115)Ba(2) O(55) C(70) 14.0(4)	O(55) Ba(2) N(30) C(19) -101.1(6)
N(30) Ba(2) O(55) C(70) 71.4(3)	O(82) Ba(2) N(30) C(19) 100.0(6)
O(100)Ba(2) N(30) C(19) 52.7(6)	O(109)Ba(2) N(30) C(19) -35.0(6)
O(115)Ba(2) N(30) C(19) 15.9(5)	O(17) ⁶ Ba(3) O(31) ¹ C(104) ¹ -160.0(5)
O(31) ¹ Ba(3) O(17) ⁶ Fe(7) ⁶ 71.3(2)	O(31) ¹ Ba(3) O(17) ⁶ C(70) ⁶ -77.22(17)
O(17) ⁶ Ba(3) O(60) C(79) 144.4(3)	O(60) Ba(3) O(17) ⁶ Fe(7) ⁶ 136.8(2)
O(60) Ba(3) O(17) ⁶ C(70) ⁶ -11.72(17)	O(87) Ba(3) O(17) ⁶ Fe(7) ⁶ -5.9(3)
O(87) Ba(3) O(17) ⁶ C(70) ⁶ -154.42(18)	O(105)Ba(3) O(17) ⁶ Fe(7) ⁶ -74.7(3)
O(105)Ba(3) O(17) ⁶ C(70) ⁶ 136.8(2)	O(107)Ba(3) O(17) ⁶ Fe(7) ⁶ -144.9(3)
O(107)Ba(3) O(17) ⁶ C(70) ⁶ 66.57(19)	O(113)Ba(3) O(17) ⁶ Fe(7) ⁶ -79.7(4)

O(113)Ba(3) O(17) ⁶ C(70) ⁶ 131.8(3)	O(17) ⁶ Ba(3) N(40) C(38) -171.3(4)
N(40) Ba(3) O(17) ⁶ Fe(7) ⁶ 60.2(3)	N(40) Ba(3) O(17) ⁶ C(70) ⁶ -88.4(3)
O(31) ¹ Ba(3) O(60) C(79) -155.8(4)	O(60) Ba(3) O(31) ¹ C(104) ¹ 85.5(4)
O(87) Ba(3) O(31) ¹ C(104) ¹ -65.1(4)	O(105)Ba(3) O(31) ¹ C(104) ¹ -118.7(4)
O(107)Ba(3) O(31) ¹ C(104) ¹ 124.6(4)	O(113)Ba(3) O(31) ¹ C(104) ¹ -6.9(6)
O(31) ¹ Ba(3) N(40) C(38) 178.2(6)	N(40) Ba(3) O(31) ¹ C(104) ¹ 13.2(4)
O(87) Ba(3) O(60) C(79) -107.0(4)	O(105)Ba(3) O(60) C(79) 65.0(5)
O(107)Ba(3) O(60) C(79) 47.2(3)	O(113)Ba(3) O(60) C(79) -15.1(4)
O(60) Ba(3) N(40) C(38) 100.0(6)	N(40) Ba(3) O(60) C(79) -73.9(3)
O(87) Ba(3) N(40) C(38) -101.1(6)	O(105)Ba(3) N(40) C(38) -54.1(6)
O(107)Ba(3) N(40) C(38) 35.6(6)	O(113)Ba(3) N(40) C(38) -15.1(5)
O(9) Fe(6) O(15) Ba(2) ⁶ -131.8(3)	O(9) Fe(6) O(15) C(79) 78.1(3)
O(15) Fe(6) O(9) C(51) -169.8(3)	N(14) Fe(6) O(9) C(51) 89.1(3)
O(9) Fe(6) N(22) C(59) 179.76(19)	O(9) Fe(6) N(22) C(69) 59.63(19)
O(9) Fe(6) N(22) C(83) -62.14(19)	N(22) Fe(6) O(9) C(51) -90.8(3)
O(9) Fe(6) N(29) C(26) -103.4(3)	O(9) Fe(6) N(29) C(56) 15.2(3)
O(9) Fe(6) N(29) C(114) 137.0(3)	N(29) Fe(6) O(9) C(51) -8.6(3)
O(15) Fe(6) O(18) C(86) 69.9(3)	O(18) Fe(6) O(15) Ba(2) ⁶ 56.5(3)
O(18) Fe(6) O(15) C(79) -93.6(3)	N(14) Fe(6) O(15) Ba(2) ⁶ -35.1(3)
N(14) Fe(6) O(15) C(79) 174.7(2)	O(15) Fe(6) N(22) C(59) -89.56(19)
O(15) Fe(6) N(22) C(69) 150.3(2)	O(15) Fe(6) N(22) C(83) 28.54(17)

N(22) Fe(6) O(15) Ba(2) ⁶ 135.7(3)	N(22) Fe(6) O(15) C(79) -14.4(2)
O(15) Fe(6) N(29) C(26) -37.7(5)	O(15) Fe(6) N(29) C(56) 81.0(5)
O(15) Fe(6) N(29) C(114) -157.2(3)	N(29) Fe(6) O(15) Ba(2) ⁶ 164.3(3)
N(29) Fe(6) O(15) C(79) 14.2(5)	N(14) Fe(6) O(18) C(86) 170.9(3)
O(18) Fe(6) N(22) C(59) 9.80(19)	O(18) Fe(6) N(22) C(69) -110.3(2)
O(18) Fe(6) N(22) C(83) 127.89(19)	N(22) Fe(6) O(18) C(86) -7.6(3)
O(18) Fe(6) N(29) C(26) 71.5(2)	O(18) Fe(6) N(29) C(56) -169.8(3)
O(18) Fe(6) N(29) C(114) -48.0(3)	N(29) Fe(6) O(18) C(86) -90.5(3)
N(14) Fe(6) N(29) C(26) 161.7(2)	N(14) Fe(6) N(29) C(56) -79.7(3)
N(14) Fe(6) N(29) C(114) 42.1(3)	N(22) Fe(6) N(29) C(26) -9.38(19)
N(22) Fe(6) N(29) C(56) 109.3(3)	N(22) Fe(6) N(29) C(114) -128.9(3)
N(29) Fe(6) N(22) C(59) 100.2(2)	N(29) Fe(6) N(22) C(69) -19.91(18)
N(29) Fe(6) N(22) C(83) -141.69(19)	O(17) Fe(7) O(25) C(104) -77.2(3)
O(25) Fe(7) O(17) Ba(3) ⁴ -53.8(3)	O(25) Fe(7) O(17) C(70) 90.1(3)
O(17) Fe(7) O(54) C(78) 179.6(3)	O(54) Fe(7) O(17) Ba(3) ⁴ 135.6(2)
O(54) Fe(7) O(17) C(70) -80.6(3)	N(52) Fe(7) O(17) Ba(3) ⁴ 39.2(3)
N(52) Fe(7) O(17) C(70) -177.0(2)	O(17) Fe(7) N(64) C(24) -26.03(17)
O(17) Fe(7) N(64) C(57) 93.0(2)	O(17) Fe(7) N(64) C(71) -147.3(2)
N(64) Fe(7) O(17) Ba(3) ⁴ -133.2(3)	N(64) Fe(7) O(17) C(70) 10.6(2)
O(25) Fe(7) N(27) C(42) -77.9(2)	O(25) Fe(7) N(27) C(48) 162.6(3)
O(25) Fe(7) N(27) C(49) 41.2(3)	N(27) Fe(7) O(25) C(104) 84.0(3)

N(52) Fe(7) O(25) C(104) -178.8(3)	O(25) Fe(7) N(64) C(24) -125.2(2)
O(25) Fe(7) N(64) C(57) -6.15(19)	O(25) Fe(7) N(64) C(71) 113.5(2)
N(64) Fe(7) O(25) C(104) 1.0(3)	O(54) Fe(7) N(27) C(42) 96.1(2)
O(54) Fe(7) N(27) C(48) -23.4(3)	O(54) Fe(7) N(27) C(49) -144.8(3)
N(27) Fe(7) O(54) C(78) 17.6(3)	N(52) Fe(7) O(54) C(78) -78.7(3)
O(54) Fe(7) N(64) C(24) 65.66(19)	O(54) Fe(7) N(64) C(57) -175.3(2)
O(54) Fe(7) N(64) C(71) -55.6(2)	N(64) Fe(7) O(54) C(78) 100.0(3)
N(52) Fe(7) N(27) C(42) -169.2(2)	N(52) Fe(7) N(27) C(48) 71.3(3)
N(52) Fe(7) N(27) C(49) -50.1(3)	N(27) Fe(7) N(64) C(24) 145.4(2)
N(27) Fe(7) N(64) C(57) -95.6(2)	N(27) Fe(7) N(64) C(71) 24.10(19)
N(64) Fe(7) N(27) C(42) 3.29(19)	N(64) Fe(7) N(27) C(48) -116.2(3)
N(64) Fe(7) N(27) C(49) 122.4(3)	Fe(6) O(9) C(51) O(37) -178.8(4)
Fe(6) O(9) C(51) C(56) -0.8(6)	Ba(2) ⁶ O(15) C(79) O(60) 16.3(4)
Ba(2) ⁶ O(15) C(79) C(83) -165.0(3)	Fe(6) O(15) C(79) O(60) 177.3(3)
Fe(6) O(15) C(79) C(83) -4.0(4)	Ba(3) ⁴ O(17) C(70) O(55) -17.2(4)
Ba(3) ⁴ O(17) C(70) C(24) 164.1(3)	Fe(7) O(17) C(70) O(55) -173.2(3)
Fe(7) O(17) C(70) C(24) 8.1(4)	Fe(6) O(18) C(86) O(45) -176.0(3)
Fe(6) O(18) C(86) C(59) 3.2(5)	Ba(1a) ¹ O(20) C(116) C(49) 148.4(4)
Fe(7) O(25) C(104) O(31) -175.6(3)	Fe(7) O(25) C(104) C(57) 4.7(5)
Ba(3) ¹ O(31) C(104) O(25) 129.4(5)	Ba(3) ¹ O(31) C(104) C(57) -50.9(7)
Ba(1a) ² O(33) C(77) C(114) -125.0(4)	Ba(1a) ⁷ O(35) C(78) O(54) -37.9(9)

Ba(1a) ⁷ O(35) C(78) C(48) 141.1(4)	Ba(1a) O(37) C(51) O(9) -44.2(10)
Ba(1a) O(37) C(51) C(56) 138.0(5)	Ba(2) ⁵ O(45) C(86) O(18) -124.0(5)
Ba(2) ⁵ O(45) C(86) C(59) 56.8(6)	Fe(7) O(54) C(78) O(35) 172.3(4)
Fe(7) O(54) C(78) C(48) -6.7(6)	Ba(2) O(55) C(70) O(17) 153.2(3)
Ba(2) O(55) C(70) C(24) -28.2(6)	Ba(3) O(60) C(79) O(15) -150.7(3)
Ba(3) O(60) C(79) C(83) 30.6(6)	Fe(6) N(22) C(59) C(86) -10.9(4)
Fe(6) N(22) C(69) C(26) 46.1(4)	Fe(6) N(22) C(83) C(79) -37.2(3)
C(59) N(22) C(69) C(26) -71.2(5)	C(69) N(22) C(59) C(86) 104.9(4)
C(59) N(22) C(83) C(79) 79.0(4)	C(83) N(22) C(59) C(86) -125.4(4)
C(69) N(22) C(83) C(79) -152.7(4)	C(83) N(22) C(69) C(26) 161.3(4)
Fe(7) N(27) C(42) C(71) -30.7(4)	Fe(7) N(27) C(48) C(78) 26.6(5)
Fe(7) N(27) C(49) C(116) -176.2(3)	C(42) N(27) C(48) C(78) -88.8(5)
C(48) N(27) C(42) C(71) 83.7(5)	C(42) N(27) C(49) C(116) -58.7(5)
C(49) N(27) C(42) C(71) -151.3(4)	C(48) N(27) C(49) C(116) 66.6(6)
C(49) N(27) C(48) C(78) 147.8(4)	Fe(6) N(29) C(26) C(69) 37.8(4)
Fe(6) N(29) C(56) C(51) -19.8(5)	Fe(6) N(29) C(114) C(77) 177.2(3)
C(26) N(29) C(56) C(51) 94.3(5)	C(56) N(29) C(26) C(69) -77.1(5)
C(26) N(29) C(114) C(77) 60.9(5)	C(114) N(29) C(26) C(69) 158.4(4)
C(56) N(29) C(114) C(77) -63.8(6)	C(114) N(29) C(56) C(51) -141.9(4)
Fe(7) N(64) C(24) C(70) 36.1(4)	Fe(7) N(64) C(57) C(104) 10.0(4)
Fe(7) N(64) C(71) C(42) -47.8(4)	C(24) N(64) C(57) C(104) 124.6(4)

C(57) N(64) C(24) C(70) -79.9(5)	C(24) N(64) C(71) C(42) -162.4(4)
C(71) N(64) C(24) C(70) 150.6(4)	C(57) N(64) C(71) C(42) 68.4(5)
C(71) N(64) C(57) C(104) -104.7(5)	N(64) C(24) C(70) O(17) -31.6(5)
N(64) C(24) C(70) O(55) 149.8(4)	N(29) C(26) C(69) N(22) -59.1(5)
N(27) C(42) C(71) N(64) 55.1(5)	N(27) C(48) C(78) O(35) 165.1(5)
N(27) C(48) C(78) O(54) -15.9(7)	N(27) C(49) C(116) O(20) -72.1(7)
O(9) C(51) C(56) N(29) 15.3(7)	O(37) C(51) C(56) N(29) -166.7(5)
N(64) C(57) C(104) O(25) -10.3(6)	N(64) C(57) C(104) O(31) 170.0(4)
N(22) C(59) C(86) O(18) 6.0(6)	N(22) C(59) C(86) O(45) -174.7(4)
O(33) C(77) C(114) N(29) 159.1(5)	O(15) C(79) C(83) N(22) 29.7(5)
O(60) C(79) C(83) N(22) -151.6(4)	

Symmetry Operators:

- | | |
|--------------------|----------------|
| (1) -X+1,-Y+1,-Z+1 | (2) -X+1,-Y,-Z |
| (3) X,Y-1,Z | (4) X+1,Y,Z |
| (5) -X+1,-Y+1,-Z | (6) X-1,Y,Z |
| (7) X,Y+1,Z | |

Appendix C

Authored Publication

1. Eagle, C. T.; **Kpogo, K. K.**; Zink, L. C.; Smith, A. E., Tetra-kis[μ -N-(2,4,6-trimethyl-phen-yl)acetamidato]- $\kappa(4)$ N:O; $\kappa(4)$ O:N-bis- [(benzo-nitrile- κ N) rhodium(II)](Rh-Rh). *Acta crystallographica. Section E, Structure reports online* **2012**, 68 (Pt 7), m877.

